Medizinische Hochschule Hannover

Klinik für Hals-, Nasen-, Ohrenheilkunde

Modeling of the human temporal bone for virtual reality surgical training

INAUGURALDISSERTATION
zur Erlangung des Grades einer Doktorin oder eines Doktors
der Humanbiologie
-Doctor rerum biologicarum humanarum-
(Dr. rer. biol. hum.)

vorgelegt von

Daniel Sieber

aus Stuttgart

Innsbruck 2021

Angenommen durch den Senat: 13.08.2021

Präsident: Prof. Dr. med. Michael P. Manns

Wissenschaftliche Betreuung: Prof. Prof. h. c. Dr. med. Thomas Lenarz

Wissenschaftliche Zweitbetreuung: Prof. Dr. med. Mads Sølvsten Sørensen

1. Referent/in: Prof. Prof. h. c. Dr. med. Thomas Lenarz
2. Referent/in: Prof. Dr. med. Mads Sølvsten Sørensen
3. Referent/in: PD Dr. med. Dietmar Böthig

Tag der mündlichen Prüfung: 13.08.2021

Prüfungsausschuss

Vorsitz: Prof. Dr. rer. biol. hum. Roland Jacobs

1. Prüfer/in: Prof. Prof. h. c. Dr. med. Thomas Lenarz
2. Prüfer/in: Prof. Dr. med. Mads Sølvsten Sørensen
3. Prüfer/in: PD Dr. med. Dietmar Böthig

Table of Content

Abstract

Modeling of the human temporal bone for virtual reality surgical training

Daniel Sieber

Simulators can be a very useful tool for the training of surgeons, especially as educational aspects of surgical residency have come under rising pressure due to work hour restrictions and increasing economization of surgical time. While it has been shown that temporal bone simulators can improve the efficiency of cadaveric training, high-fidelity anatomy models and variable practice conditions may be needed for more advanced learner levels. Existing simulator systems either feature anatomy models of low-quality or are limited to constant practice training as only one anatomy is available. To overcome this limitation, a novel process was developed within the framework of this dissertation which allows the relative efficient production of high-fidelity anatomical computer models as well as their implementation in virtual reality surgical simulation.

Eight fresh adult human temporal bones were digitized using Cone Beam Computed Tomography (CBCT) and destructive micro-slicing by serial grinding and optical imaging. The resulting multimodal image stacks were reconstructed and registered in 3D. Segmentation of critical structures was performed using threshold-based techniques for bone structures and threshold supported manual techniques for soft tissue structures.

Six anatomies could successfully be implemented into the Visible Ear Simulator software complete with instructional guides for different temporal bone surgical procedures. The CBCT and micro-slicing datasets were combined to achieve this, with a CBCT based geometry model for haptic simulation working in a concerted way with the micro-slicing color based visual model. Manual tinting was applied in segments which had compromised appearance as an artefact of specimen preparation for micro-slicing. Along the same lines, some bony defects in the drillable segments as a result of artefacts in CBCT imaging were manually corrected.

The publication of the OpenEar datasets and their implementation into the Visible Ear Simulator mark the beginning of a new era in surgical simulation of otologic surgery. It will now be possible to study the effects of task variability in temporal bone surgical training without having to make compromises when it comes to the visual quality of the underlying datasets. This is expected to increase trainee's performance in simulation training due to the better development of a Generalized Motor Program and training the surgeons attention to more anatomical variables. While patient specific surgical rehearsal is still hindered by clinical imaging fidelity, the processes developed within this dissertation

could prove essential in the creation of training data for machine learning techniques powering such simulations and clinical Augmented Reality applications in the future.

Interactive apps featuring high-fidelity 3D anatomy models as described here, could become an important addition to conventional textbooks for medical students. Residents can increase their understanding of the anatomy and make cadaveric dissection training more efficient by using surgical simulators. With the current work, surgical simulators are expected to also stay relevant for intermediate learners who need high-fidelity anatomy models and the option to train in different anatomies to create variable practice conditions. Additional studies will be needed to further develop the evidence basis allowing a more widespread and systematic use of surgical simulators in surgical training curricula.

Kurzzusammenfassung

Modellierung des humanen Felsenbeins für das chirurgische Training in virtueller Realität

Daniel Sieber

Chirurgisches Training im Simulator kann ein sehr nützliches Element in der Ausbildung von Chirurgen darstellen, insbesondere da Lehraspekte in der Facharztausbildung durch Arbeitszeitbeschränkungen und einer zunehmenden Ökonomisierung der Zeit im Operationssaal unter Druck geraten. Während der positive Effekt von Simulatoren auf die Effizienz des Trainings im Felsenbeinpräparat bereits gezeigt werden konnte, wird angenommen, dass für fortgeschrittene Lernende anatomische Modelle hoher Qualität und abwechslungsreiche Trainingsszenarien benötigt werden. In den bislang verfügbaren Simulator Systemen sind hingegen die anatomischen Modelle entweder von niedriger Qualität oder auf das konstante Training in einer einzelnen Anatomie beschränkt. Um diese Einschränkungen zu überwinden, wurde im Rahmen der vorliegenden Dissertation ein neuartiger Prozess zur effizienten Produktion qualitativ hochwertiger anatomischer Computermodelle und deren Implementierung in die virtuelle Realität chirurgischer Simulatoren entwickelt.

Acht frische humane Felsenbeine wurden mit Hilfe von Digitaler Volumentomografie (DVT) sowie optischer Hartschliffhistologie digitalisiert. Die resultierenden multimodalen Bilddaten wurden anschließend dreidimensional rekonstruiert und zueinander registriert. Die Segmentierung der kritischen Strukturen für knöcherne Segmente erfolgte schwellenwertbasiert, während die Segmentierung von Weichgewebssegmenten mit manuellen Methoden erfolgte.

Sechs Anatomien wurden in den Visible Ear Simulator implementiert und stehen nun auch im Rahmen von geführten Anleitungen für verschiedene virtuelle Eingriffe am Felsenbein zur Verfügung. Dazu wurden die DVT- und Schnittbild-Datensätze vereint, wobei ein geometrisches Modell zur haptischen Simulation auf DVT Basis konzertiert mit einem visuellen Modell auf Basis von Schliffbildern zusammenspielt. Manuelle Texturen wurden in jenen Segmenten hinzugefügt, deren Aussehen durch die Probenvorbereitung für den Hartschliff kompromittiert wurde. Knochendefekte als Folge von Artefakten aus der DVT Bildgebung wurden ebenfalls manuell korrigiert.

Die Publikation der OpenEar Datensätze und ihre Implementierung in einen Simulator läuten ein neues Zeitalter in der Simulation otologischer Chirurgie ein. Es wird nun möglich sein, den Einfluss variabler Trainingsszenarien auf den Trainingserfolg zu erforschen, ohne dabei Kompromisse in Bezug auf die visuelle Qualität der zugrundeliegenden Datensätze machen zu müssen. Es ist zu erwarten, dass die Erfolge der Lernenden auf Grund der verbesserten Anlage von generalisierten Bewegungsabläufen

sowie der Erweiterung der Aufmerksamkeit auf mehr anatomische Variablen größer ausfallen werden. Einer brauchbaren patientenspezifischen Operationssimulation steht derzeit noch die Qualität der klinischen Bildgebung entgegen. Der hier beschriebene Prozess könnte jedoch für die Produktion von Trainingsdaten für das maschinelle Lernen essenziell sein, welches für patientenspezifische Simulation und augmentierte klinische Realität von großer Bedeutung ist.

Interaktive Apps auf Basis qualitativ hochwertiger anatomischer Modelle wie in dieser Arbeit beschrieben, können zukünftig schon für Studierende der Medizin eine wichtige Ergänzung zu anatomischen Lehrbüchern sein. In der Facharztausbildung können das Verständnis der Anatomie sowie die Effizienz des Trainings im Präparat verbessert werden. Mit der hier vorgestellten Arbeit kann die Relevanz chirurgischer Simulation auch auf fortgeschrittene Lernende erweitert werden, welche anatomische Modelle in hoher Qualität und abwechslungsreichere Trainingsoptionen benötigen. Weitere Studien sind nötig, um die evidenzbasierte, flächendeckende und systematische Integration chirurgischer Simulatoren in das Curriculum der chirurgischen Ausbildung zu erreichen.

Foreword

I still remember when I first met Peter Trier and Mads Sølvsten Sørensen in 2009 at the *Computer Aided Surgery around the Head* conference in Paris in 2009. I was a freshman developer of surgical tools for cochlear implant surgery and Peter and Mads were presenting the first version of their otology surgical simulator in the anatomical preparation lab. I was deeply impressed with the technology and the way young surgeons interacted with the simulator in a natural and fun way.

From today's perspective of course the simulator they presented at the time seems prototypical. One had to wear red/blue glasses to see a stereoscopic image which falsified the visible colors quite a bit. Also, the user interface at the time consisted of dozens of technical controls and keyboard shortcuts and was hard to master even in the scales of digital natives. But the core components which make up the magic of the Visible Ear Simulator until today were there already. On the one hand it is the interaction of the user with the three-dimensional digital model of the human ear through a haptic force feedback device, creating a virtual reality experience which really made sense beyond a pure showcase for the first time in my personal experience. But most impressive was the quality of the underlying Visible Ear dataset which Mads had already started working on more than a decade before. The three-dimensional interaction with this high-fidelity digital model of the human temporal bone including the use of transparency and sectioning provided insights into the anatomy of the human ear which neither textbooks nor cadaveric specimen could provide.

After Paris, I stayed in touch with Peter and Mads and became a volunteer in the team beta-testing every new version of Visible Ear Simulator. Many things have naturally been improved over the last ten years. The cluttered user interface was replaced over time by a cleaner design inherently limiting the user's adjustment options to configurations maintaining a realistic simulation. The initial stereoscopy concept using red/blue glasses was first updated to polarized 3D screens and finally to the digital binoculars of the new and fully digital operating microscopes. The visuals and physics simulation constantly evolved with every new version.

An invariant remark which we heard when presenting the simulator all around the world, was that surgeons desired more anatomies to be included in the system. While the benefit of adding more anatomies was evident to the developer's team, there was no clear path towards achieving them. The laboriousness of the original cryo-sectioning method used in the Visible Ear dataset was prohibitive to scaling up to more anatomies. On the other hand, sacrificing the high quality of the original dataset in exchange for a faster ability to create more anatomical models using (micro)CT scans did not seem a good option either. The promises of artificial intelligence to morph the Visible Ear dataset to any clinical patient CT series could not be materialized either given the time and resources available.

When my professional career brought me to Hannover in 2012 to work with the amazing group of Professor Thomas Lenarz, things changed. Having access to Peter Erfurt's specimen preparation laboratory and experiencing some of his advanced preparation techniques was a golden opportunity. In 2014 the idea of creating a more efficient way of creating digital temporal bones through a combination of CT and micro-slicing techniques was born. After a while of experimenting with different embedding and imaging techniques in 2015 we had grown confident, that it might be possible to create high-fidelity anatomical models of the temporal bone in a more scalable way which could produce more models in shorter time. In 2016 we started working with actual temporal bone specimen. Peter Erfurt optimized the staining and embedding processes in the first samples Alpha and Beta, while I was busy fine tuning the workflow of micro-slicing and optical microscopy. With the support of Samuel John, the alignment of slices and reconstruction into 3D could be mastered even though the hurdles found were much more difficult and resistant to being overcome than expected.

The following months appear blurred in hindsight, as I was working long hours every day grinding, digitizing, post-processing and segmenting temporal bone specimen. But the privilege of being allowed to see the beauty of the human anatomy unfold in front of me with every new slice was more than enough reward, and at times the seven minutes between two slices was almost unbearably long and I could not stop going before the dawn of morning.

Once all data was captured it still took a significant period of time and the motivated helping hands of Gabriel Ribeiro Dos Santos to finalize the datasets in preparation of publication and to overcome many small challenges in the reconstruction, segmentation, 3D modeling and presentation of the data. At this point in time, all contributors were dedicated to publishing the datasets in full to enable the scientific community to work with the raw data or final result as suitable. We were more than happy that one of the most prestigious Open Data journals accepted our work.

Finally, the time had come to integrate OpenEar datasets into the Visible Ear Simulator. But it soon became clear that while much time had been spent to create the "truest" possible digital representation of the temporal bone specimen, a real time computer-based simulation of ear surgery had additional and sometimes competing requirements. Finding a good compromise between maintaining an adequate digital representation of the original specimen while achieving a visually appealing and stable simulation resembling temporal bone dissection ultimately required active participation of a physician (Mads), a software engineer (Peter Trier) and the data originator (myself). We are happy and proud that as a result, Visible Ear Simulator 3.5 features six new anatomies from OpenEar.

After more than five years of interdisciplinary work of a fantastic team of experts, we've been able to deliver on the promise of taking high-fidelity modeling of the human temporal bone for virtual reality surgical training to a new level which will hopefully extend the possibilities of surgical simulation in our field worldwide. I feel deeply grateful for the fantastic experiences during this time, for everything I've learned and for being allowed to contribute to this fascinating technology.

Introduction

The evolution of surgical training and education has been closely linked to the history of the art of surgery itself. Surprisingly from today's perspective, the Hippocratic oath in its ancient form explicitly forbade physicians to operate on their patients. [1] So surgeons and surgery were historically considered separate from medicine for ages, and the history of training of surgeons reflects this. [2] While training of physicians was provided within the infrastructure of academic settings relatively early, surgery was considered a craft and training of surgeons was hence provided in the form of apprenticeships for ages. The concept of apprenticeships is still deeply rooted in training of surgeons until today, with senior physicians highly invested and actively involved in advancing the education of their assigned residents. [2] With its pivotal teaching paradigm of "See one, do one, teach one" the apprenticeship concept is considered the most successful mechanism for knowledge transfer until today and has proven to work, in that most surgeons today are a product of this system and performing surgery in a successful way. [3] In recent years however, educational aspects of surgical residency have come under rising pressure in many clinics as per work-hour restrictions and an increasing economization of surgical time, leaving senior surgeons with less opportunity to pass on their knowledge to the next generation. [2,3]

Surgical simulation can be very useful in this context, as it gives trainees the opportunity to learn certain aspects of surgery on their own, allowing them to use the valuable time with their mentors more efficiently. [4] While surgical simulation reaches back to the first documented surgical procedure in ancient India 600 BC where leaf and clay models were used to simulate nasal reconstruction, in modern times simulators based on computer technology have seen a distinct rise in interest during the last three decades. [5] Numerous simulator systems have been developed for a wide range of surgical procedures and many parts of the human body. These simulators offer the advantage of allowing distributed surgical training opportunities outside of working hours and eventually even away from the healthcare facility. [6] They offer an environment in which trainees have an infinite number of attempts in an environment in which it is safe to fail and try out things which would be unethical to try in patients. [2] Offering such a stress-free environment and being able to gradually increase the complexity of training reduces cognitive load and could make learning more efficient. [7] Gamification and competitive elements can be used to boost the engagement of residents in simulation training. [8] As a consequence of these advantages, surgical simulation centers have been established in some clinics. [9]

When it comes to simulating surgery of the human temporal bone -representing a particularly challenging anatomical area- several training options have been established over the years. While the most prominent simulation of ear surgery used is obviously training in cadaveric specimen, such

specimens have become a scarce and precious resource. [10] To overcome this scarcity, artificial temporal bone models from 3D plastics printing techniques have been established and allow simulation with good physical realism despite some need for perfecting the materials and anatomical accuracy. [11] Several virtual reality surgical simulators providing immersive training environments with the help of advanced computer graphics and haptic force feedback instruments have been introduced as further alternatives to cadaveric specimen. The Voxel-Man™ is the only commercially available system today [12] and comes with a complete hardware system including two haptic force-feedback devices and a 3D screen. Several temporal bone simulators are developed in academic environments at Stanford [13], Ohio State University [14] and Melbourne University [15] but are not available publicly. Finally, The Visible Ear Simulator (VES) [16] is a simulation system, which is available as an academic freeware allowing (but also requiring) users to obtain hardware from third party suppliers. It has been one of the most far developed systems in the field and is different from beforementioned simulators in that it is not based on computed tomography type images, but on the sophisticated Visible Ear cryosection dataset [17] of a human temporal bone including soft tissue structures. VES is therefore providing a higher fidelity anatomy model underlying the surgical simulation compared to other simulators and has demonstrated to be a valid training tool boosting the mastoidectomy performance in otorhinolaryngology residents [4]. Unfortunately, high-fidelity data of the human temporal bone such as the Visible Ear dataset is not widely available and in fact, the Visible Ear remained the only such dataset for more than fifteen years. This means that while VES allowed a higher simulation quality when compared to other simulators, it had the disadvantage that training was limited to repeating the same training scenario over and over.

This was identified as a potentially limiting factor for the simulator as it has been suggested in the field of motor skill learning that variable tasks practice could provide even better training when compared to constant task practice. [18] So, while repetition is an important concept in learning, adding variability to the practice task may improve generalization and transfer to novel tasks. [19] Interestingly, while novice residents showed a steep initial learning curve when using Visible Ear Simulator, studies revealed a plateau in the mean performance around the nineth repetition [20], and it could be discussed whether one aspect of this plateau effect is that constant repetition of the same scenario just yields no further learning effect beyond a certain point.

The goal of this dissertation was to develop an efficient novel method enabling the creation of a whole library of high-fidelity digital models of the human temporal bone as well as the implementation and validation of these models in the Visible Ear Simulator. As the imaging modalities used previously in model creation for otologic simulators all had their advantages and disadvantages, we decided to try combining the advantages of each imaging modality to achieve the fidelity needed to provide an

optimal simulation experience while keeping the effort for the creation of new models at a level yielding sufficient training scenarios. The implementation into the virtual reality simulator was seen foremost as a software engineering task, but it was clear that a considerable effort should be put into validating the virtual dissection experience and eliminate any artefacts in the original data which could falsify simulation.

The results of the research performed within this dissertation are documented in two peer reviewed journal publications in which the candidate was the first and corresponding author:

The first publication in *Nature Scientific Data* [21] describes the novel process of digitizing temporal bones including processing of cadaveric specimen, multimodal imaging of these specimen and subsequent reconstruction, registration and segmentation of resulting datasets including a description of process errors and limitations. A description of how to access and use the raw data from the experiments as well as all results thereof is given as per the open data nature of this publication.

The second aspect of this work - integration into the virtual reality simulator system- was published in *Otology & Neurotology* [22] and describes data requirements for implementation in the simulator, technical details regarding the implementation, postprocessing steps to increase realism of the simulation as well as learnings from our research which should be considered when using clinical imaging for patient-specific simulation and planning.

Nature Scientific Data: The OpenEar library of 3D models of the human temporal bone based on computed tomography and micro-slicing

Submitted: 30 August 2018

Accepted: 8 November 2018

Published: 8 January 2019

SCIENTIFIC DATA

OPEN

Data Descriptor: The OpenEar library of 3D models of the human temporal bone based on computed tomography and micro-slicing

Received: 30 August 2018
Accepted: 8 November 2018
Published: 8 January 2019

Daniel Sieber[1], Peter Erfurt[2], Samuel John[3], Gabriel Ribeiro Dos Santos[1], Daniel Schurzig[1], Mads Sølvsten Sørensen[4] & Thomas Lenarz[2]

Virtual reality surgical simulation of temporal bone surgery requires digitized models of the full anatomical region in high quality and colour information to allow realistic texturization. Existing datasets which are usually based on microCT imaging are unable to fulfil these requirements as per the limited specimen size, and lack of colour information. The OpenEar Dataset provides a library consisting of eight three-dimensional models of the human temporal bone to enable surgical training including colour data. Each dataset is based on a combination of multimodal imaging including Cone Beam Computed Tomography (CBCT) and micro-slicing. 3D reconstruction of micro-slicing images and subsequent registration to CBCT images allowed for relatively efficient multimodal segmentation of inner ear compartments, middle ear bones, tympanic membrane, relevant nerve structures, blood vessels and the temporal bone. Raw data from the experiment as well as voxel data and triangulated models from the segmentation are provided in full for use in surgical simulators or any other application which relies on high quality models of the human temporal bone.

Design Type(s)	modeling and simulation objective • replicate design • source-based data transformation objective
Measurement Type(s)	3D structure determination assay • histological assay
Technology Type(s)	Cone-Beam Computed Tomography • optical microscope
Factor Type(s)	
Sample Characteristic(s)	Homo sapiens • ear

[1]MED-EL Elektromedizinische Geräte GesmbH, Innsbruck, Austria. [2]Hannover Medical School, Dept. Otorhinolaryngology, Hannover Germany. [3]Hörsys GmbH, Hannover, Germany. [4]Rigshospitalet, University of Copenhagen, Copenhagen, Denmark. Correspondence and requests for materials should be addressed to D.S. (email: daniel.sieber@medel.com)

Background & Summary

Surgical interventions to treat hearing disorders, including hearing implants such as cochlear implants, middle ear implants or bone conduction implants require profound knowledge of the anatomy of the human temporal bone[1]. The level of experience of surgeons is therefore crucial to ensure optimal outcomes and low complication rates, necessitating extensive surgical training in preparation for ear surgery[2]. Until now, surgical training typically takes place in the operation theatres[3] and in temporal bone laboratories, where surgeons are enabled to practice identification of anatomical landmarks on human cadaveric specimen[4,5]. However, in many places it has become increasingly difficult to obtain a sufficient number of temporal bones due to lack of availability because of ethical, cultural, regulatory and/or financial reasons[6]. This situation led to the development of alternative training options such as artificial temporal bones from polymer materials[7–14] or computer based surgical simulators, where haptic feedback devices are used in combination with advanced computer graphics to create a virtual reality training environment[15–19]. None of the mentioned systems is meant to entirely replace working with cadaveric specimen, but all of them offer a hazard free training environment which has the potential to be very effective in training surgeons at relatively low running costs. In fact, computer based surgical simulation allows the user to repeat procedures as often as desired while adding a new level of motivation for training by giving interactive feedback to the trainee. Recent studies[20–23] have been able to demonstrate that with just two hours of self-directed simulator training a significant improvement of temporal bone dissection abilities measured in cadaveric specimen can be demonstrated in entry level surgeons.

Most of the currently available simulation systems are limited by the fact that they are based on low-quality datasets. Those datasets are acquired by Computed Tomography (CT) which results in low detail models and lack of information on soft tissue structures such as membranes. micro CT imaging-based data might be able to overcome the lack of details, however current Micro CT machines only allow scanning of small specimen and it is therefore impossible to model a sufficiently big portion of the anatomy for surgical simulation. For both CT and micro CT based datasets there is no colour information available and so texturing of models for simulation is performed manually resulting in quite unnatural colouring. The Visible Ear Simulator (VES) freeware[19] available at https://ves.alexandra.dk is currently the only simulator providing higher fidelity simulation as it is based on naturally coloured cryosection data[24] and 3D rendered at 125 voxels/mm^3. On the other hand, as the creation and processing of cryosection data is extremely laborious, over more than ten years the VES has been limited to only one anatomy which limits the learning experience by neglecting the significant learning potential of inter individual variability of anatomy[25–27].

The aim of the OpenEar project was therefore to develop a new approach and method which allows for much more efficient creation of high fidelity coloured models of the human temporal bone. Such an efficient method was found in the combination of imaging using ionizing radiation and micro-slicing of cadaveric human temporal bone specimens. Both imaging modalities were three dimensionally reconstructed, registered and segmented. An overview of all process steps is provided in Fig. 1. As a result, raster/voxel imaging data of eight digitized human temporal bones is provided, including segmentations of all relevant anatomical structures and triangulated 3D models thereof. The entire dataset is provided to the public in full to allow for surgical training or research relying on high-quality models of the human ear such as navigated/robotic surgery, development of automated segmentation algorithms and finite-element simulations of the middle and inner ear mechanics.

The OpenEar represents a valuable addition to the datasets which had previously been available to the field of surgical simulation. Compared to datasets created using clinical CT imaging, the OpenEar dataset provides a much higher level of detail, particularly when it comes to delicate soft tissue structures such as the tympanic membrane or basilar membrane. In contrast to datasets based on micro CT imaging, the OpenEar dataset is able to provide a sufficient model size to cover all aspects of middle and inner ear surgery and comparable to temporal bone specimen used in clinical education courses.

Like the Visible Ear dataset, the OpenEar dataset provides high fidelity volumetric geometry data including colour information which enables surgical simulators to be textured based on the actual colours of the anatomical specimen. This allows to overcome the need to rely on manual false colour texturing used in simulations based on data from CT/micro CT imaging. The Visible Ear dataset continues to provide an excellent quality temporal bone model for surgical simulation, while the OpenEar dataset enriches the learning experience by introducing the significant factor of anatomical variation in eight unique human ears.

Methods

Eight fresh human temporal bone specimens from four adult subjects were used to create this dataset. Temporal bones were kindly donated by the Institute of Pathology of the Hannover Medical School. They were obtained from patients who contributed their corpses to medical education and research. As the specimens were used anonymously, no approval by the institutional ethical board was necessary.

Specimen Preparation

Specimens were scanned using a 3D ACCUITOMO 170 Digital Cone Beam Computed Tomography (CBCT) scanner (J. MORITA TOKYO MFG. CORP., Japan) within a period of one hour after specimen

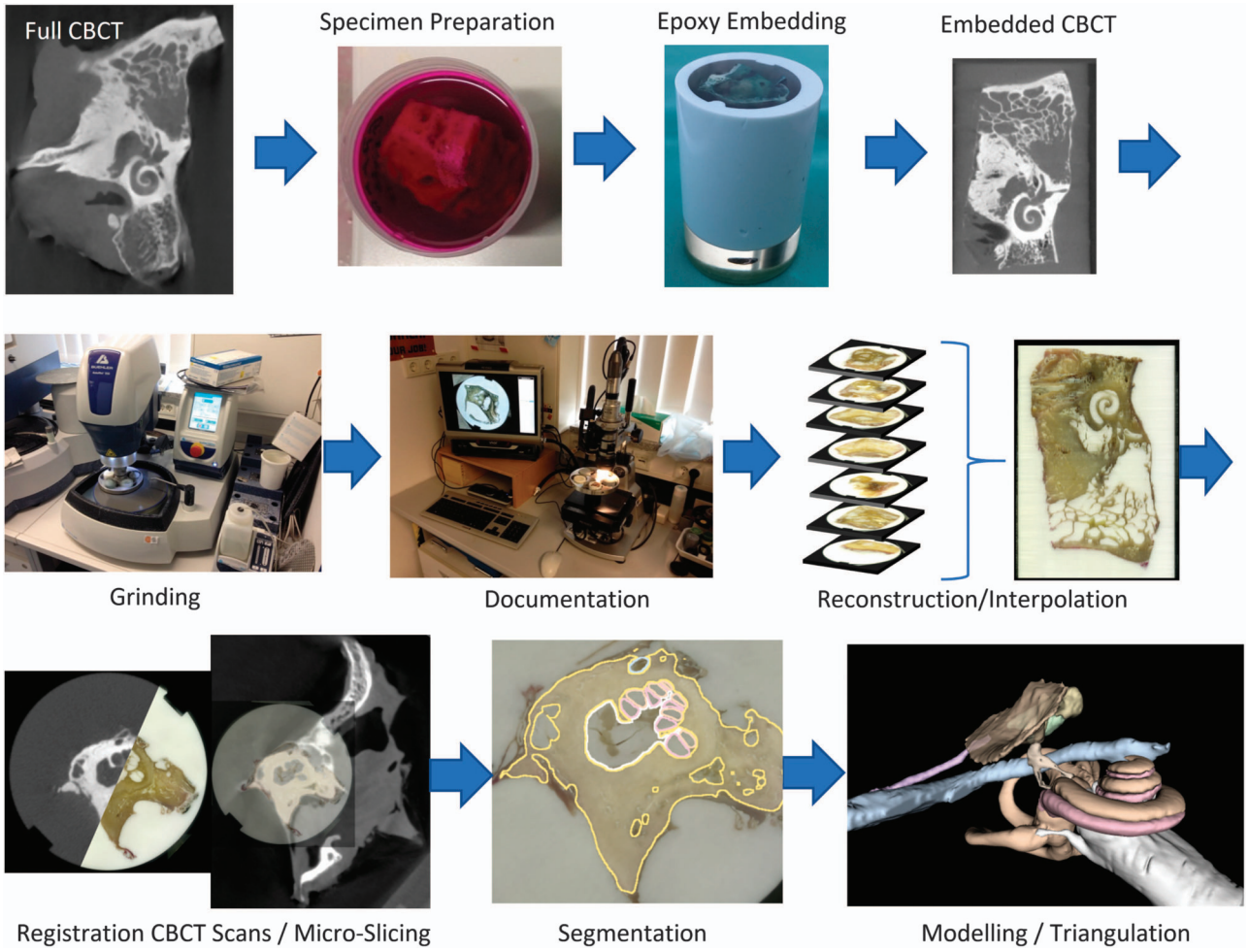

Figure 1. **Overview of processes used in creation of the OpenEar Dataset.**

sampling. Resulting CT images were reconstructed and exported as DICOM using the i-Dixel software (J. MORITA TOKYO MFG. CORP., Japan) with a voxel size of 0.250 mm.

After CBCT imaging, specimens were cut to fit an embedding mould and fully immersed in a fixation solution of 4% Formol in phosphate buffered saline (PBS). To allow for better penetration of the fixation solution and further process fluids into the inner ear lumina, a small opening was drilled into the superior semi-circular canal, and fixation solution was applied to the superior semi-circular canal using a syringe and cannula to optimally fix the intracochlear structures. After 72 h of storage in the fixation solution, specimens were rinsed in PBS to remove Formol from the specimens. The specimens were dehydrated in four steps by sequential immersion in 70, 90 and 100% Ethanol and afterwards 100% Methanol for 2 days each. For improved contrast of the soft tissue structures against the embedding epoxy, 0.1% Acid Fuchsin was added during the Ethanol steps. Afterwards, specimens were dried at room temperature in a fume hood for about one hour. Finally, the specimens were embedded in epoxy resin (SPECI-FIX 40, STRUERS, Denmark) to immobilize and preserve any mobile structures inside the temporal bone like membranes or the ossicular chain during further process steps. To improve penetration of the epoxy resin into the smaller lumina of the temporal bone, the embedded specimens were put in a vacuum desiccator. Embedded specimens were cured at room temperature for at least 7 days before continuing with further process steps.

After embedding, all specimens were scanned again using CBCT, to also capture the outer geometry of the epoxy overmould to be used for referencing the different imaging modalities. Scanning mode was set to 'HiRes' this time, scanning parameters were set to 80 kV tube voltage, 2 mA tube current, 360° scanning angle and 60x60mm Field of View (FOV). Reconstruction and DICOM export were performed in the same manner as before mentioned, but at a 0.125 mm voxel size.

Micro-Slicing

Micro-slicing was performed by sequential grinding and microscopic documentation of the specimens. Grinding was performed using an AutoMet250 Grinder-Polisher (BUEHLER, Lake Bluff, IL, USA)

Segment	Micro-Slicing	CBCT Embedded Specimen	CBCT Full Specimen
Scala Tympani/Vestibuli	X	X	
Malleus/Incus/Stapes		X	
Facial Nerve/Chorda		X	
Tympanic Membrane/EAC	X		X
Sinus/Carotis Interna			X
Bone			X

Table 1. Image modality used for segmentation of different anatomical structures.

equipped with silicon carbide (SIC) grinding paper with a Grit of P 800. After each removal, the novel layer was documented using a VHX-2000 measurement microscope (KEYENCE Corporation, Osaka, Japan) equipped with a VH-Z20UR zoom lens at 20x magnification mode using image stitching functionality. The effective removal was determined by measuring the height of the remaining overmould using a micrometre gauge.

Alignment of the images from micro-slicing as a prerequisite step for reconstruction of the image stack, was performed by custom made software using Python scripting and the packages of the Anaconda collection (Continuum Analytics, Austin, TX, US). A template matching technique was implemented to align the images along the overmould outline which served as reference geometry due to its relative invariance across images. A brute force search approach was first used to find the approximate translation and rotation of the overmould outline in the image, followed by a local optimization method to find the best translation, rotation, shear and scale of the overmould in the image.

Due to the relatively large size of the images (~3700 × 3700 pixels) the computational effort to perform such operation makes it unattractive to perform the computation on the central processing units (CPUs) of modern personal computers. Instead it was decided to implement the described operation on a graphics processing unit (GPU) which allows for a massive parallelization of the required computations.

Reconstruction/Registration

The slice thickness in histological sections is inhomogeneous as per the unavoidable technical tolerances of the used grinding process. To be able to use the acquired images with existing software for processing of medical three-dimensional images, slices had to be homogenized. The aligned images were therefore interpolated to a homogeneous slice thickness of 150 µm using a virtual image stack. The original images were put on the positions in the virtual image stack, which came closest to their original position to keep interpolation related losses in image quality minimal. Those positions in the stack which did not have an original image assigned to them, were then linearly interpolated between the nearest neighbouring original images.

Reconstruction of the micro-slicing image stack was performed using 3D Slicer 4.8.0 (http://www.slicer.org). The data from CBCT imaging was also imported into 3D Slicer as DICOM series. After a rough manual alignment of the high-resolution embedded CBCT scan with the micro-slicing images, 3D Slicer's built-in BRAINSfit algorithm was used to automatically register both imaging modalities. In a second step, the low-resolution, larger CBCT scan of the unembedded temporal bone was registered to the high-resolution CBCT scan using a manual landmark-based registration, followed by the automatic BRAINSfit registration algorithm. After completion of the two registrations mentioned, it became possible to display all three imaging modalities, the large portion low-resolution CBCT, the high resolution embedded CBCT and the reconstructed micro-slicing data aligned in parallel.

Segmentation

A threshold supported manual paint segmentation technique was chosen for segmentation of the datasets using 3D Slicer. Small structures were segmented using the high resolution embedded CBCT dataset to have access to the best possible image quality. Larger structures were segmented using the larger low resolution unembedded CBCT scan to be able to model the biggest possible portion of the temporal bone. Multimodal overlay visualization was utilized in those anatomic structures which are partially delimited by bony structures and partially by soft tissue structures. Table 1 gives an overview of the anatomical structures and imaging modalities used for segmentation of these structures.

3D Surface Model Creation

Segmented volumes were converted to three-dimensional triangulated surface models of all anatomical structures. The bone segment was additionally exported as a voxel model as per the requirements of surgical simulators. Triangulation was performed in 3D Slicer and included moderate smoothing during model creation. Finally, the mesh quality and complexity were optimized using free software tools Graphite, Meshlab and Meshmixer (Autodesk, San Rafael, CA, USA).

Step-by-Step Process Descriptions

Further details on the processes used to create the OpenEar dataset including step-by-step description of all process steps are included in Supplementary File 1 of this Data Descriptor.

Code Availability

All custom-made software which was created to align and interpolate micro-slicing data is available in full and without restrictions at the Zenodo open access research data repository[28,29].

All software tools used for the postprocessing of image data are either freeware or Open Source where code can be accessed via the individual software project websites.

3D Slicer is available at https://www.slicer.org/

Meshlab is available at http://www.meshlab.net/

Graphite is available at http://alice.loria.fr/software/graphite/

Meshmixer is available at http://www.meshmixer.com/

Data Records

As a result of the described process we are able to provide three-dimensionally reconstructed, co-registered sets of CBCT scans and micro-slicing colour images of the human temporal bone. Eight digitized human temporal bones were uploaded to the Zenodo open access research data repository and are available for download free of charge through a permanent Digital Object Identifier (DOI) (Data Citation 1). They may be shared, used and adapted even for commercial use with the requirement of attributing to this original work as per a Creative Commons Attribution 4.0 License.

Volume datasets from all imaging modalities performed in this project are provided as 3D Nearly Raw Raster Data (NRRD) images in the final data processing stage. CBCT images are provided as isotropic voxel data at a resolution of 125 µm. To allow access to the higher in-plane resolution of those images, micro-slicing data is provided at an inhomogeneous $50 \times 50 \times 150$ µm voxel resolution. Coordinate directions are invariant across all imaging modalities provided. Additionally, all raw data from the experiment, including CT scans in DICOM format and micro-slicing images stored as TIFF files are provided to enable the community to work with the original data and eventually improve the above described reconstruction, registration and segmentation processes.

Segmentations of scala tympani, scala vestibuli, malleus, incus, stapes, facial nerve, chorda tympani, tympanic membrane, external auditory canal, sigmoid sinus and dura, carotid artery and bone are provided at a 125 µm isotropic voxel resolution as 3D NRRD images and can be viewed with any of the co-registered imaging modalities in the background. Additionally, triangulated models of those segments are provided with an optimized mesh quality using about 70 vertices/mm^2 surface area in Polygon File Format (PLY) format which can also easily be converted to the common STL file format using 3D Slicer (e.g. for 3D printing).

The data repository contains a compressed subfolder for each of the datasets labelled with the specimen identifier. The eight temporal bone datasets were labelled Alpha, Beta, Gamma, Delta, Epsilon, Zeta, Eta and Theta. The compressed subfolder for each specimen contains the data as described in Table 2.

Technical Validation

The numerical representation of the human temporal bone provided in this work is limited by its nature to only be able reproduce the colour and structures found in temporal bone specimens ex-vivo and post-mortem. These may differ from the colours and structures found intraoperatively in patients in-vivo, despite all efforts to process specimen immediately after becoming available.

Furthermore, several of the process steps in the creation of data may result in certain technical inaccuracies:

- Dehydration of specimens during preparation for embedding may result in shrinkage of certain soft tissue structures in the embedded datasets. E.g. the facial nerve may shrink and no longer fill out its bony canal entirely
- Mechanical forces applied for fixation of the embedded specimens in the grinding machine holder may result in geometric deformations of the specimens in the micro-slicing data
- The stitching of images as performed with the optical microscope may lead to minor inaccuracies in the optical image acquisition in the micro-slicing data
- The measurement of remaining overmould height after each grinding step in micro-slicing involves a certain measurement error particularly in a somewhat elastic specimen
- 3D Reconstruction of the micro-slicing data relies on algorithmic identification of the outline of the specimens embedding as well as the overmould height measurement determining the position of each slice in the image stack. Above mentioned inaccuracies in the experimental setup as well as numerical errors may result in reconstruction inaccuracies.
- Interpolation of the reconstructed micro slicing data to create a homogeneously spaced image stack may result in certain image artefacts.
- Registration of the micro-slicing and computed tomography images is based on the identical accurate imaging representation in both modalities. As per the above described inaccuracies of both the 3D micro-slicing and CT image modalities, as well as due to numerical errors in the registration process, inaccuracies may occur.

Steps	Description of files	File format
CBCT Unembedded	Folders containing DICOM series of files representing a CBCT scan of the unembedded temporal bone specimen right after specimen sampling (not available for ALPHA and BETA)	DICOM (.dcm)
CBCT Embedded	Folders containing DICOM series of files representing a CBCT scan of the specimen after cutting, dying, drying and embedding into the epoxy overmould	DICOM (.dcm)
Microslicing Raw	Series of images from micro-slicing grinding process, each image documents the embedded specimen after removal of material using the grinding machine	TIFF (.tiff)
Reconstruction Microslicing	3D reconstructed colour datasets from micro-slicing after alignment of slices and interpolation to a homogenous spaced image stack as volumetric voxel data Transformations: Comma separated value table where each row contains the nine entries of a 3x3 transformation matrix of one micro-slicing image from the stack in C-like/row-major order	NRRD (.nrrd) CSV (.csv)
	Materials for Reconstruction: Target images containing the outline of the epoxy overmould used for alignment of the images from micro-slicing Layer Positions: Comma separated value table with the information on the position of each micro-slicing image in the stack as described by its distance to the initial slices	GIMP/PNG/SVG (.xcf)/(.png)/(.svg) CSV (.csv)
Registred Slicer Volumes	3D reconstructed grayscale datasets from CBCT @ 125 µm resolution as volumetric voxel data • CBCT_Unembedded: Unembedded CBCT registered to align with micro-slicing • CBCT_Embedded: Embedded CBCT registered to align with micro-slicing, resized to the coordinate space size of the unembedded CBCT	NRRD (.nrrd) NRRD (.nrrd)
	Transformations: Transformation matrices used to register datasets to each other Accuracy assessment: (not available for ETA) Meshlab screenshot of the Hausdorff analysis Text file with results from geometric and volumetric analysis 3D Slicer segmentation file delineating overmould in CBCT and micro-slicing	.H5 (.h5) PNG (.png) TXT (.txt) NRRD (.nrrd)
Segmentation	3D Slicer segmentation file assigning voxels of the registred CBCT volumes to one of the anatomical structures delineated	NRRD (.nrrd)
3D Models	Triangulated, smoothed 3D models of all anatomical structures as segmented in 3D Slicer after mesh quality optimization @ ~70 vertices / mm^2 Bone volume as volumetric voxel data	PLY (.ply) NRRD (.nrrd)

Table 2. Data content per compressed specimen subfolder (e.g. Alpha).

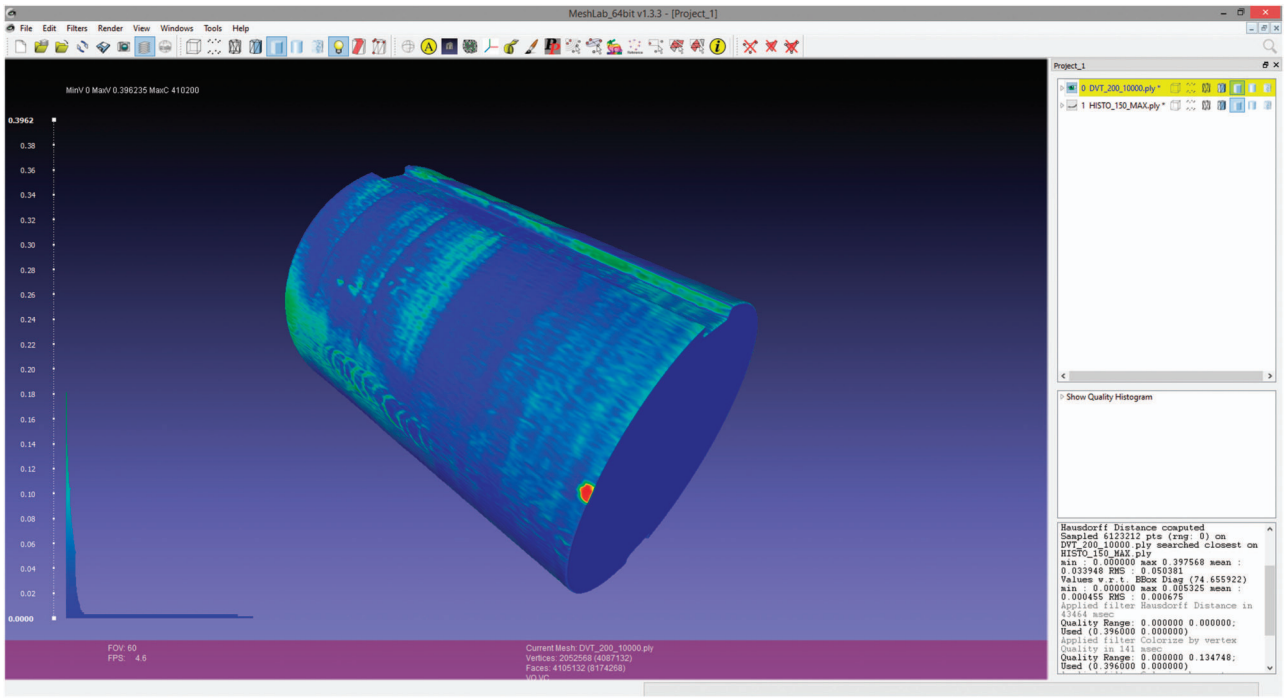

Figure 2. Visualization of differences between CBCT and micro-slicing data for the Zeta dataset using the Meshlab Hausdorff distance analysis.

Regarding the computed tomography imaging, Lund *et al.*[30] found that the accuracy of the ACCUITOMO CBCT device used in this experiment can be assumed to be below the voxel size of 0.125 mm.

Quantification of the overall accuracy of the micro-slicing data proves more difficult due to the high number of interconnected process steps and influencing factors, and the possible inhomogeneity of inaccuracies within the volume. A comparison of volumetric and geometric properties of the final product from acquisition, reconstruction and registration of micro-slicing with the CBCT as reference

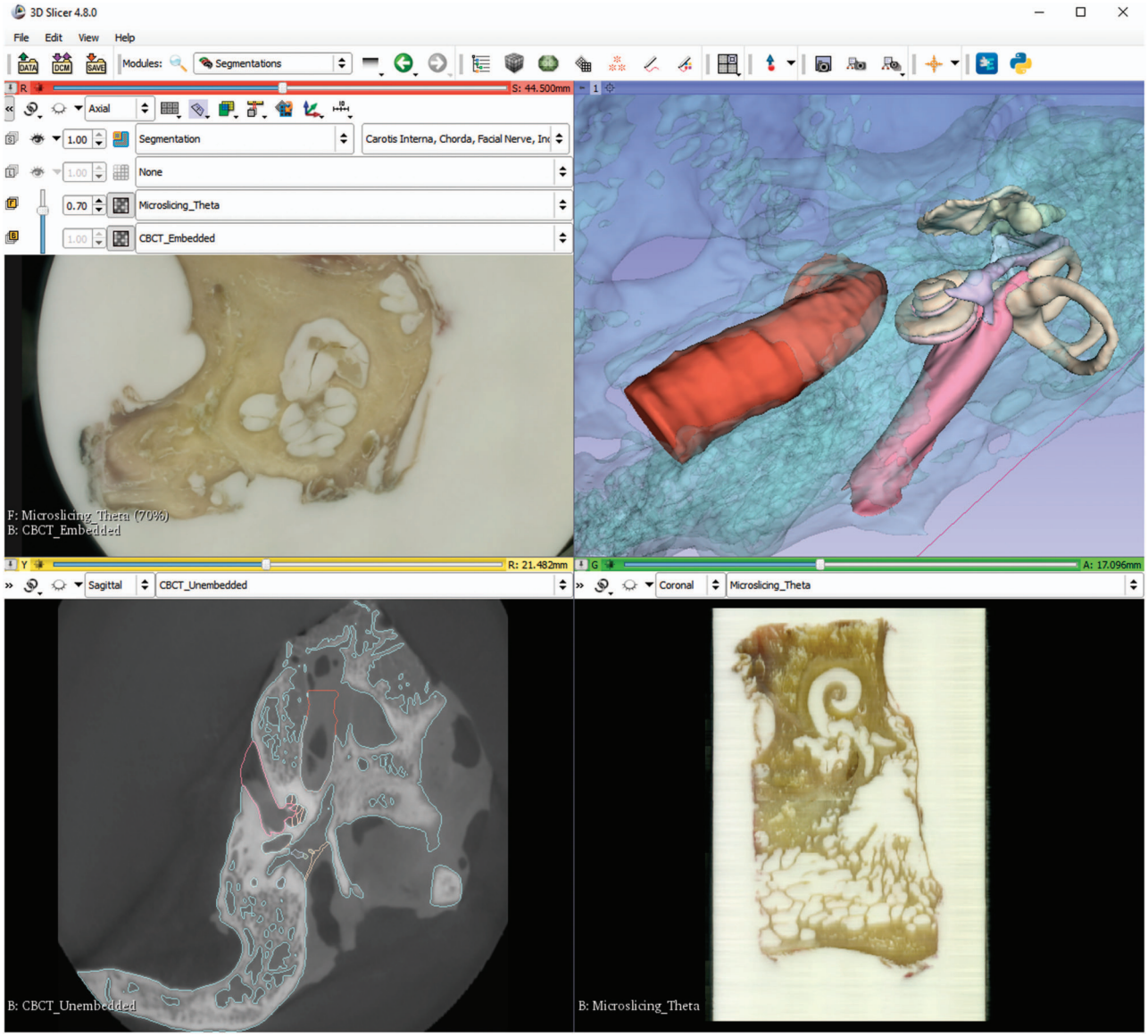

Figure 3. 3D Slicer visualization of different imaging modalities of the Theta dataset. (**a**) Image fusion slice with 30% CBCT and 70% micro-slicing. (**b**) Three-dimensional reconstruction of anatomical segments from delineation. (**c**) CBCT slice with anatomy segmentation delineation overlay. (**d**) Reconstructed slice from micro-slicing.

was chosen as most viable option. Threshold based segmentations of the epoxy overmould outline in the CBCT and micro-slicing modalities were analytically compared using the Meshlab Hausdorff distance filter[31] yielding the mean and maximum geometric error between CBCT and micro-slicing. Figure 2 exemplary shows the visualization of the Hausdorff distance analysis and histogram of error for one dataset. The Meshlab Compute Geometric Measures function allowed for the calculation of the volumetric error of the micro-slicing image related to the CBCT images. Colour coded is the distance between the surface of reconstructed overmold geometry from micro-slicing and CBCT imaging. Visible error/deformations of the epoxy overmold include e.g. screw indentations from mounting the specimen in the grinding machine holder in different positions.

Results for the geometric and volumetric errors for each of the datasets are summarized in Table 3. The described analysis could unfortunately not be performed for dataset Eta, due to an artefact in the CBCT acquisition which made segmenting the overmould outline impossible.

High fidelity surgical simulators currently operate at a voxel resolution of about 125 voxels/mm^3[19] and a corresponding isotropic pixel size of about 200 µm. The above described accuracies of the CBCT and the micro-slicing datasets are therefore considered to be acceptable as they lie within the pixel resolution of the computer simulation which they were primarily created for. However, the OpenEar dataset may be limited for applications requiring higher levels of detail and accuracy such as e.g. cochlear microanatomy.

Dataset	Geometric error [mm]		Volumetric error [%]
	Mean	Max	
Alpha	0.064	0.736	0.349
Beta	0.090	0.951	0.929
Gamma	0.082	0.734	0.753
Delta	0.087	0.627	0.646
Epsilon	0.056	0.529	0.296
Zeta	0.034	0.398	0.370
Eta	—	—	—
Theta	0.043	0.288	0.128

Table 3. Geometric and volumetric error for datasets of the OpenEar library.

Usage Notes

The OpenEar datasets allow for an entirely new view on the anatomy of the human temporal bone. The co-registration of reconstructed CBCT and micro-slicing data allows for viewing two-dimensional slices of the ear seamless and/or simultaneous in radiation based and optical modalities. When looking at a mid-modiolar section of the inner ear, for instance, the CBCT image will give the viewer a solid understanding of where the bony constraints of the inner ear space are located and allow for semi-automatic threshold-based segmentation techniques. Being able to amend or change to the information from the micro-slicing images, on the other hand, allows for a more complete picture and more precise segmentations as also soft tissue structures like e.g. the basilar membrane or tympanic membrane can easily be located.

For viewing of the data, 3D Slicer is the recommended free software package which was also used during the creation of the datasets, however there are numerous software options to work with TIFF, DICOM or NRRD data which may be considered.

When using 3D Slicer to work with the datasets, it is recommended to load the reconstructed micro-slicing dataset, as well as the registered 3D Slicer volumes of the CBCT unembedded and embedded specimen and the segmentation file. Figure 3 shows how to use the 'Slice Viewer' controls, to view two image volumes simultaneously as foreground and background layer, as well as the segmentation overlay and 3D representation of the geometric segmentation.

References

1. Gulya, A. J., Minor, L. B., Glasscock, M. E. & Poe, D. *Glasscock-Shambaugh Surgery of the Ear*. (People's Medical Publishing House, 2010).
2. Wiet, G. J., Sørensen, M. S. & Andersen, S. A. W. Otologic skills training. *Otolaryngol Clin North Am* **50**(5), 933–945 (2017).
3. Geibel, J. & Longo, W. Evolution of surgical skills training. *World J Gastroenterol* **12**(20), 3219–3224 (2006).
4. Mowry, S. E. & Hansen, M. R. Resident participation in cadaveric temporal bone dissection correlates with improved performance on a standardized skill assessment instrument. *Otol Neurotol.* **35,** 77–83 (2014).
5. Awad, Z., Tornari, C., Ahmed, S. & Tolley, N. S. Construct validity of cadaveric temporal bones for training and assessment in mastoidectomy. *Laryngoscope* **125,** 2376–2381 (2015).
6. Frithioff, A., Sørensen, M. S. & Andersen, S. A. W. European status on temporal bone training: a questionnaire study. *Eur Arch Otorhinolaryngol* **275**(2), 357–363 (2018).
7. Begall, K. & Vorwerk, U. Artificial petrous bone produced by stereolithography for microsurgical dissection exercises. *ORL* **60,** 241–245 (1998).
8. Suzuki, M. *et al.* Rapid prototyping of temporal bone for surgical training and medical education. *Acta Otolaryngol.* **124,** 400–402 (2004).
9. Bakhos, D., Velut, S., Robier, A., Al Zahrani, M. & Lescanne, E. Three-dimensional modeling of the temporal bone for surgical training. *Otol Neurotol.* **31**(2), 328–334 (2010).
10. Röösli, C., Hoon Sim, J., Möckel, H., Mokosch, M. & Probst, R. An Artificial Temporal Bone as a Training Tool for Cochlear Implantation. *Otology&Neurotology* **34**(6), 1048–1051 (2013).
11. ENT Surgery/Temporal Bone Archive*Phacon Company Website* https://www.phacon.de/en/produkt-kategorie/ent-surgery/temporal-bone/ (2018).
12. Awad, Z. *et al.* Feasibility of a synthetic temporal bone for training in mastoidectomy: face, content and concurrent validity. *Otol Neurotol.* **35,** 1813–1818 (2014).
13. Mowry, S. A., Jammal, H., Myer, C., Solares, C.A. & Weinberger, P. A novel bone simulation model using 3d printing techniques. *Otol Neurotol.* **36,** 1562–1565 (2015).
14. Takahashi, K. *et al.* Creating an optimal 3d printed model for temporal bone dissection training. *Ann Otol Rhinol Laryngol* **126** (7), 530–536 (2017).
15. Pflesser, B., Petersik, A., Tiede, U., Höhne, K. H. & Leuwer, R. Volume cutting for virtualpetrous bone surgery. *Comput Aided Surg* **7**(2), 74–83 (2002).
16. Wiet, G. J. *et al.* Virtual temporal bone dissection: an interactive surgical simulator. *Otolaryngol Head Neck Surg* **127,** 79–83 (2002).
17. Morris, D. & Blevins, N. H. Visuohaptic simulation of bone surgery for training and evaluation. *IEEE Comput Graph Appl* **26,** 48–57 (2006).
18. O'Leary, S. J. *et al.* Validation of a networked virtual reality simulation of temporal bone surgery. *Laryngoscope* **118,** 1040–1046 (2008).

19. Soerensen, M. S., Mosegaard, J. & Trier, P. The Visible Ear Simulator: A Public PC Application for GPU-Accelerated Haptic 3D Simulation of Ear Surgery Based on the Visible Ear Data. *Otol Neurotol.* **30,** 484–487 (2009).
20. Zhao, Y. C., Kennedy, G., Yukawa, K., Pyman, B. & O'Leary, S. Improving temporal bone dissection using self-directed virtual reality simulations: results of a randomized blinded control trial. *Otolaryngol Head Neck Surg* **144**(3)**,** 357–364 (2011).
21. Francis, H. W. *et al.* Technical skills improve after practice on a virtual-reality temporal bone simulator. *Laryngoscope* **122,** 1385–1391 (2012).
22. Wiet, G. J. *et al.* Virtual temporal bone dissection system: development and testing. *Laryngoscope* **122,** S1–S12 (2012).
23. Andersen, S. A. W., Foghsgaard, S., Konge, L., Cayé-Thomasen, P. & Soerensen, M. S. The Effect of Self-Directed Virtual Reality Simulation on Dissection Training Performance in Mastoidectomy. *Laryngoscope* **126,** 1883–1888 (2016).
24. Soerensen, M. S. The Visible Ear: A Digital Image Library of the Temporal Bone. *ORL* **64,** 378–381 (2002).
25. Tolsdorff, B. *et al.* Individual models for virtual bone drilling in mastoid surgery. *Comput Aided Surg* **14,** 21–27 (2009).
26. Wiet, G. J., Schmalbrock, P., Powell, K. & Stredney, D. Use of ultra-high-resolution data for temporal bone dissection simulation. *Otolaryngol Head Neck Surg* **133,** 911–915 (2005).
27. Arora, A. *et al.* Virtual reality case-specific rehearsal in temporal bone surgery: a preliminary evaluation. *Int J Surg* **12,** 141–145 (2014).
28. John, S. & Sieber, D. M. Source code for: reconstruct_volume_from_RGB_slices. *Zenodo* https://doi.org/10.5281/zenodo.1344923 (2018).
29. John, S. Source code for: pattern_finder_gpu. *Zenodo* https://doi.org/10.5281/zenodo.1400785 (2018).
30. Lund, H., Gröndahl, K. & Gröndahl, H. G. Accuracy and precision of linear measurements in cone beam computed tomography Accuitomo tomograms obtained with different reconstruction techniques. *Dentomaxillofac Radiol.* **38**(6)**,** 379–386 (2009).
31. Cignoni, P., Rocchini, C. & Scopigno, R. Metro: measuring error on simplified surfaces *Computer Graphics Forum* **17**(2), 167–174 (1998).

Data Citation

1. Sieber, D. M. *et al. Zenodo* https://doi.org/10.5281/zenodo.1473724 (2018).

Acknowledgements

The authors would like to acknowledge the work of Peter Trier Mikkelsen who has driven the field of surgical simulation through the constant evolution of the Visible Ear Simulator software in an unparalleled way for the last decade, and who greatly inspired the creators of the OpenEar dataset.

Author Contributions

Daniel Sieber is the creator of the OpenEar dataset, captured all raw data for the dataset, created the methodology for reconstruction and registration and performed segmentation and 3D modelling of all datasets. Peter Erfurt supported the creation of the datasets, performed sampling of specimen and preparation for micro-slicing, acquisition of CBCT images. Samuel John supported the development of methods to reconstruct micro-slicing and significantly contributed to the custom-made software for alignment of images. Gabriel Ribeiro Dos Santos supported segmentation of some datasets. Daniel Schurzig contributed to the compilation of data and manuscript creation. Mads Sølvsten Sørensen contributed his scientific and technical experience from the Visible Ear dataset creation and performed validation of datasets and references. Thomas Lenarz contributed his scientific advice and access to his facilities and performed validation of datasets.

Additional Information

Supplementary information accompanies this paper at http://www.nature.com/sdata.

Competing interests: The authors declare no competing interests.

How to cite this article: Sieber, D. *et al.* The OpenEar library of 3D models of the human temporal bone based on computed tomography and micro-slicing. *Sci. Data.* 6:180297 doi: 10.1038/sdata.2018.297 (2019).

Publisher's note: Springer Nature remains neutral with regard to jurisdictional claims in published maps and institutional affiliations.

Otology & Neurotology: OpenEar image data enables case variation in high fidelity virtual reality ear surgery

Submitted: 31 July 2020

Accepted: 13 January 2021

OpenEar image data enables case variation in high fidelity virtual reality ear surgery

Daniel Manuel Sieber[1], Steven Arild Wuyts Andersen[2], Mads Sølvsten Sørensen[2] and Peter Trier Mikkelsen[3]

[1] *MED-EL Elektromedizinische Geräte GesmbH, Innsbruck, Austria*
[2] *Dept. of Otorhinolaryngology, Rigshospitalet, University of Copenhagen, Denmark*
[3] *Alexandra Instituttet, Aarhus, Denmark*

Address Correspondence to Dipl.-Ing. Daniel Manuel Sieber, MED-EL Elektromedizinische Geräte GesmbH, Electrodes / Surgical Research & Development, Fürstenweg 77A, A-6020 Innsbruck, daniel.sieber@medel.com

Conflicts of Interest and Source of Funding: Dr. Andersen has received a postdoc grant by the Independent Research Fund Denmark (8026-00003B). The Visible Ear Simulator is developed with support from Oticon Medical, MED-EL and the Oticon Foundation. The authors have no other funding sources or conflicts of interest to declare.

Abstract

Background: Virtual reality (VR) simulation is an established option for temporal bone surgical training. Most VR simulators are based on CT imaging whereas the Visible Ear Simulator (VES) is based on high-fidelity cryosections of a single temporal bone specimen. Recently published OpenEar datasets combine cone-beam computed tomography (CBCT) and micro-slicing to achieve similar model quality. This study explores integration of OpenEar datasets into VES to enable case variation in simulation with implications for patient-specific modeling based on CBCT.

Methods: The OpenEar dataset consists of segmented, co-registered, multimodal imaging sets of human temporal bones. We derived drillable bone segments from the dataset as well as triangulated surface models of critical structures such as facial nerve or dura. Realistic visualization was achieved using coloring from micro-slicing, custom tinting and texture maps. Resulting models were validated by clinical experts.

Results: Six out of the eight OpenEar datasets could be integrated in VES complete with instructional guides for various temporal bone surgical procedures. Resulting models were of high quality because of postprocessing steps taken to increase realism including colorization and imaging artefact removal. Bone artefacts were common in CBCT, resulting in dehiscences that most often could not be found in the ground truth micro-slicing data.

Conclusion: New anatomy models are included in VES version 3.5 freeware and provide case variation for training which could help trainees to learn more quickly and transferably under variable practice conditions. The use of CBCT for VR simulation models without postprocessing results in bone artefacts, which should be considered when using clinical imaging for patient-specific simulation, surgical rehearsal and planning.

Keywords: virtual reality simulation; temporal bone surgical training; patient-specific simulation; 3D modelling; post-processing.

Introduction

Surgery of the human temporal bone requires a high level of understanding with regards to the three-dimensional location of anatomical landmarks and important neural and vascular structures.[1] Training of novice surgeons still relies heavily on dissection of cadaveric specimens despite challenges to provide enough temporal bones in many centers.[2] Surgical simulators can be an important addition to the early stage cadaveric training of novice surgeons in temporal bone labs. It is well-documented that temporal bone simulators can improve the technical skills of trainees and optimize the potential and efficiency of cadaveric training.[3] However, patient-specific simulation[4] for the more experienced surgeons rehearsing and planning in complicated cases may imply higher requirements of realism and quality in simulation.

Most surgical simulators are based on medium resolution grayscale image data from clinical computed tomography (CT)[5], which provides no anatomical color information nor detailed geometry information on the more delicate bony or soft tissue structures such as the ossicles or the tympanic membrane. This low level of graphic fidelity can be a major hurdle in creating realistic and immersive VR environments for surgical training and planning.

A stack of high-fidelity digital image data[6] resulting from a laborious cryosection process was used in the development of the Visible Ear Simulator (VES) freeware.[7] The quality and realism of this anatomical model is higher, but the amount of work needed for manual segmenting and rendering has yielded only a single anatomy. This is a common concern among teachers and trainees because experience from practicing on multiple anatomies (i.e. case variation) is generally considered to be important.[8]

The recently published OpenEar dataset[9] used clinical cone-beam CT (CBCT) and high resolution CBCT in combination with anatomical micro-slicing to increase accuracy and efficacy in segmentation and to achieve a similar visual quality as the Visible Ear 3D model using a less laborious process. We hypothesize that we could apply these datasets to provide additional high-fidelity virtual reality models for temporal bone surgical training.

Material and Methods

Data summary

The OpenEar dataset consists of eight digitized adult human temporal bones available for free download from the Zenodo OpenData repository.[10] Each dataset in the series is based on a co-registered multimodal imaging set, including clinical type CBCT of the entire temporal bone and high resolution CBCT, as well as micro-slicing of a cropped specimen as shown in Figure 1 (left). Segmentations (i.e. delineations) of scala tympani, scala vestibuli, malleus, incus, stapes, tympanic membrane, facial nerve, chorda tympani, cochleovestibular nerve, sigmoid sinus/dura and carotid artery are provided.

VR simulator

The Visible Ear Simulator freeware (VES), first published in 2009, has evolved over several iterations technologically, didactically, and in relation to the source data material: The first versions (1.0 through 1.3) focused entirely on the Visible Ear dataset[6] whereas version 2.0 introduced a modular software concept that allowed developers to load models based on other datasets into the simulator. In this paper, we present the integration of the OpenEar datasets[9] in the newest version 3.5[11] that has a fully modular

system, allowing for the user's creation of training scenarios and tutorials as well as user addition of new anatomies.

Figure 1. *Left: An example of the OpenEar dataset (Delta) showing the embedded specimen. Note the level of detail and color representation in the micro-slicing data as well as the cochlear compartments, modiolus, and osseous spiral lamina being clearly visible. Right: 3D reconstruction of the full dataset in the Visible Ear Simulator for surgical training. The embedded part from micro-slicing is highlighted.*

Data requirements: drillable bone segment

In order to integrate new anatomies such as the OpenEar library into the VES, the drillable osseous segment of the temporal bone must be available as a three-dimensional, isotropic voxel model at a high resolution of 0.2mm or better. For a realistic simulation, two models work in concert: a central processing unit (CPU) based haptic bone model, which allows physical simulation of drilling through interaction with the user input from a haptic device, and a corresponding graphics processing unit (GPU) based model, which provides 3D imaging and advanced optical effects like subsurface scattering. Through precise co-registration, the two models are aligned to ensure that the physical and visual models interact properly.

Data acquisition and processing: drillable bone segment voxel pipeline

CBCT data from the OpenEar library was resampled to an isometric voxel size of 0.15mm using the Fiji software[12] setting the resolution 25% higher compared to the original Visible Ear dataset to provide more anatomical detail. A transfer function was applied in 3DSlicer[13] to remove noise and artefacts from the scans, identify bone voxels through a Hounsfield threshold limit, and adjust the Hounsfield dynamic range to match that of VES. A custom software tool was created to apply slight Gaussian filtering to achieve smooth surfaces. Tissue density values for haptic simulation in the simulator were also based on CBCT Hounsfield scale data.

Color data for each bone voxel was derived from the micro-slicing datasets of the OpenEar library. These datasets are originally anisotropic due to the nature of the micro-slicing process yielding higher in-slice resolution compared to the slice-to-slice resolution. Therefore, these were resampled to an isometric resolution. To accommodate the differences in size of the CBCT and micro-slicing datasets, a simple algorithm was created to sample colors in the micro-slicing dataset and achieve realistic color variation in the remaining bone in the model.
For manual postprocessing in relation to bony defects, a "voxel spray" tool was introduced into VES which can be used to fill artefactual bony voids manually where needed.

Data processing of non-drillable segments: triangulated segments pipeline

Manual segmentations of critical structure segments (nerves, blood vessels, dura) from the OpenEar dataset were exported as triangulated surface models. Surface normals were computed for all surfaces, and geometric decimation was applied to reduce the number of polygons in some segments which yielded models that could not be handled efficiently. Resulting surface models needed to be free of CBCT artefacts[14] such as holes, internal surfaces, non-manifold geometries and inverted surface normals for the sake of realism and to avoid problems in the physics simulation (e.g. contact detection between drill and anatomical segment). Therefore, new high-fidelity triangulation meshes with a defined number of elements and a uniform triangle size were created to optimize the models for fast real-time physics simulation using the Graphite software tool.[15] Meshmixer[16] was used to repair remaining defects in the models, such as noisy surface patches. Meshlab[17] was used to check the resulting segments and fix instances of inverted inner and outer surfaces, which would make the use of segments in physics simulations impossible.

For the graphical model, additional color maps were created. In the middle ear ossicles each vertex of the surface triangulation was assigned the corresponding color value from the micro-slicing dataset (Figure 2). Non bony segments such as the dura and facial nerve were colored using UV mapping—a computer graphics method to project 2D images onto 3D models. This required the surface of the 3D object being UV unwrapped (i.e. a 2D parametrization of the 3D model). A commercial software package[18] was used to produce the UV maps for the larger models. Color for each element was determined by using a search position 0.05mm inside the segment element surface normal to avoid artefacts caused by the micro-slicing embedding resin.

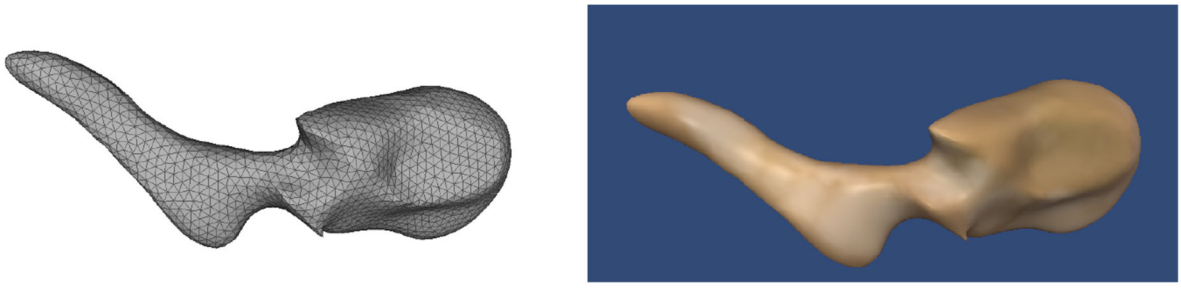

Figure 2. *An example of modelling based on segmentation of the temporal bone structures. Malleus after MeshLab processing (left) and after vertex colorization (right).*

To further enhance the graphic realism of the data, textures were applied with manual painting of blood vessels on the facial nerve and dura segments (Figure 3, right) using Blender software.[19] This enhancement is considered important because the vascular pattern on these structures visible through a thin layer of bone can be a visual cue e.g. during posterior tympanotomy drilling. Such optical surface information is always lost even in micro-slicing as an inherent artefact of the sectioning, segmentation, and reconstruction, in which the reconstructed 3D surface consists of stacked pixels selected stochastically on either side of a segment border in a 2D image. Improvements of such visual cues and graphics realism in the simulation environment seem to positively impact drilling performance as illustrated in the increased average performance (adjusted for other factors) from version 1.3 to version 2.1 and 3.0 of the Visible Ear Simulator[20].

Some of the segments appeared visually flat despite colorization, pattern tinting and manual texturization. In reality, thin segments feature translucency, but most real-time visualization calculations -such as those needed for simulation- do not support this because of performance constraints. To simulate the effect of translucency, an efficient method was developed to reconstruct a view dependent

model thickness using spherical harmonics.[21] To calculate these spherical harmonic coefficients[22], a signed distance field was computed representing the closest distance to a surface for every voxel, and subsequently used inside the shader to simulate translucency in real time.
The final process step in implementing the triangulated segments was the modeling of collision detection and physics. Collisions are detected using signed distance fields. The physics simulation is driven by a very simple mesh discretization using only spheres for fast intersection tests and surface skinning.[23]

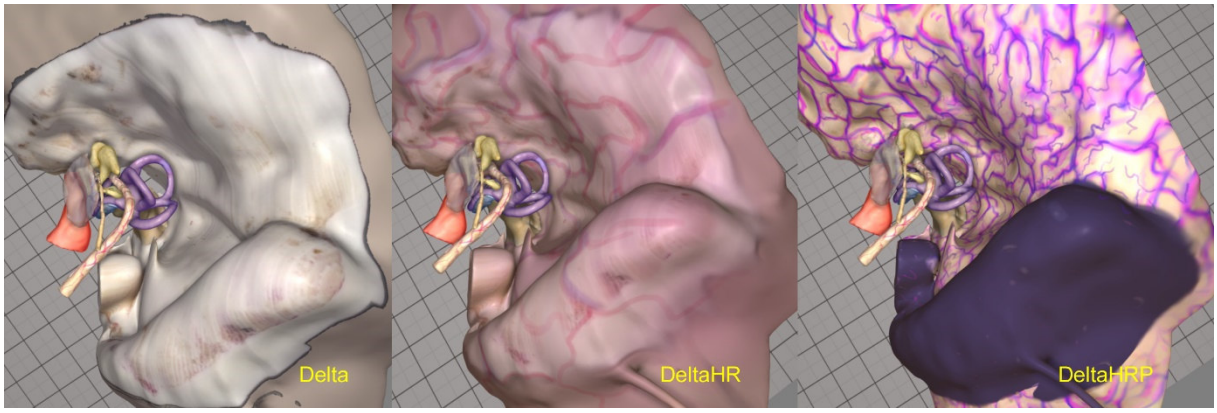

Figure 3. *Example of texture mapping to enhance realism (Delta OpenEar dataset). Left: UV mapping. Middle: Basic color tinting + minor texture. Right: Major texture mapping using artwork created in the Blender software.*

Validation of visual quality and anatomical validity

The resulting 3D models including the artistic enhancement of some segments were evaluated by nine experienced clinical experts from six clinics in four different countries from a viewpoint closely resembling the perspective of an operating surgeon. The experts rated the usefulness of each segment for surgical navigation for the newly implemented anatomies from the OpenEar dataset in direct comparison to the original Visible Ear dataset using a 5-point Likert scale.

Results

Six datasets from the OpenEar library (Delta, Epsilon, Eta, Gamma, Theta and Zeta) were processed using the described pipeline. Datasets Alpha and Beta were not included because the quality was lower and not suited for integration. Each of the seven digital specimens (six OpenEar + one Visible Ear dataset) can now be used for training in VES—both as a left or right ear through mirroring. The current version 3.5 of the Visible Ear Simulator is available as an academic freeware from https://ves.alexandra.dk/ and will run on PCs/laptops running 64bit Microsoft Windows 7 or later and featuring a sufficiently powerful NVIDIA® graphics processor (RTX2070 or better is recommended for optimal performance). A Geomagic Touch® device (3D systems, Rock Hill, SC, USA) is needed for haptic 3D control of the interactive surgical tools and for drilling with force feedback. Various tutorials for training of novice surgeons are available for each specimen with on-screen step-by-step guides for meatoplasty, cortical and full mastoidectomy, posterior tympanotomy and CI insertion, front-to-back attico-antro-mastoidectomy, and translabyrinthine as well as fossa media approaches to the inner auditory canal. Learning support functions include transparency and slicing to “see into the bone”, collision warnings, optional color-coding of bone volumes to be removed (simulator-integrated tutor-function) corresponding to the step-by-step guides, and even haptic guidance of CI electrode handling.

For the integrated OpenEar datasets, the bone segment geometry of the virtual temporal bones was created from the clinical CBCT dataset, which has a large field-of-view. This allows simulation of e.g. a full mastoidectomy and cochlear implant bed creation. For the core part of the temporal bone for which color data from micro-slicing was available (i.e. the embedded specimen), the bone volume is colored according to the respective micro-slicing colors (Figure 1, left). This includes the mastoid, external ear canal, tympanic cavity, middle ear ossicles, and round window niche. These structures will therefore closely resemble the colors found in an actual cadaveric temporal bone. For the voxels outside of the micro-slicing dataset, the CBCT bone volume was manually colored (Figure 1, right). The authors have made resulting UV maps as well as 3D models including vertex coloring available for the Delta dataset as a sample[24].

The authors also evaluated the fidelity of each of the VR models and frequently observed bone voxel defects in the 3D models (Table 1), imitating for example a dehiscence at the horizontal or vertical segment of the facial nerve, or bony defects at the interface with dura (Figure 4). These defects were often less prominent using the high-resolution CBCT as source material when compared to the clinical CBCT. However, not all defects were artefacts of processing the CBCT to make 3D models: in a few cases, actual defects and dehiscences were also found in micro-slicing. For example, in the Eta dataset, a dehiscence of the superior semi-circular canal was found in both the CBCT and the micro-slicing datasets; and in the Epsilon dataset, there seems to be an extensive dehiscence of the horizontal part of the facial nerve, which in the micro-slicing is merely a partial dehiscence. These examples show that it can be impossible to judge whether a bone defect is merely an artefact in CBCT imaging or an actual anatomical finding without access to ground truth imaging such as micro-slicing. For the scala tympani, several of the OpenEar models had bony voxel artefacts "growing" inside the scala making it difficult or impossible to insert a CI electrode in the simulator using the dataset without manual postprocessing. Finally, the CBCT models in two cases (Theta and DeltaHR) also capped the incus in an artificial layer of bone that is not a part of the structure.

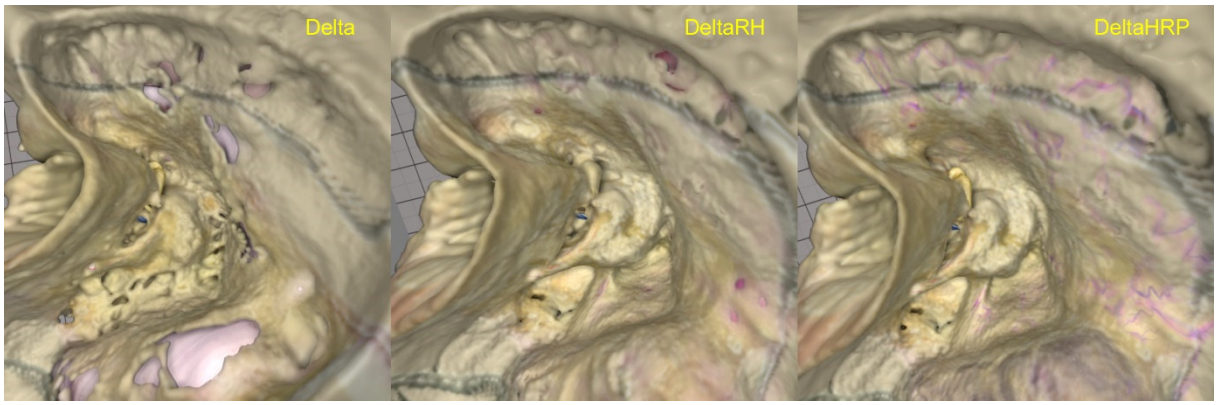

Figure 4. *Examples of how bony defects appear in the differently processed datasets of Delta during a virtual drilling of an anatomical mastoidectomy. Left: The clinical CBCT dataset has large artefacts seen as dehiscences at dura and sinus. Middle: The high-resolution CBCT dataset has smaller dehiscence artefacts but the ossicles are embedded in bone. Right: The manually post-processed high-resolution dataset has no bone artefacts.*

Table 1. *Fidelity of virtual reality 3D models before manual postprocessing. All artefacts were removed for final integration in VES.*

Source material (resolution)	Dataset	Voxel artefacts/defects in the 3D model							
		External surface	Dura	Sigmoid sinus	Labyrinth	Facial nerve	Lateral face of carotid	Scala tympani	Ossicles
Micro-slicing (50μm)	**Visible Ear**	–	–	–	–	–	–	– CI electrode insertion easy	–
Clinical cone-beam CT (250μm)	**OpenEar: Theta**	–	–	–	–	–	–	+ Narrow due to artefacts, CI electrode insertion difficult	+ Incus capped in some bone
	OpenEar: Zeta	–	–	–	–	–	–	++ Very narrow due to artefacts, CI electrode insertion impossible	–
	OpenEar: Gamma	–	–	–	–	+ Bone voxel defect	+ Bone voxel defect	– CI electrode insertion easy	–
	OpenEar: Eta	–	(+) Bone voxel defect in micro-slicing too	+ Bone voxel defect	(+) Bone voxel defect in micro-slicing too: SSC dehiscence in fossa media.	++ Large bone voxel defect	+ Bone voxel defect	+ Narrow due to artefacts, CI electrode insertion difficult	–
	OpenEar: Epsilon	+ Bone voxel defect	+ Bone voxel defect	–	–	+(+) Large bone voxel defect. Partial dehiscence in micro-slicing too.	–	– CI electrode insertion easy	–
	OpenEar: Delta	+ Bone voxel defect	+++ Very large bone voxel defect	+++ Very large bone voxel defect	–	++ Large bone voxel defect	++ Large bone voxel defect	+ Narrow due to artefacts, CI electrode insertion difficult	–
High-resolution cone-beam CT (125μm)	**OpenEar: Delta HR**	+ Bone voxel defect	+ Bone voxel defect	+ Bone voxel defect	+ Bone voxel defect. Promontory defect inferior to the stapes footplate	+ Bone voxel defect	+ Bone voxel defect	++ Very narrow, CI electrode insertion impossible	+++ Incus embedded in bone
	OpenEar: Delta HR with post-processing	–	–	–	–	–	–	– CI electrode insertion easy	–

– No artefacts or defects, i.e. normal anatomy in micro-slicing as well as the 3D model.
(+) Bone defect in micro-slicing as well as the 3D model.
+ Bone voxel artefact in the 3D model only.

The fidelity of models can be improved by 1) increasing the quality of the data acquisition (i.e. increasing scan resolution), 2) by voxel post-processing and 3) by using texture maps to represent blood vessels and other visual cues. The Delta dataset may serve as an example of what was done in VES version 3.5: The external surface towards the dura and the sigmoid sinus had many gross defects when the clinical CBCT dataset (0.25mm resolution) was used for 3D modelling (Figure 5, left). However, even at a better resolution (0.125mm) some of these defects persisted (Figure 5, middle). With manual postprocessing using the voxel spray tool and drilling, these defects could be corrected (Figure 5, right) along with correction of other bony artefacts such as the incus being embedded in bone (Figure 4, middle), a defect of the promontory wall, and bony artefacts inside scala tympani. Finally, adding texture maps (Figure 3, middle and right) provides further realism of the simulation (Figure 4 middle and right). These postprocessing procedures still require extensive manual labor, pushing the time to integrate a new anatomy into the simulator to 25-30 hours which could be optimized by automatization over time.

Ultimately all artefacts mentioned in Table 1 and beyond were removed for the implementation in VES during postprocessing of all included OpenEar models. Resulting virtual models included in VES version 3.5 provide the highest quality of models for training (i.e. similar to the DeltaHRP in Figure 5) approaching a similar visual quality as compared to the original Visible Ear models. Nonetheless, to demonstrate the challenges and effects of imaging and postprocessing on fidelity and realism, all three Delta models (i.e. based on the clinical CBCT, high-resolution CBCT, and high-resolution CBCT with manual postprocessing) are available in VES 3.5. The expert evaluation of the OpenEar models revealed similar ratings for the OpenEar models (range avg 3.7-4.1) and the Visible Ear 3.5 models (avg 4.2). A clear improvement was found between the low-resolution Delta models (avg 3.4), high resolution DeltaHR models (avg 3.6) and final simulator implementation including manual postprocessing DeltaHRP (avg 4.1). Questionnaire and detailed evaluation results for individual structures are found in Supplemental Digital Content 1.

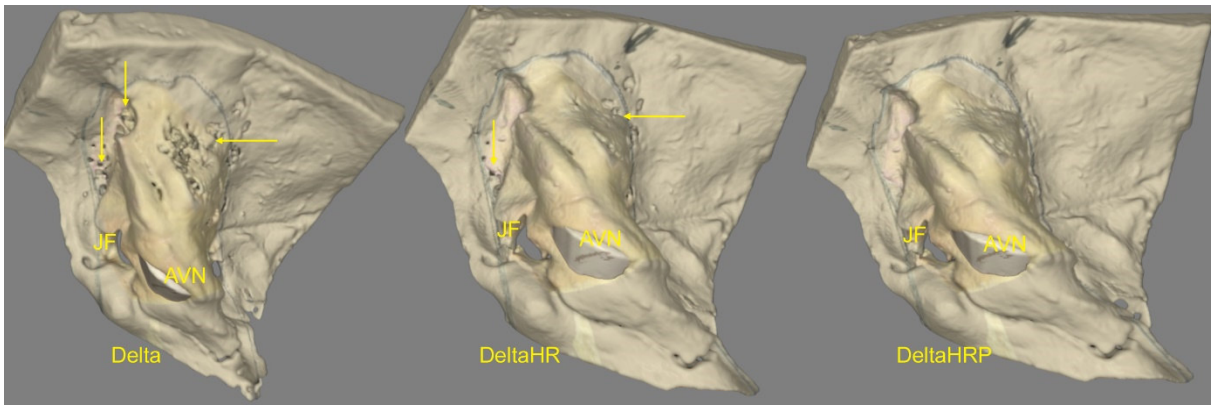

Figure 5. *Different 3D reconstructions of the OpenEar dataset (Delta). Left: Model based on the clinical type CBCT + automatic smoothing routines. Middle: Model based on the high-resolution CBCT + automatic smoothing routines. Right: Model based on the high-resolution CBCT + automatic smoothing routing + manual postprocessing. Arrows mark bony defects (i.e. artefacts). Abbreviations: JF - jugular foramen, AVN - acusticovestibular nerve.*

Discussion

We present a process for developing high-fidelity VR simulation based on the publicly available OpenEar datasets. The aim of the OpenEar project was to develop a new method to create digital temporal bone specimens in a time efficient way and to focus on those structures needed to adequately simulate the most common otologic procedures including middle and inner ear surgery. Even though the original Visible Ear data remains unparalleled as a complete digital representation of the human temporal bone including e.g. brain and skin segments, the OpenEar data has been successfully used to expand the number of anatomies in high-fidelity virtual temporal bone training. A group of international experts has evaluated the implementation of the OpenEar anatomies in the simulator and rated the new models almost as highly as the original Visible Ear models. The creation of patient-specific high-fidelity models for pre-surgical rehearsal and planning requires high-resolution imaging, accurate and fast segmentation, as well as methods to warp and apply meaningful coloring to grayscale type data. While the latter could be solved in software engineering given adequate time and resources, clinically available imaging quality and segmentation methods are currently hindering advances in this field.
Two studies have investigated the use of clinical imaging for patient-specific VR simulation, with both studies based on cadaveric material: Arora et al. used clinical CT[25] and Locketz et al. used clinical CBCT.[26] Both groups report substantial need for manual interaction to achieve usable models. In a recent study[27], novice simulator users supported patient specific simulator rehearsal before surgery. However, this recommendation was based on the drilling of a single bone rendered from microCT, which is not applicable for use in patients.

Our study further highlights that while clinical CBCT can be used to generate patient-specific models, there might be considerable defects and artefacts in the resulting 3D models. Most of these abnormalities are artefacts resulting from the acquisition, processing and reconstruction of the data for 3D modelling and could not be found in the ground truth micro-slicing data material. However, as some of the defects represented true defects also found in the micro-slicing data, there is no clinically available way of knowing whether defects are true or artefacts from clinical CBCT imaging. Consequently, this might mislead surgeons regardless of whether standard review of the clinical imaging is done pre-operatively in a clinical imaging viewer (i.e. DICOM viewer) or whether data is modelled for 3D VR visualization. The experienced surgeon will be aware of bias inherent to CBCT such as apparent dehiscences but also bias due to the reconstruction and visualization in the virtual reality environment. Manual postprocessing can of course be added, but besides being time consuming and resource intensive, this provides no guarantee of a “truer” representation without ground truth imaging available.

Nonetheless, 3D modeling offers advantages such as interaction with the dataset through drilling and CI electrode insertion. The manual postprocessing with closure of defects and removal of artefacts needed for a solid simulation is however still not feasible or attractive in clinical routine where time of physicians is extremely precious. We therefore propose to do this mainly when establishing a case library for temporal bone surgical training as in this study, which has made six new cases available within the latest version of VES complete with many tutorials for drilling mastoidectomy, CI insertion and more. The simulator software is provided as academic freeware online.[11]
The implementation of the OpenEar datasets represents a valuable extension of the Visible Ear Simulator capabilities, as it allows training of surgical procedures covering more anatomical variations without sacrificing some of the fundamental advantages of model colorization based on empirically obtained data. Being able to offer variability of practice could increase the learning speed in simulator training significantly when compared to constant practice[28], as it allows learners to sample a useful range of parameter-sets (in our case: anatomical variations) and observe outcomes (in our case: surgical successes

or traumata) dependent on their actions. Furthermore, Huet et. al.[29] found in aviation simulator participants, that variable practice training may accelerate the education of attention to more useful informational variables. Translated into our application, surgical simulator trainees in constant practice settings could e.g. depend too much on a certain anatomical landmark which is prominent in their single anatomy scenario. By adding anatomical variation and variable practice to the simulation, trainees would realize they cannot rely on this landmark only and add further landmarks into their decision-making process, improving transferability of their simulator-acquired skills. With the addition of further anatomies it is anticipated, that simulations will stay attractive up to a higher number of repetitions, which may aid in internalizing the surgical procedure at an even higher level than what has been found in previous work where an apparent plateau in performance is observed after only few repetitions of training.[30,31]

Even though basic surgical skills can effectively be learned using low fidelity simulation (such as for example box trainers in laparoscopy) most studies have only investigated this for novice learners.[32] A high graphical realism as pursued by the Visible Ear and OpenEar models might be more important in complex procedures [33] where accurate visual cues are important and higher fidelity of the simulation is beneficial for more advanced learners.[34]

Further studies using a contemporary validity framework [35] are needed to demonstrate that the positive effects of variability of practice can also be observed in temporal bone surgical simulation and to create validity evidence supporting increased fidelity of the graphics.

After more than 15 one-eared VES years, the OpenEar project has made six additional digital temporal bone datasets available to the scientific community. With the integration into the latest version 3.5 of the Visible Ear Simulator, these are now also available for surgical training in a high-fidelity surgical simulator environment for the benefit of VR training of ear surgery. The modularization of the simulator and the possibility for users to create their own tutorials, could take surgical simulation to a new and community-based level. This project yielded several simple but novel solutions to technological challenges encountered in the process development as well as insights into implications of using clinical CBCT for patient-specific simulation.

References

1. Gulya AJ, Minor LB, Glasscock ME, Poe D. Glasscock-Shambaugh Surgery of the Ear. People's Medical Publishing House, 2010.
2. Frithioff A, Sørensen MS, Andersen SAW. European status on temporal bone training: a questionnaire study. *Eur Arch Otorhinolaryngol.* 2018; 275:357–363.
3. Lui JT, Hoy MY. Evaluating the Effect of Virtual Reality Temporal Bone Simulation on Mastoidectomy Performance: A Meta-analysis. *Otolaryngol Head Neck Surg*. 2017; 156:1018–24.
4. Sethia R, Wiet GJ. Preoperative preparation for otologic surgery: temporal bone simulation. *Curr Opin Otolaryngol Head Neck Surg*. 2015; 23(5):355-9.
5. Tolsdorff B, et al. Individual models for virtual bone drilling in mastoid surgery. *Comput Aided Surg.* 2009; 14:21–27.
6. Sørensen MS, Dobrzeniecki AB, Larsen P, Frisch T, Sporring J, Darvann TA. The visible ear: a digital image library of the temporal bone. *ORL J Otorhinolaryngol Relat Spec*. 2002; 64(6):378–81.

7. Sørensen MS, Mosegaard J, Trier P. The Visible Ear Simulator: A Public PC Application for GPU-Accelerated Haptic 3D Simulation of Ear Surgery Based on the Visible Ear Data. *Otol Neurotol.* 2009; 30:484–487.
8. Cook DA, Hamstra SJ, Brydges R, et al. Comparative effectiveness of instructional design features in simulation-based education: systematic review and meta-analysis. *Med Teach.* 2013; 35(1):e867–98.
9. Sieber DM, Erfurt P, John S, et. al. The OpenEar library of 3D models of the human temporal bone based on computed tomography and micro-slicing. *Scientific Data*. 2019; 6:180297.
10. Sieber DM, Erfurt P, John S, et.al. The OpenEar library of 3D models of the human temporal bone based on computed tomography and micro-slicing [Data set]. *Zenodo*. 2019; http://doi.org/10.5281/zenodo.1473724
11. The Visible Ear Simulator. Available from https://ves.alexandra.dk. Last accessed: 23 October 2020.
12. Schindelin J, Arganda-Carreras I, Frise E, et al. Fiji: an open-source platform for biological-image analysis. *Nature Methods.* 2012; 9(7): 676–682.
13. Fedorov A, Beichel R, Kalpathy-Cramer J, et. al. 3D Slicer as an Image Computing Platform for the Quantitative Imaging Network. *Magn Reson Imaging.* 2012; 30(9):1323–1341.
14. Hsieh J. Computed Tomography: Principles, Design, Artifacts, and Recent Advances. SPIE Press, 2003. 183–187.
15. Institute National de Recherche en Informatique et en Automatique, Graphite Software. Available at: http://alice.loria.fr/software/graphite/. Last accessed: 23 October 2020.
16. Autodesk, Meshmixer. Available at: http://www.meshmixer.com/. Last accessed: 23 October 2020.
17. Cignoni P, Callieri M, Corsini M, Dellepiane M, Ganovelli F, Ranzuglia G. MeshLab: an Open-Source Mesh Processing Tool. *Eurographics Italian Chapter Conference*. 2008; 129–136.
18. 3D-IO Games & Video Production GmbH, Unwrella Software. Available at: https://www.unwrella.com/. Last accessed: 23 October 2020.
19. Blender free and open source 3D creation suite. Available at: https://www.blender.org/. Last accessed: 23 October 2020.
20. Andersen SAW, Park YS, Sørensen MS, Konge L. Reliable Assessment of Surgical Technical Skills Is Dependent on Context: An Exploration of Different Variables Using Generalizability Theory. *Acad Med*. 2020 Jun 23. doi: 10.1097/ACM.0000000000003550. Epub ahead of print. PMID: 32590473.
21. Barré-Brisebois C, Bouchard M. GDC talk 2011 at: https://www.gdcvault.com/play/1014538/Approximating-Translucency-for-a-Fast . Last accessed: 23 October 2020.
22. Green, R. Spherical Harmonic Lighting. Sony Computer Entertainment America, 2003.
23. Mueller M, Chentanez N. Solid Simulation of Oriented Particles. *ACM Transactions on Graphics*. Siggraph, 2011.
24. Sieber DM, Andersen SAW, Sørensen MS, Trier P. OpenEar color example from Visible Ear Simulator anatomy Delta [Data set]. *Zenodo*. 2020; https://doi.org/10.5281/zenodo.4362584

25. Arora A, Swords C, Khemani S et.al. Virtual reality case-specific rehearsal in temporal bone surgery: a preliminary evaluation. *Int J Surg.* 2014;12(2):141–5.

26. Locketz GD, Lui JT, Chan S, et al. Anatomy-Specific Virtual Reality Simulation in Temporal Bone Dissection: Perceived Utility and Impact on Surgeon Confidence. *Otolaryngol Head Neck Surg*. 2017; 156(6):1142–1149.

27. Compton EC, Agrawal SK, Ladak HM, Chan S, Hoy M, Nakoneshny C, Siegel L, Dort JC, Lui JT. Assessment of a virtual reality temporal bone surgical simulator: a national face and content validity study. J Otolaryngology Head Neck Surg. 2020 Apr 7;49(1):17. doi: 10.1186/s40463-020-00411-y.

28. Schmidt RA. A schema theory of discrete motor skill learning. *Psychological Review.* 1975; 82(4): 225-260.

29. Huet M, Jacobs DM, Camachon C, Missenard O, Gray R, Montagne G. The education of attention as explanation of variability of practice effects: learning the final approach phase in a flight simulator. *J Exp Psychol Hum Percept Perform*. 2011;37(6):1841-54.

30. Andersen SA, Konge L, Cayé-Thomasen P, Sørensen MS. Learning Curves of Virtual Mastoidectomy in Distributed and Massed Practice. *JAMA Otolaryngol Head Neck Surg*. 2015; 141(10):913–8.

31. Andersen SA, Konge L, Mikkelsen PT, Cayé-Thomasen P, Sørensen MS. Mapping the plateau of novices in virtual reality simulation training of mastoidectomy. *Laryngoscope.* 2017; 127(4):907–914.

32. Lefor AK, Harada K, Kawahira H, Mitsuishi M. The effect of simulator fidelity on procedure skill training: a literature review. *Int J Med Educ*. 2020 May 18;11:97-106. doi: 10.5116/ijme.5ea6.ae73. PMID: 32425176; PMCID: PMC7246118.

33. Sarmah P, Voss J, Ho A, Veneziano D, Somani B. Low vs. high fidelity: the importance of 'realism' in the simulation of a stone treatment procedure. *Curr Opin Urol*. 2017 Jul;27(4):316-322. doi: 10.1097/MOU.0000000000000401. PMID: 28403125

34. Sidhu RS, Park J, Brydges R, MacRae HM, Dubrowski A. Laboratory-based vascular anastomosis training: a randomized controlled trial evaluating the effects of bench model fidelity and level of training on skill acquisition. *J Vasc Surg*. 2007 Feb;45(2):343-9. doi: 10.1016/j.jvs.2006.09.040. PMID: 17264015.

35. Cook DA, Beckman TJ. Current concepts in validity and reliability for psychometric instruments: theory and application. *Am J Med*. 2006 Feb;119(2):166.e7-16. doi:10.1016/j.amjmed.2005.10.036. PMID: 16443422.

List of Supplemental Digital Content

Refer to Dissertation Attachments:

Questionnaire: Evaluation of the VES3.5 OpenEar scenarios and controls.

Supplemental table 1: Average rating of the nine raters for each structure.

Summary and Discussion

Within the framework of this dissertation a novel process was developed which allows the relative efficient production of high-fidelity anatomical computer models as well as their implementation in state-of-the-art virtual reality surgical simulation. Eight fully digitized 3D models of the human temporal bone were created and exemplarily integrated into the Visible Ear Simulator.

Eight fresh adult human temporal bones were scanned using Cone Beam Computed Tomography (CBCT), cut to size, stained, dehydrated, embedded in epoxy and scanned using CBCT again. Destructive micro-slicing was performed by serial grinding and optical documentation of the revealed layer of the epoxy embedded specimen. The resulting image stack was aligned, reconstructed in 3D and registered to the CBCT scans of the specimen in full size and after epoxy embedding. Multimodal segmentation of critical structures was performed using threshold-based techniques for bone structures and threshold supported manual techniques for soft tissue structures. All segmented structures were made available as voxel volumes as well as converted triangulated surface models.

Previous research by other groups has been aimed at providing similar digital representations of the human ear. The infamous Visible Human project [23] made the entire human body available in a digital format, however despite the immense efforts undertaken to ensure high levels of detail, these datasets were not deemed feasible for the simulation of temporal bone surgery. On the other hand, they motivated the researchers of the Visible Ear project to commence their work, creating a dataset like the Visible Human but dedicated to ear anatomy only and providing a much greater level of detail [17]. While this dataset was of excellent quality, the time and effort needed in its production was very high with just the time for segmentation alone estimated at 450 hours for one anatomy [16] yielding only one digital anatomy out of several years' work. Rau et. al. [24] developed a method to reduce the processing time in micro-slicing by using an automated grinding sectioning and subsequent 3D image reconstruction of epoxy embedded specimen. Their work was however focused on the middle and inner ear structures and limited to smaller size specimen making it unsuitable for use in simulations requiring the full temporal bone to be modelled to achieve enough overview. So the majority of digital models of the human temporal bone feasible for surgical simulation are still CT or micro CT based and entirely lack color information and, in many cases, the geometrical accuracy of certain anatomical structures which are not well represented in CT imaging can be quite poor.

It was discovered during creation and preliminary presentation of our data that there was a high level of interest in the scientific community to obtain access to such digital temporal bone models for various applications, some far beyond surgical simulation. It was therefore decided to adjust the publication strategy and become as transparent as possible from an Open Science viewpoint with the

idea of making the research conducted as accessible, reproducible and community available as possible. Three basic principles of Open Science were particularly prioritized in the OpenEar project. To improve the accessibility and impact of our work, an Open Access journal was chosen for publication of the methodology used and the datasets resulting from the work. Furthermore, to be able to guarantee free long-term availability of the results of this work to the scientific community, the complete raw data from our experiments and all results from the processes applied were published Open Data using the Zenodo repository hosted by CERN data center. Open Source and free software were used in this work and all custom created software code within the framework of this work was uploaded to the Open-Source platform Github to ensure our work is reproducible and can be improved and built on by the scientific community in the future.

As in the development of any novel process, the creation of OpenEar datasets went through a learning curve and some aspects of the process can still be further improved over time. The concept behind our experiments is fortunately still considered fully valid and the proposed concatenation of process steps described above could serve to create further high-fidelity models in the future. However, several details within the described process steps deserve further optimization to improve the data quality and/or reduce the effort needed in some of the later steps in the process. While specimen sampling did not seem to have considerable negative impacts on the model quality, the specimen preparation and embedding techniques could potentially be further improved. For the application in VR surgical simulation, it would be advantageous to better preserve the visual properties of the nerve structures such as facial nerve or chorda tympani. Eventually the nerves could be subject of a targeted fixation avoiding shrinkage during subsequent drying steps. Another potential field for improvements is the setup for micro-slicing, where the specimen holder should be optimized such that local deformations of the embedded specimen are reduced, which would make correct reconstruction of the data significantly more efficient. It could be suggested to use a specimen holder which clamps the entire circumference of the specimen with a defined force distributing pressure evenly and consistently compared to the current solution which significantly deforms the specimen at the contact location with the pointed radial fixation screw. Advances in optical microscopy systems might offer additional improvements in optical imaging quality and reduce motion artefacts introduced by the micro-table and image stitching functions used in the current work. Further automatization of the process along the lines of [24] could further improve the efficacy of the micro-slicing process. Another field for potential improvement is the CT imaging used for segmentation of the datasets. The relatively low resolution and fidelity of these datasets significantly decreased the efficiency of the model creation process in the current work. It would therefore be highly recommended for future work, to perform high-resolution, high-fidelity micro-CT imaging or even Synchrotron imaging [25] in addition to the clinical CBCT imaging to reduce the amount of manual segmentation needed in model creation.

Despite being a significant efficiency improvement in time and resources spent per anatomy created, the new process remains laborious. While acquisition of CBCT image can be performed rather fast, the micro-slicing process without automatization still consumes plenty of time. The reconstruction time for the micro-slicing data could be greatly reduced if artefacts such as the local deformation of the embedding overmold could be overcome. Segmentation and integration of datasets into the simulator including significant manual editing is additionally time and labor intensive. In summary, in our experience, once the described process had been established, the overall time to create a new training anatomy in the simulator is significantly lower than e.g., the Visible Ear dataset [16]. However, we are evidently still far away from an automated patient-specific high-fidelity simulation without the need for a disproportional investment of surgeons' time.

While two of the datasets from the initial process development phase had to be excluded for data quality reasons, six out of the eight OpenEar anatomies could successfully be implemented into the Visible Ear Simulator software complete with instructional guides for different temporal bone surgical procedures. The CBCT and micro-slicing datasets were fusioned to achieve this, with the CBCT based geometry model for haptic simulation working in a precisely concerted way with the micro-slicing color based visual model. Manual tinting was applied in segments which had compromised visual quality as an artefact of specimen preparation for micro-slicing. Along the same lines, some bony defects in the drillable segments as a result of artefacts in CBCT imaging were manually patched.

The publication of the OpenEar datasets and their implementation into the Visible Ear Simulator mark the beginning of a new era in surgical simulation of otologic surgery. It will now be possible to study the effects of variability of practice in temporal bone surgical training without having to make compromises when it comes to the visual qualities of the underlying datasets. This is expected to increase trainee's performance in simulation training due to the better development of a Generalized Motor Program [18] and training the surgeons attention to more anatomical variables [19]. What is still missing in this regard is representations of pediatric anatomy as well as malformed and pathologic anatomy. While pediatric specimens remain more difficult to obtain, such specimens could be digitized and modelled using the same process which we have described in this work. Providing models of anatomical malformations and pathologic ears represents a much greater challenge as the occurrence of these special cases is relatively low in the general public and not necessarily obvious in donors which are willing to provide their bodies to science post-mortem.

So, while this work has been able to demonstrate that it is possible to create high-fidelity models of the human temporal bone in a relative efficient way, the question remains how useful it is to just increase the number of available models of adult temporal bones with normal non-pathologic anatomy beyond a certain point. This highlights the need for the above-mentioned focus on pediatric,

malformed and pathologic ear model creation. On the other hand, creating more digital anatomies might be an important key element on the way to patient-specific rehearsal of surgery based on clinical CT imaging, which is considered a technology which could be needed and within reach in the not-so-distant future. While the current clinical imaging does not provide sufficient resolution and fidelity to distinguish between imaging artefacts and actual anatomical specialties (e.g., bony dehiscences), the progress made in clinical scanners in the last decades [26] gives hope that sufficient image quality will become available in the foreseeable future. To be able to then also provide meaningful coloring for such false-colored baseline images, modern day deep-learning techniques could probably extract color information from an existing training database which includes ground-truth color data, and apply an artificial yet realistic coloration to models automatically created from clinical imaging on this basis. As machine learning techniques usually rely on large scale datasets for training, the processes described in our work -or an optimized version thereof- could be useful or even a prerequisite in the creation of training data for this future technology. Another technology which might require realistic and colored visualization based on false-color imaging is the new generation of fully digital operating microscopes [27,28] which could project high-fidelity patient-specific digital models into the surgeon's binoculars in an Augmented Reality manner, to further improve patient safety and surgical performance in actual patient surgery. Such systems have in fact very similar requirements as surgical simulators aiming at high-fidelity patient-specific simulation which could result in interesting development synergies.

In whatever direction the outlook regarding future developments of our work will develop, what is available today already extends the possibilities in surgical training worldwide. The increasing uptick in simulator capabilities has not yet been fully reflected in the widespread modifications of surgical curricula needed. However, based on our experiences and published data [29] surgical simulation training could and should be strategically positioned at several different levels during the career of medical students as well as novice and intermediate level surgeons.

Using simulators and their anatomical models could be of great benefit already in the education of medical students. [30,31] While conventional textbooks are always limited by the need to project information into two-dimensional images and text description, interactive use of the available 3D models can provide students with additional and motivational insight into the tree-dimensional geometry of the human temporal bone in our experience. As interactive drilling is not needed for the use of simulators as an 'advanced textbook' a haptic force-feedback device is not needed in this use case, eventually allowing the use of simulators on the students' own computers. Even when it is decided to make a simulation system available for this audience as a centralized service, the risk of broken hardware and resulting need of maintenance can greatly be reduced by removal of the haptic force feedback device which is more vulnerable than other parts of the simulator due to its moving

parts and eventually fragile components. Such system could therefore be a very competitive tool in the education of medical students from a cost-benefit perspective.

Simulation of drilling in the temporal bone including haptic force-feedback could be added in the second step of the training and remain exclusively reserved for more far-advanced medical students and entry-level residents. At this stage, tutor-assisted and eventually more low-fidelity simulation in a single anatomy is an option to keep cognitive load moderate and maximize steepness of the early learning curve. [32] There may be further target groups which this stage of training could be relevant for to make the clinical processes more efficient, including advanced surgical nurses and other healthcare professionals involved in patient treatment which should have a good understanding of what is happening in the surgical theatre.

Once the initial learning curve is completed, it may be advisable to transfer and solidify the simulator learned skills in surgical dissection training using physical 3D-printed models of the temporal bone and further on in cadaveric specimen under the supervision and with feedback from the mentoring expert surgeon.

The final stage of simulator training might be indicated when the performance in cadaveric specimen is deemed sufficient by the mentoring expert surgeon and before moving into operating in patients. At this stage, variable practice VR surgical training in a range of high-fidelity anatomy models – as just made available by the products of this dissertation- could help to prepare surgeons for some of the anatomical variations to be expected in patients and to further improve the efficacy of the continued parallel dissection training in cadaveric specimen. [33,34]

While the general validity and usefulness of surgical simulator training is well proven in literature including the studies mentioned above, further studies are needed to support the suggested integration into surgical training curriculum or a modification thereof. Most importantly, the positive effects of variable practice conditions observed in other fields of education and training [19, 29] must be shown to also be relevant in the field of temporal bone surgical training. Such study comparing constant versus variable practice conditions using different VES set-ups in the National Danish temporal bone course has already been scheduled. Further studies which are considered important to boost the creation of an evidence-based training curriculum should be aimed at better understanding the correlations between simulator fidelity and training efficacy in learners of different competency levels. Based on the literature [32], it is anticipated that low-fidelity graphics could be sufficient in novice learners, whereas high-fidelity simulation might prove superior in intermediate and advanced learners.

To be able to satisfy the need for surgical simulator training worldwide, access to simulator systems must be improved on a global scale in the future. Simulators must be affordable and should not require the need for users to individually purchase computer hardware and haptic force feedback devices needed to make full use of the simulator capabilities.

A lifetime's work is probably still needed to carefully develop these exciting technologies further, making them a strong and evidence-based integral part of surgical training worldwide. This includes not only further technical development of the existing systems, but also their clinical validation, establishing simulation centers in all teaching clinics and integrating simulation into the training curricula globally as exemplarily described above. Strong partnerships with all stakeholders involved in such effort will be needed to succeed. This includes not only the university clinics being the 'owners' of surgical training, but also e.g. public health insurance providers and industrial partners. If these ambitious goals can be met, it is in the strong belief of the author, that surgical simulation in education and training has the potential of improving the efficacy of surgical skills acquirement and ultimately the lives of patients worldwide.

References

[1] L Edelstein. From the hippocratic oath: text, translation, and interpretation. Baltimore (MD): Johns Hopkins Press; 1943.

[2] C. B. Franzese and S. P. Stringer, “The evolution of surgical training: perspectives on educational models from the past to the future.,” *Otolaryngologic clinics of North America*, vol. 40, no. 6, pp. 1227–35, vii, Dec. 2007, doi: 10.1016/j.otc.2007.07.004.

[3] J. Walter, “Surgical education for the twenty-first century: beyond the apprentice model.,” *Obstetrics and gynecology clinics of North America*, vol. 33, no. 2, pp. 233–6,vii, Jun. 2006, doi: 10.1016/j.ogc.2006.01.003.

[4] S. A. W. Andersen, S. Foghsgaard, L. Konge, P. Cayé-Thomasen, and M. S. Sørensen, “The effect of self-directed virtual reality simulation on dissection training performance in mastoidectomy.,” *The Laryngoscope*, vol. 126, no. 8, pp. 1883–1888, Aug. 2016, doi: 10.1002/lary.25710.

[5] R. A. Agha and A. J. Fowler, “The role and validity of surgical simulation.,” *International Surgery*, vol. 100, no. 2, pp. 350–357, Feb. 2015, doi: 10.9738/INTSURG-D-14-00004.1.

[6] M. Frendø, L. Konge, P. Cayé-Thomasen, M. S. Sørensen, and S. A. W. Andersen, “Decentralized Virtual Reality Training of Mastoidectomy Improves Cadaver Dissection Performance: A Prospective, Controlled Cohort Study.,” *Otology & Neurotology*, vol. 41, no. 4, pp. 476–481, Apr. 2020, doi: 10.1097/MAO.0000000000002541.

[7] S. A. W. Andersen, P. T. Mikkelsen, L. Konge, P. Cayé-Thomasen, and M. S. Sørensen, “Cognitive Load in Mastoidectomy Skills Training: Virtual Reality Simulation and Traditional Dissection Compared.,” *Journal of surgical education*, vol. 73, no. 1, pp. 45–50, 2016, doi: 10.1016/j.jsurg.2015.09.010.

[8] B. P. Kerfoot and N. Kissane, “The use of gamification to boost residents’ engagement in simulation training.,” *JAMA surgery*, vol. 149, no. 11, pp. 1208–1209, Nov. 2014, doi: 10.1001/jamasurg.2014.1779.

[9] L. Konge et al., “The Simulation Centre at Rigshospitalet, Copenhagen, Denmark,” *Journal of Surgical Education*, vol. 72, no. 2, pp. 362–365, 2015, doi: https://doi.org/10.1016/j.jsurg.2014.11.012.

[10] Frithioff, A., M. S. Sørensen and S. A. W. Andersen. "European Status on Temporal Bone Training: A Questionnaire Study." *Eur Arch Otorhinolaryngol* 275, no. 2 (2018): 357-363.

[11] T. S. Kashikar, T. F. Kerwin, A. C. Moberly, and G. J. Wiet, “A review of simulation applications in temporal bone surgery.,” *Laryngoscope investigative otolaryngology*, vol. 4, no. 4, pp. 420–424, Aug. 2019, doi: 10.1002/lio2.277.

[12] Varoquier, M., C. P. Hoffmann, C. Perrenot, N. Tran and C. Parietti-Winkler. "Construct, Face, and Content Validation on Voxel-Man(R) Simulator for Otologic Surgical Training." *Int J Otolaryngol* 2017, (2017): 2707690.

[13] Compton EC, Agrawal SK, Ladak HM, Chan S, Hoy M, Nakoneshny C, Siegel L, Dort JC, Lui JT. Assessment of a virtual reality temporal bone surgical simulator: a national face and content validity study. *J Otolaryngology Head Neck Surg*. 2020 Apr 7;49(1):17. doi: 10.1186/s40463-020-00411-y.

[14] Wiet, G. J., P. Schmalbrock, K. Powell and D. Stredney. "Use of Ultra-High-Resolution Data for Temporal Bone Dissection Simulation." *Otolaryngol Head Neck Surg* 133, no. 6 (2005): 911-5.

[15] Zhao, Y. C., G. Kennedy, K. Yukawa, B. Pyman and S. O'Leary. "Improving Temporal Bone Dissection Using Self-Directed Virtual Reality Simulation: Results of a Randomized Blinded Control Trial." *Otolaryngol Head Neck Surg* 144, no. 3 (2011): 357-64.

[16] Sørensen, M. S., J. Mosegaard and P. Trier. "The Visible Ear Simulator: A Public Pc Application for Gpu-Accelerated Haptic 3d Simulation of Ear Surgery Based on the Visible Ear Data." *Otol Neurotol* 30, no. 4 (2009): 484-7.

[17] Sørensen, M. S., A. B. Dobrzeniecki, P. Larsen, T. Frisch, J. Sporring and T. A. Darvann. "The Visible Ear: A Digital Image Library of the Temporal Bone." *ORL J Otorhinolaryngol Relat Spec* 64, no. 6 (2002): 378-81.

[18] Schmidt, Richard A. "A Schema Theory of Discrete Motor Skill Learning." *Psychological Review* 82, no. 4 (1975): 225-260.

[19] Huet, M., D. M. Jacobs, C. Camachon, O. Missenard, R. Gray and G. Montagne. "The Education of Attention as Explanation of Variability of Practice Effects: Learning the Final Approach Phase in a Flight Simulator." *J Exp Psychol Hum Percept Perform* 37, no. 6 (2011): 1841-54.

[20] S. A. W. Andersen, L. Konge, P. Cayé-Thomasen, and M. S. Sørensen, “Learning Curves of Virtual Mastoidectomy in Distributed and Massed Practice.,” *JAMA Otolaryngology– Head & Neck Surgery*, vol. 141, no. 10, pp. 913–8, Oct. 2015.

[21] Sieber, D., P. Erfurt, S. John, G. R. D. Santos, D. Schurzig, M. S. Sørensen and T. Lenarz. "The Openear Library of 3D Models of the Human Temporal Bone Based on Computed Tomography and Micro-Slicing." *Sci Data* 6, (2019): 180297.

[22] Sieber, D., S.A.W. Andersen, M.S. Sørensen, P. Trier. ”OpenEar image data enables case variation in high fidelity virtual reality ear surgery.” *Otol Neurotol*, Revision under review

[23] Spitzer, Victor M. and David G. Whitlock. "The Visible Human Dataset: The Anatomical Platform for Human Simulation." *The Anatomical Record* 253, no. 2 (1998): 49-57.

[24] Rau, T. S., W. Wurfel, T. Lenarz and O. Majdani. "Three-Dimensional Histological Specimen Preparation for Accurate Imaging and Spatial Reconstruction of the Middle and Inner Ear." *Int J Comput Assist Radiol Surg* 8, no. 4 (2013): 481-509.

[25] Li, H., N. Schart-Moren, S. A. Rohani, H. M. Ladak, H. Rask-Andersen and S. Agrawal. "Synchrotron Radiation-Based Reconstruction of the Human Spiral Ganglion: Implications for Cochlear Implantation." *Ear Hear* 41, no. 1 (2020): 173-181.

[26] Hata, A., M. Yanagawa, O. Honda, N. Kikuchi, T. Miyata, S. Tsukagoshi, A. Uranishi and N. Tomiyama. "Effect of Matrix Size on the Image Quality of Ultra-High-Resolution Ct of the Lung: Comparison of 512 X 512, 1024 X 1024, and 2048 X 2048." *Acad Radiol* 25, no. 7 (2018): 869-876.

[27] BHS Technologies, "World's First Roboticscope" https://www.bhs-technologies.com/roboticscope/?lang=en (accessed 01. November 2020).

[28] Munich Surgical Imaging GmbH, "See the Difference - ARRISCOPE" https://www.munichimaging.de/en/ (accessed 01 November 2020).

[29] Bernardo, A. "Virtual Reality and Simulation in Neurosurgical Training." *World Neurosurg* 106, (2017): 1015-1029.

[30] Venail, F., A. Deveze, B. Lallemant, N. Guevara and M. Mondain. "Enhancement of temporal bone anatomy learning with computer 3D rendered imaging software." *Med Teach* (2010) 32(7): e282-288. doi:10.3109/0142159X.2010.490280

[31] Triepels, C. P. R., C. F. A. Smeets, K. J. B. Notten, R. Kruitwagen, J. J. Futterer, T. F. M. Vergeldt and S. M. J. Van Kuijk. "Does three-dimensional anatomy improve student understanding?" *Clin Anat* (2020) 33(1): 25-33.

[32] Lefor, A. K., K. Harada, H. Kawahira and M. Mitsuishi. "The Effect of Simulator Fidelity on Procedure Skill Training: A Literature Review." *Int J Med Educ* 11, (2020): 97-106.

[33] Sarmah, P., J. Voss, A. Ho, D. Veneziano and B. Somani. "Low Vs. High Fidelity: The Importance of 'Realism' in the Simulation of a Stone Treatment Procedure." *Curr Opin Urol* 27, no. 4 (2017): 316-322.

[34] Sidhu, R. S., J. Park, R. Brydges, H. M. MacRae and A. Dubrowski. "Laboratory-Based Vascular Anastomosis Training: A Randomized Controlled Trial Evaluating the Effects of Bench Model Fidelity and Level of Training on Skill Acquisition." *J Vasc Surg* 45, no. 2 (2007): 343-9

Danksagungen

Die vorliegende Arbeit konnte nur aufgrund vieler wunderbarer Unterstützer entstehen.

Größter Dank gebührt meinem Doktorvater, Herrn Prof. Prof. h.c. Dr. med. Thomas Lenarz, der mich an der Medizinischen Hochschule Hannover aufgenommen und mir während meiner Zeit dort die faszinierende Welt der HNO-Chirurgie eröffnet und meiner Forschung im Bereich der Hörimplantate ganz neue Dimensionen ermöglicht hat.

Ebenso großer Dank geht an Univ.-Doz. Dipl.-Ing. Dr. Dr. h.c. mult. Ingeborg Hochmair für die einmalige Möglichkeit, in verantwortungsvoller Position und berufsbegleitend, diese Dissertation anfertigen zu dürfen und für viele spannende Jahre, in denen ich an ihrer wahrlich großartigen Vision mitarbeiten durfte, Hörverlust als Barriere für Kommunikation und Lebensqualität zu überwinden.

Ich möchte mich herzlich bei meinem Zweitbetreuer, Prof. Dr. med. Mads Sølvsten Sørensen für seine Unterstützung und die Inspiration zu dieser Arbeit bedanken, welche durch seine bahnbrechende Forschung im Bereich der Modellierung des menschlichen Felsenbeines entstanden ist.

Einer der wichtigsten Unterstützer dieser Arbeit war Herr Peter Erfurt. Ich bedanke mich vielmals dafür, dass ich die einmalige Möglichkeit hatte und in seinem Labor mit Präparaten arbeiten durfte sowie für seine tatkräftige Unterstützung bei der Probenherstellung, histologischen Schlifferstellung und vielem mehr.

Für seine erhebliche und unersetzliche Unterstützung, insbesondere bei der Entwicklung der programmatischen Rekonstruktion histologischer Bilddaten, bedanke ich mich vielmals bei Herrn Dipl.-Inform. Samuel John.

Von ganzem Herzen möchte ich dem Programmierer und Mastermind des Visible Ear Simulator, Herrn Peter Trier Mikkelsen (MSc) für seine Unterstützung, die langjährige Zusammenarbeit und mehr als ein Jahrzehnt grenzüberschreitender Freundschaft und Verbundenheit danken.

Ich danke den klinischen Experten, welche uns bei der Bewertung der anatomischen Modelle unterstützt haben, darunter Prof. Peter Roland, Prof. Joachim Müller, Dr. Kristen Rak, Prof. Joachim Schmutzhard, Prof. Paul van de Heyning, Prof. Helge Rask-Andersen, Prof. Rolf Salcher und Prof. Omid Majdani.

Schließlich danke ich meiner Familie, meinen Kollegen und Freunden für ihre Ermutigung diese Arbeit zu beginnen, ihr Verständnis für die vielen Stunden, welche in dieses Projekt geflossen sind und ihren Beistand während der herausfordernden Phasen dieser Arbeit.

Erklärung des Doktoranden

Hiermit erkläre ich, dass ich die Dissertation

Modeling of the human temporal bone for virtual reality surgical training

selbstständig verfasst habe.

Bei der Anfertigung wurden folgende Hilfen Dritter in Anspruch genommen:

Peter Erfurt, Labortechniker, Hilfe bei der Erstellung von histologischen Schliffen und CT Studien

Samuel John, Programmierer, Hilfe bei der algorithmischen Rekonstruktion der Bilddaten

Gabriel Ribeiro dos Santos, Student, Hilfe bei der Datensatzsegmentierung

Daniel Schurzig, Wissenschaftler, Hilfe bei der Manuskriptkorrektur für *Scientific Data*

Peter Trier Mikkelsen, Programmierer, Hilfe bei der Implementierung im Visible Ear Simulator

Steven Arild Wuyts Andersen, Wissenschaftler, Hilfe bei der Manuskriptkorrektur für *O&N*

Mads Sølvsten Sørensen, Zweitbetreuer, Hilfe bei der Manuskriptkorrektur beider Publikationen

Thomas Lenarz, Erstbetreuer, Hilfe bei der Manuskripterstellung für *Scientific Data*

Ich habe keine entgeltliche Hilfe von Vermittlungs- bzw. Beratungsdiensten (Promotionsberater oder anderer Personen) in Anspruch genommen. Niemand hat von mir unmittelbar oder mittelbar entgeltliche Leistungen für Arbeiten erhalten, die im Zusammenhang mit dem Inhalt der vorgelegten Dissertation stehen.

Ich habe die Dissertation an folgenden Institutionen angefertigt:

1.) Medizinische Hochschule Hannover, Carl-Neuberg-Straße 1, D-30625 Hannover
2.) MED-EL Elektromedizinische Geräte GesmbH, Fürstenweg 77A, A-6020 Innsbruck

Die Dissertation wurde bisher nicht für eine Prüfung oder Promotion oder für einen ähnlichen Zweck zur Beurteilung eingereicht.

Ich versichere, dass ich die vorstehenden Angaben nach bestem Wissen vollständig und der Wahrheit entsprechend gemacht habe.

Appendix

Otology & Neurotology – Editor's Letter of Acceptance for Publication

Otology & Neurotology - Supplementary Digital Content

SDC Questionnaire Surgical Experts: Evaluation of the VES3.5 OpenEar scenarios and controls.

SDC Table 1: Average rating of the nine raters for each structure.

Nature Scientific Data - Supplementary Information

Step-by-Step Protocols of OpenEar Creation Process

- Protocol of micro slicing of epoxy embedded temporal bone specimen
- Protocol of creation of target image from image stack
- Protocol of alignment and interpolation of micro slicing data
- Protocol of reconstruction / registration of micro slicing data
- Protocol of segmentation and modeling of anatomy

Date: Jan 13, 2021
To: "Daniel Manuel Sieber" daniel.sieber@medel.com
From: "Otology and Neurotology" marianna.hagan@wolterskluwer.com
Subject: O&N Decision for ON-20-877R2

RE: ON-20-877R2, entitled "OpenEar image data enables case variation in high fidelity virtual reality ear surgery"

Dear Mr Sieber,

I am pleased to inform you that your manuscript has been accepted for publication by Otology & Neurotology. The Editors who reviewed your work felt that it was original and would make a valuable contribution to the Otologic literature.

All manuscript materials will be forwarded to production for placement in an upcoming issue. You will receive additional correspondence from our production team about the progress of your article, but you can expect to receive galley proofs from the production team in about 6-8 weeks.

After corrections have been received, your article will be eligible to publish ahead of print and scheduled for an upcoming issue. To accelerate publication in an issue, some articles may be selected for online only publication. Online articles are still listed in the print table of contents for the selected issue and all papers are indexed the same whether they are in print or online. Should you have any questions about your paper post-acceptance, please do not hesitate to contact the editorial office.

On behalf of the entire Editorial Board, I would like to thank you for submitting your work to Otology & Neurotology.

Your username is: ********
****

Sincerely,

Lawrence Lustig, M.D.
Editor-in-Chief
Otology & Neurotology

OPEN ACCESS INFORMATION
If you indicated in the revision stage that you would like your submission, if accepted, to be made open access, please go directly to step 2. If you have not yet indicated that you would like your accepted article to be open access, please follow the steps below to complete the process:
1. Notify the journal office via email that you would like this article to be available open access. Please send your Email to marianna.hagan@wolterskluwer.com. Please include your article title and manuscript number.
2. A License to Publish (LTP) form must be completed for your submission to be made available open access. Please download the form from http://links.lww.com/LWW-ES/A49, sign it, and Email the completed form to the journal office.
3. **Within 48 hours of receiving this e-mail:** Go to http://wolterskluwer.qconnect.com to pay for open access. If you have not previously used this site to place an order, you will need to register for an account (your login will be different from your Editorial Manager login). When placing your order, you will be asked for the following information. Please enter exactly as shown:
a. Article Title - OpenEar image data enables case variation in high fidelity virtual reality ear surgery
b. Manuscript Number - ON-20-877R2
The cost for publishing an article as open access can be found at https://wkauthorservices.editage.com/open-access/hybrid.html.

Evaluation of the VES3.5 OpenEar scenarios and controls.

Each page contains two images from a drilled mastoidectomy scenario in the Visible Ear Simulator.

Please consider if each structure listed is represented in a way that provides useful visual cues for surgical navigation.

Please rate the quality from 1 (poor-not useful) to 5 (good-sufficient for safe navigation) with X in the following table:

VES 3.5	Score				
Item	1	2	3	4	5
Dura					
Sigmoid sinus					
Lateral semicircular canal					
Incus					
Chorda tympani					
Facial nerve					
Stapes					
Round Window					

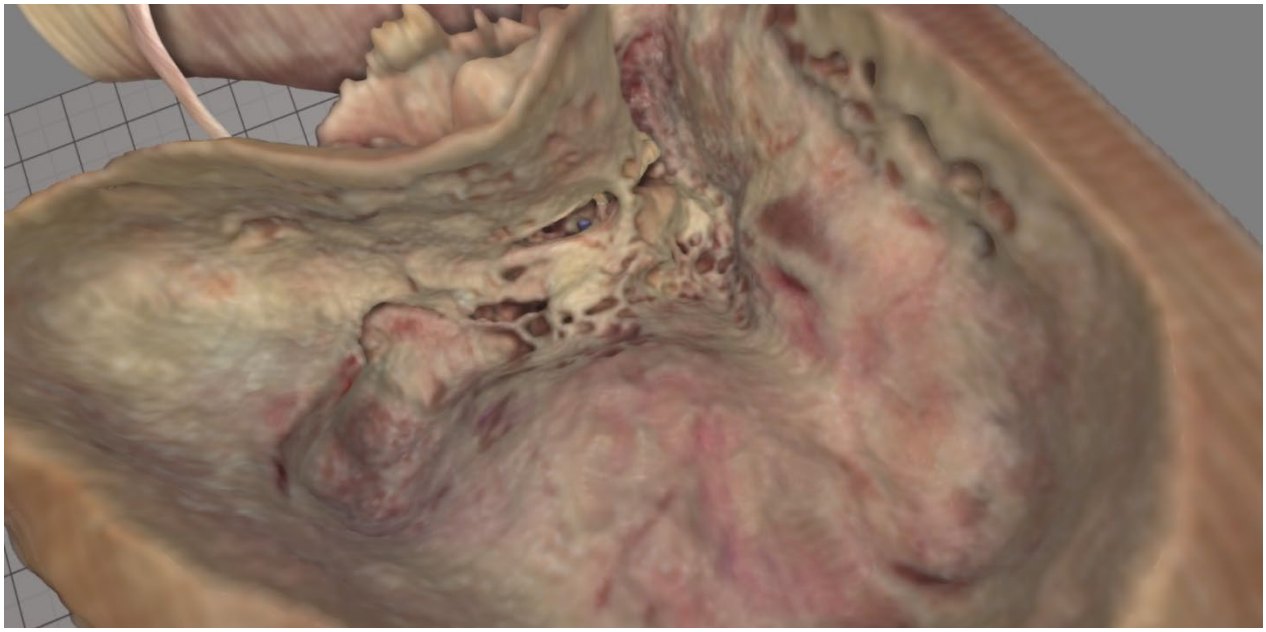

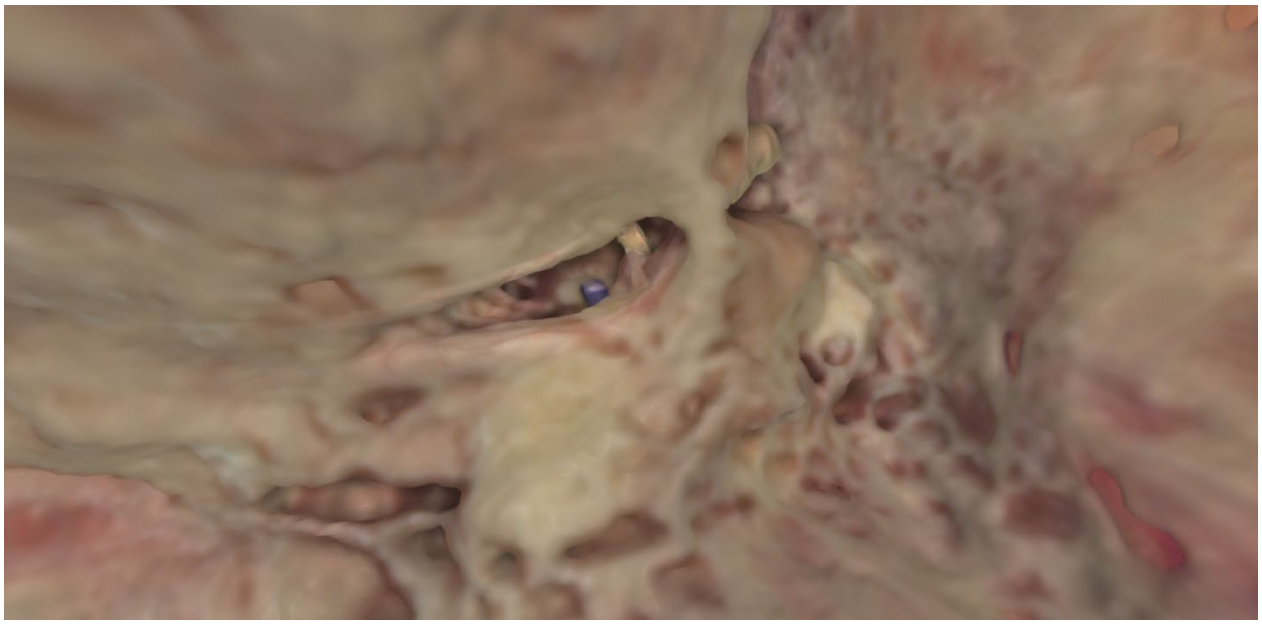

Evaluation of the VES3.5 OpenEar scenarios and controls.

Each page contains two images from a drilled mastoidectomy scenario in the Visible Ear Simulator.

Please consider if each structure listed is represented in a way that provides useful visual cues for surgical navigation.

Please rate the quality from 1 (poor-not useful) to 5 (good-sufficient for safe navigation) with X in the following table:

VES 2.0	Score				
Item	1	2	3	4	5
Dura					
Sigmoid sinus					
Lateral semicircular canal					
Incus					
Chorda tympani					
Facial nerve					
Stapes					
Round Window					

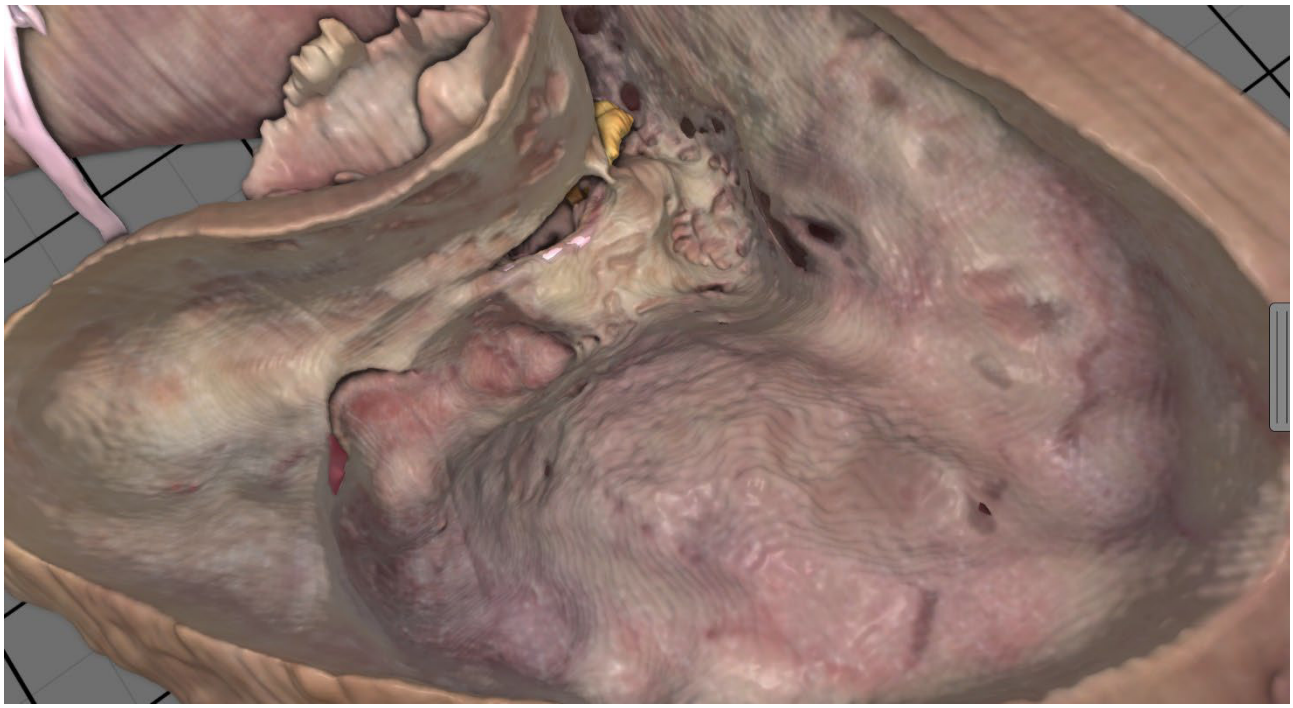

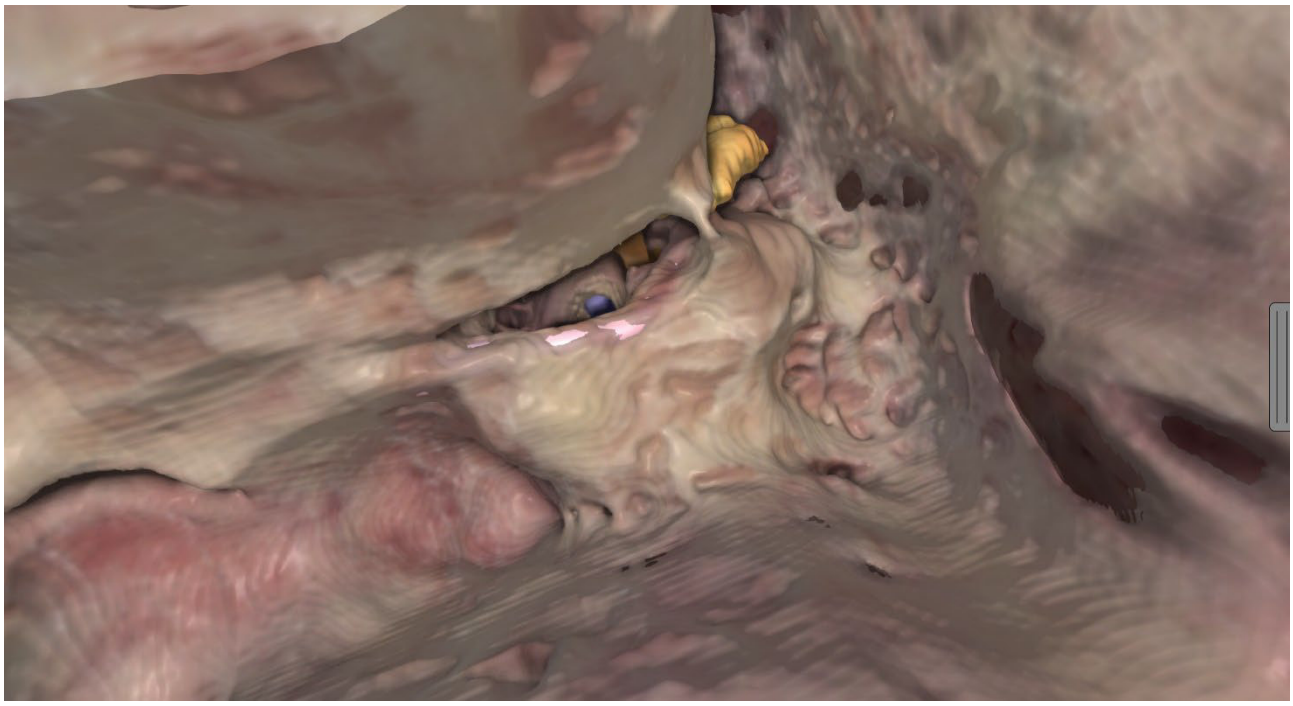

Evaluation of the VES3.5 OpenEar scenarios and controls.

Each page contains two images from a drilled mastoidectomy scenario in the Visible Ear Simulator.

Please consider if each structure listed is represented in a way that provides useful visual cues for surgical navigation.

Please rate the quality from 1 (poor-not useful) to 5 (good-sufficient for safe navigation) with X in the following table:

VES 1.3	Score				
Item	1	2	3	4	5
Dura					
Sigmoid sinus					
Lateral semicircular canal					
Incus					
Chorda tympani					
Facial nerve					
Stapes					
Round Window					

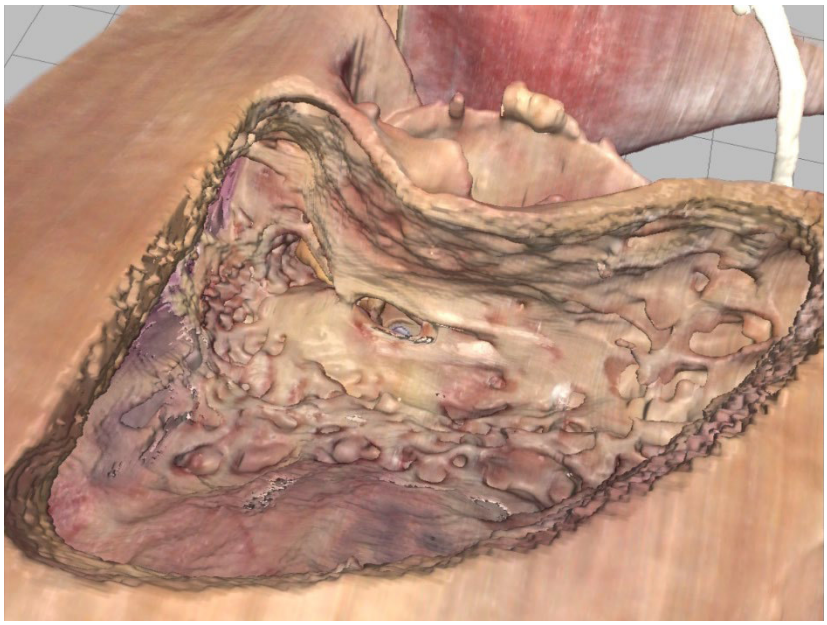

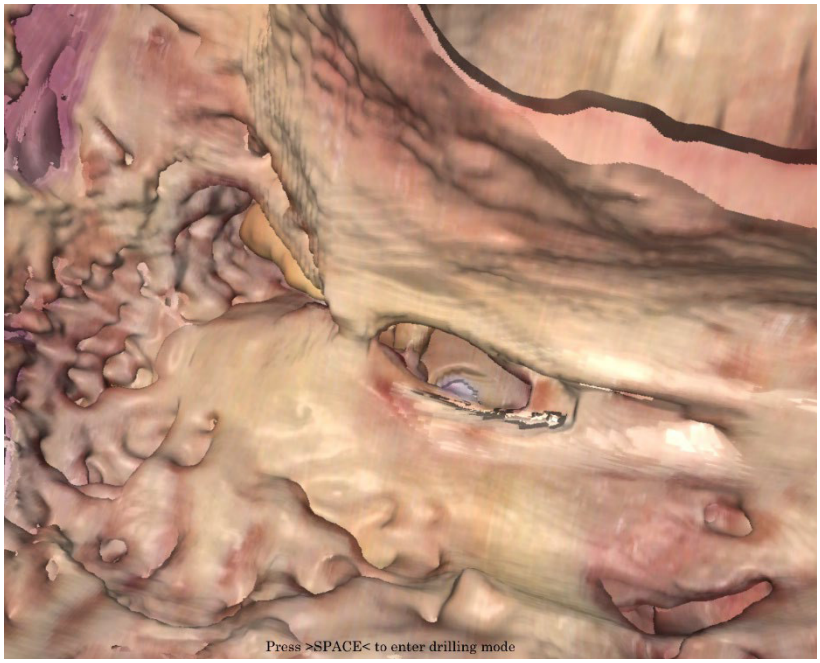

Evaluation of the VES3.5 OpenEar scenarios and controls.

Each page contains two images from a drilled mastoidectomy scenario in the Visible Ear Simulator.

Please consider if each structure listed is represented in a way that provides useful visual cues for surgical navigation.

Please rate the quality from 1 (poor-not useful) to 5 (good-sufficient for safe navigation) with X in the following table:

Delta	Score				
Item	1	2	3	4	5
Dura					
Sigmoid sinus					
Lateral semicircular canal					
Incus					
Chorda tympani					
Facial nerve					
Stapes					
Round Window					

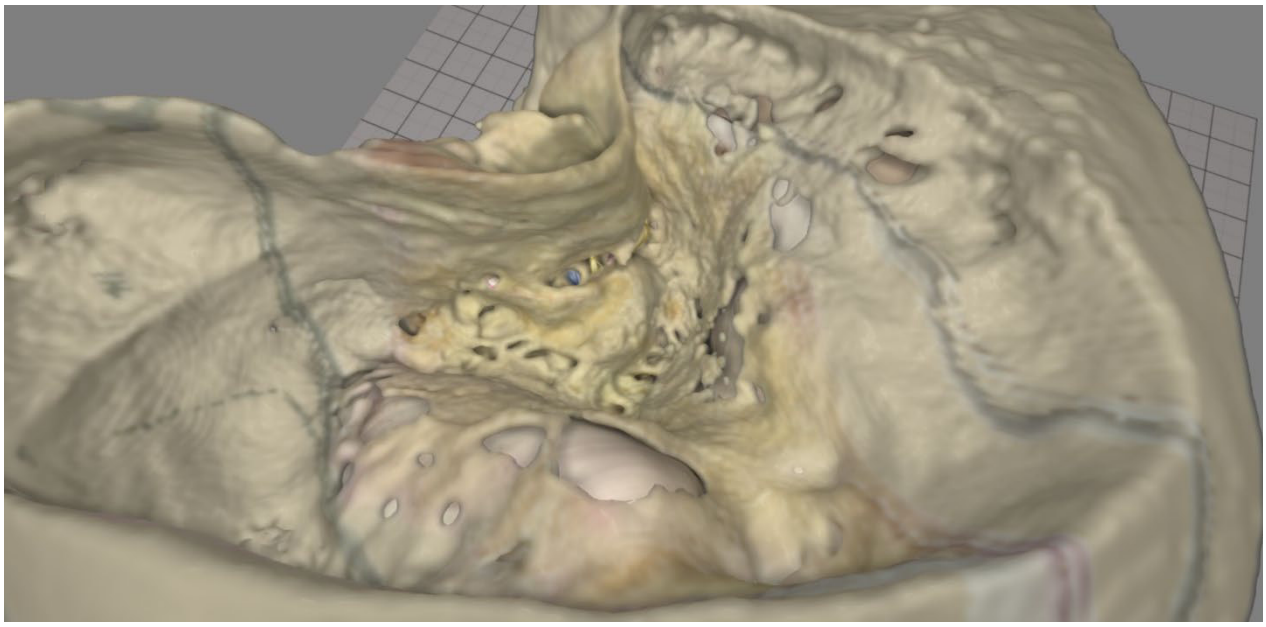

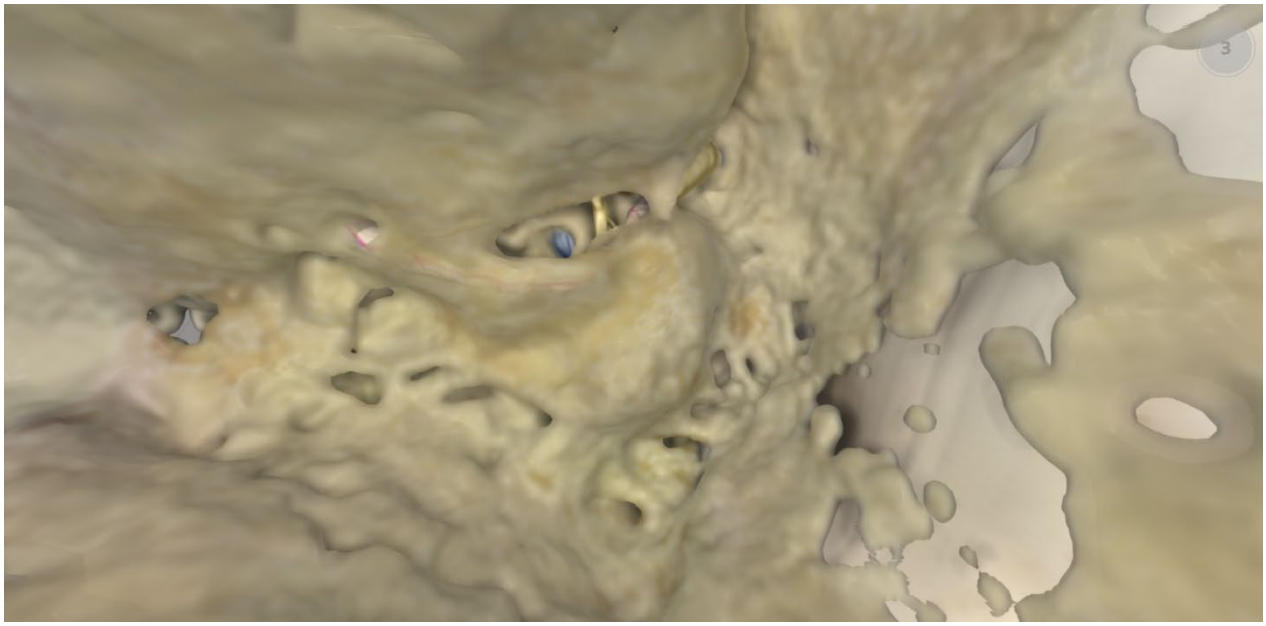

Evaluation of the VES3.5 OpenEar scenarios and controls.

Each page contains two images from a drilled mastoidectomy scenario in the Visible Ear Simulator.

Please consider if each structure listed is represented in a way that provides useful visual cues for surgical navigation.

Please rate the quality from 1 (poor-not useful) to 5 (good-sufficient for safe navigation) with X in the following table:

DeltaHR	Score				
Item	1	2	3	4	5
Dura					
Sigmoid sinus					
Lateral semicircular canal					
Incus					
Chorda tympani					
Facial nerve					
Stapes					
Round Window					

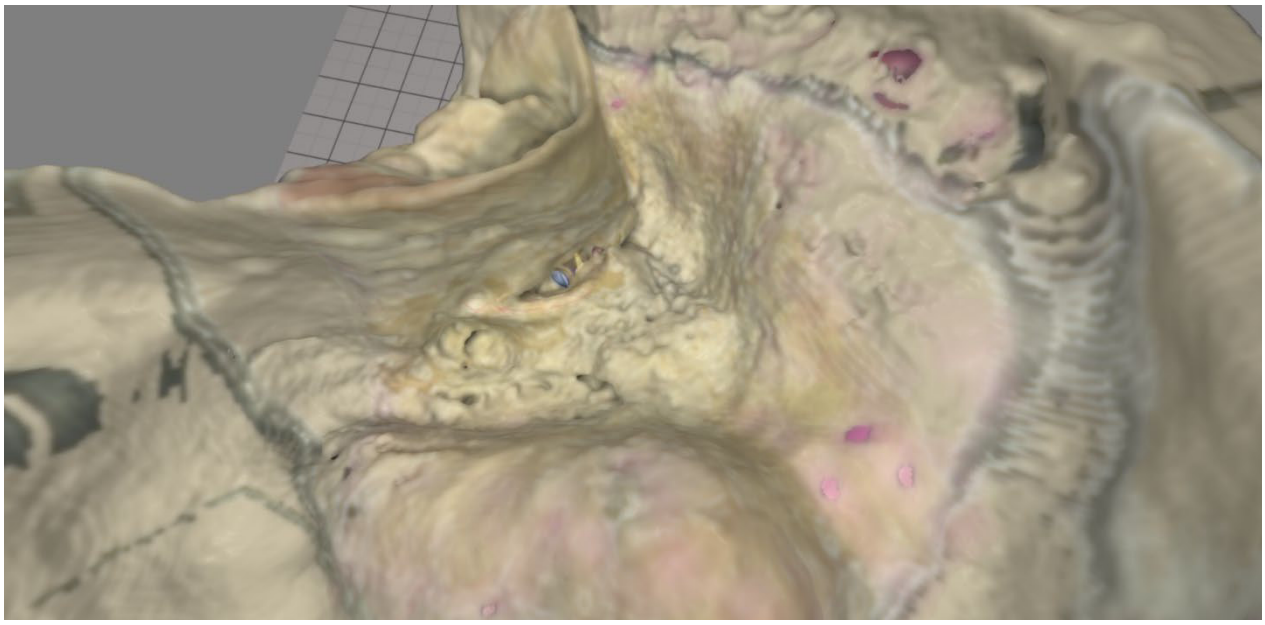

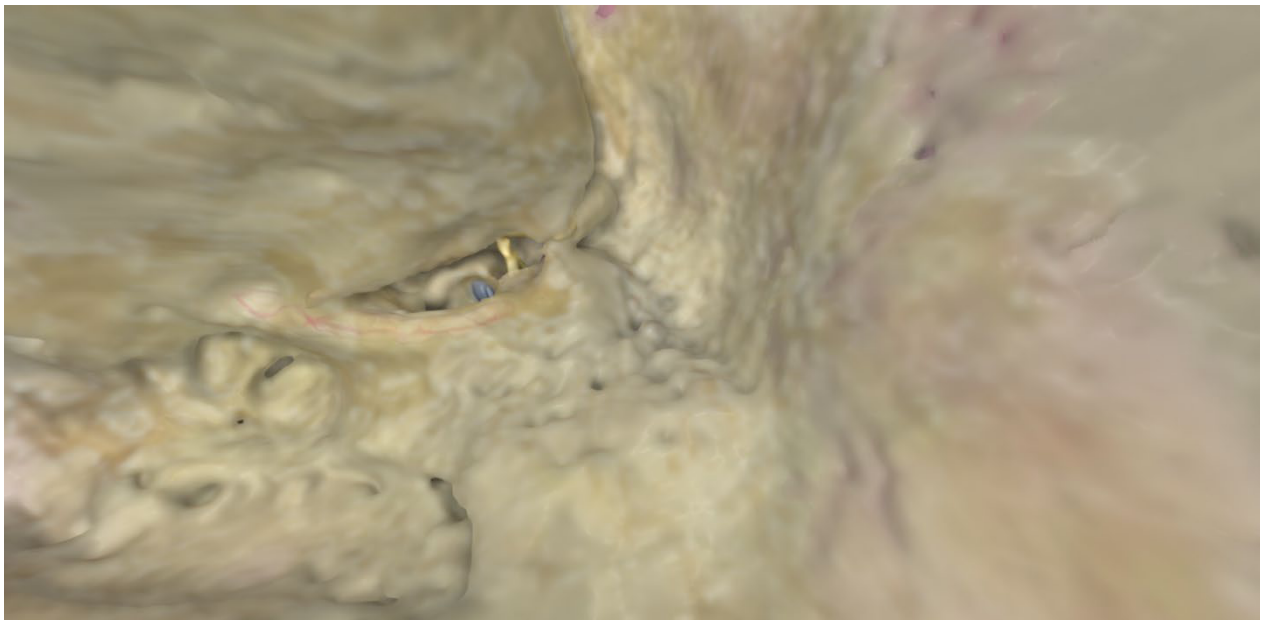

Evaluation of the VES3.5 OpenEar scenarios and controls.

Each page contains two images from a drilled mastoidectomy scenario in the Visible Ear Simulator.

Please consider if each structure listed is represented in a way that provides useful visual cues for surgical navigation.

Please rate the quality from 1 (poor-not useful) to 5 (good-sufficient for safe navigation) with X in the following table:

DeltaHRP	Score				
Item	1	2	3	4	5
Dura					
Sigmoid sinus					
Lateral semicircular canal					
Incus					
Chorda tympani					
Facial nerve					
Stapes					
Round Window					

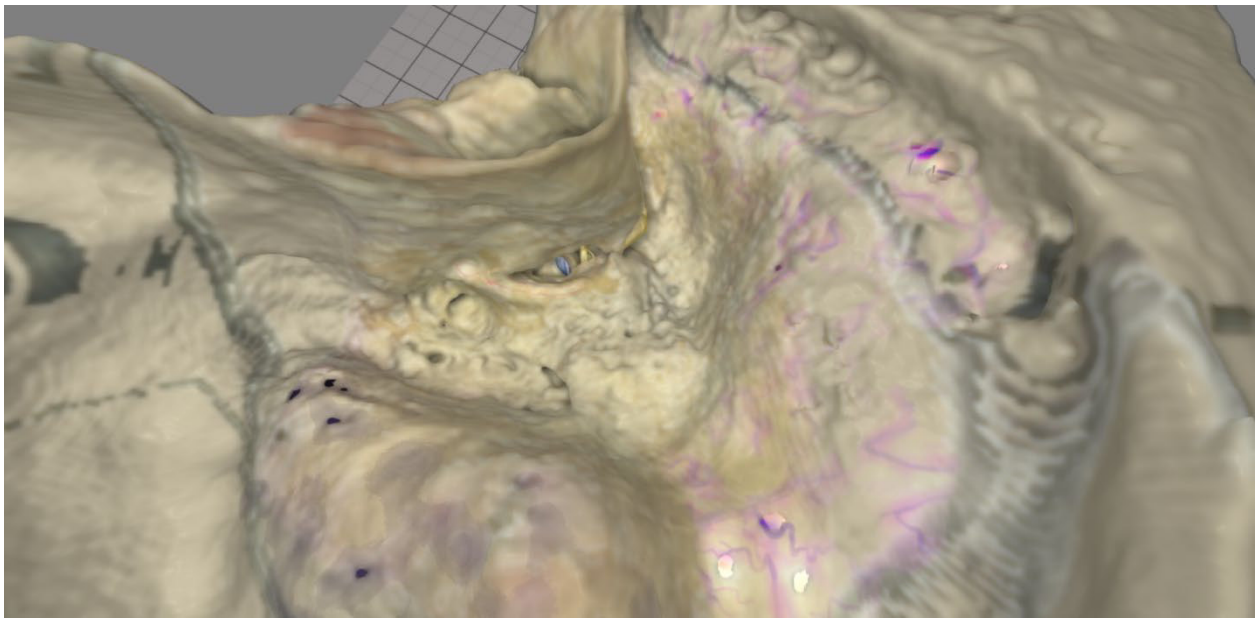

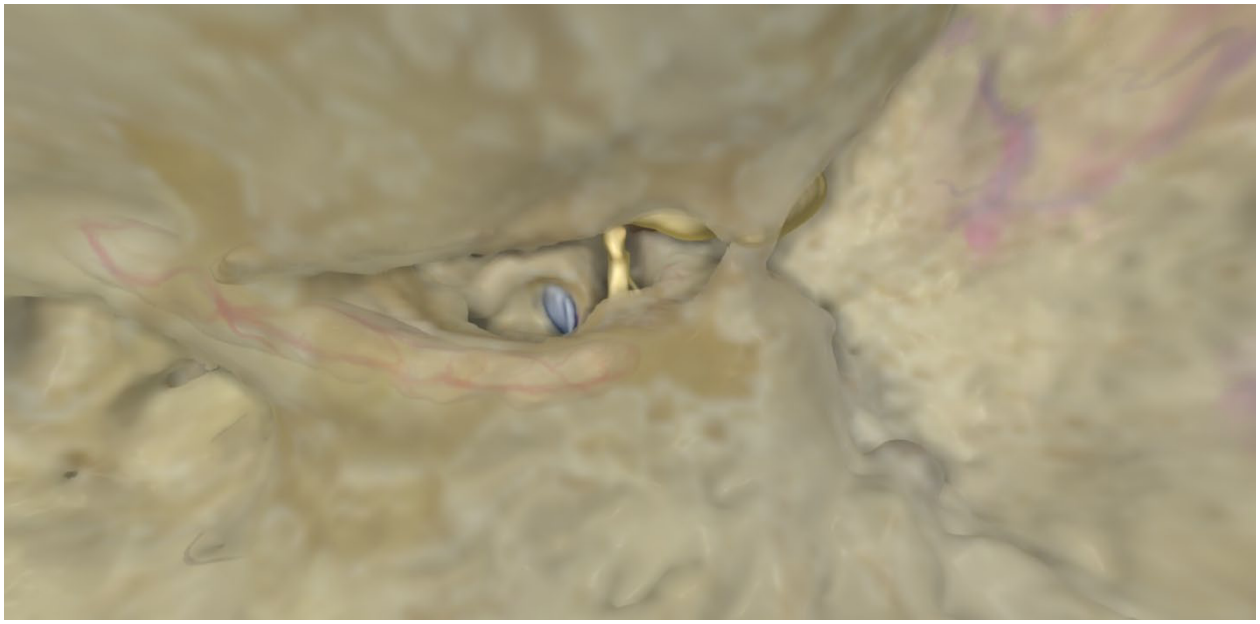

Evaluation of the VES3.5 OpenEar scenarios and controls.

Each page contains two images from a drilled mastoidectomy scenario in the Visible Ear Simulator.

Please consider if each structure listed is represented in a way that provides useful visual cues for surgical navigation.

Please rate the quality from 1 (poor-not useful) to 5 (good-sufficient for safe navigation) with X in the following table:

Epsilon	Score				
Item	1	2	3	4	5
Dura					
Sigmoid sinus					
Lateral semicircular canal					
Incus					
Chorda tympani					
Facial nerve					
Stapes					
Round Window					

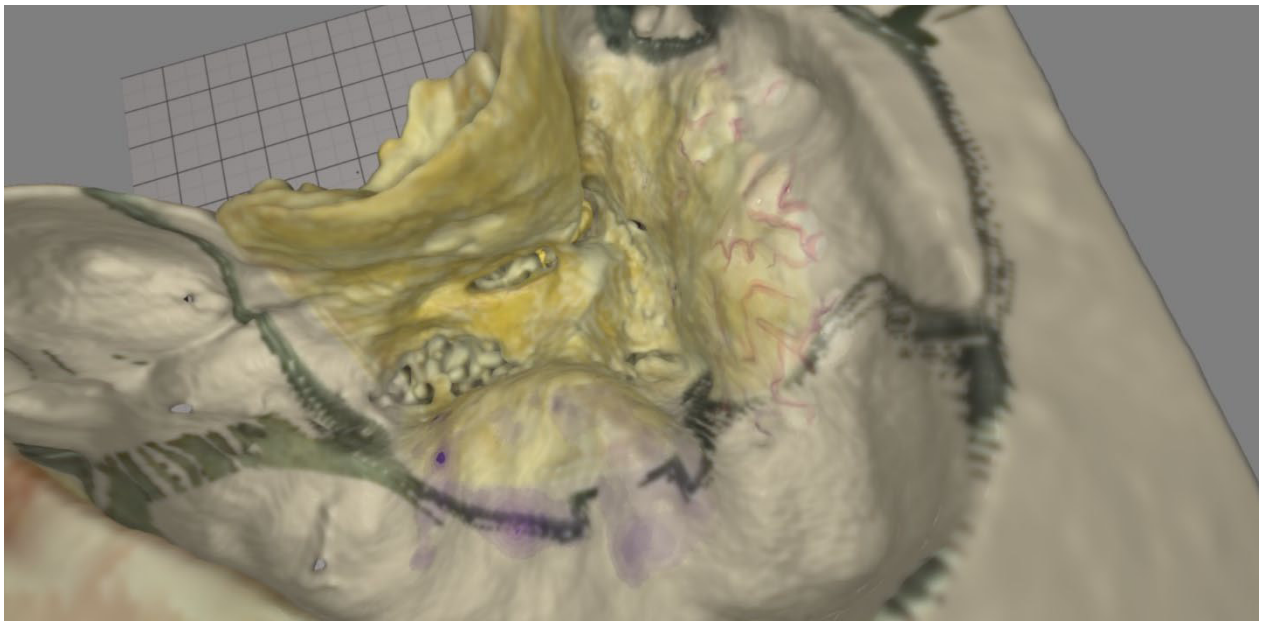

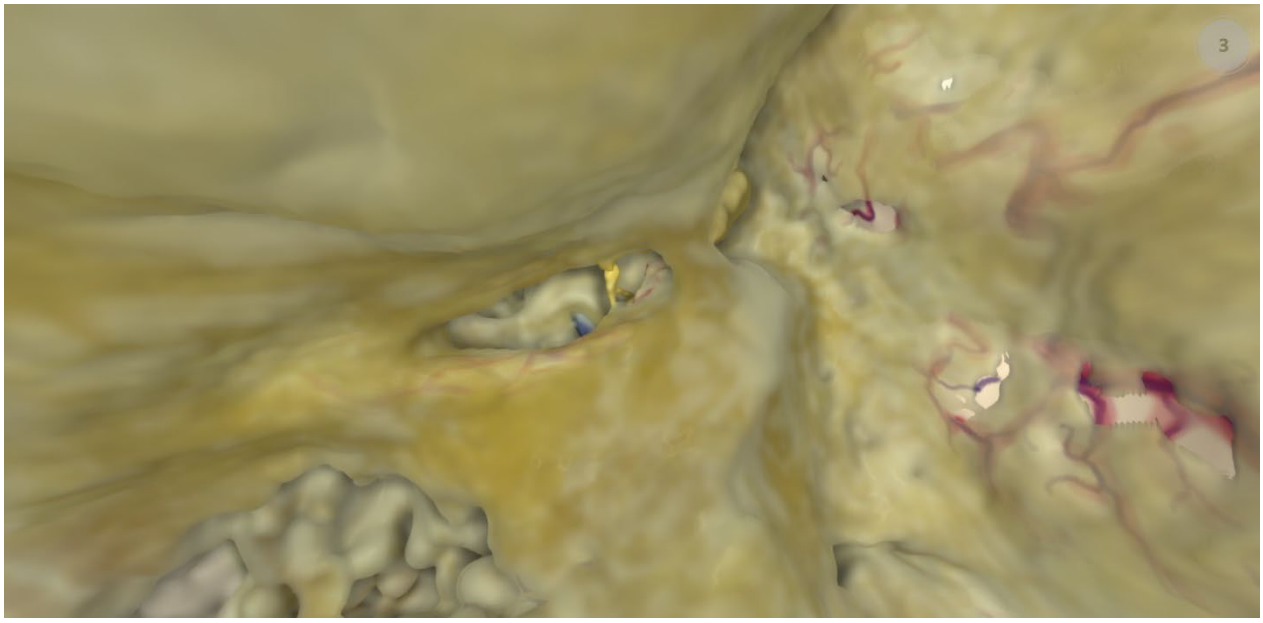

Evaluation of the VES3.5 OpenEar scenarios and controls.

Each page contains two images from a drilled mastoidectomy scenario in the Visible Ear Simulator.

Please consider if each structure listed is represented in a way that provides useful visual cues for surgical navigation.

Please rate the quality from 1 (poor-not useful) to 5 (good-sufficient for safe navigation) with X in the following table:

Eta	Score				
Item	1	2	3	4	5
Dura					
Sigmoid sinus					
Lateral semicircular canal					
Incus					
Chorda tympani					
Facial nerve					
Stapes					
Round Window					

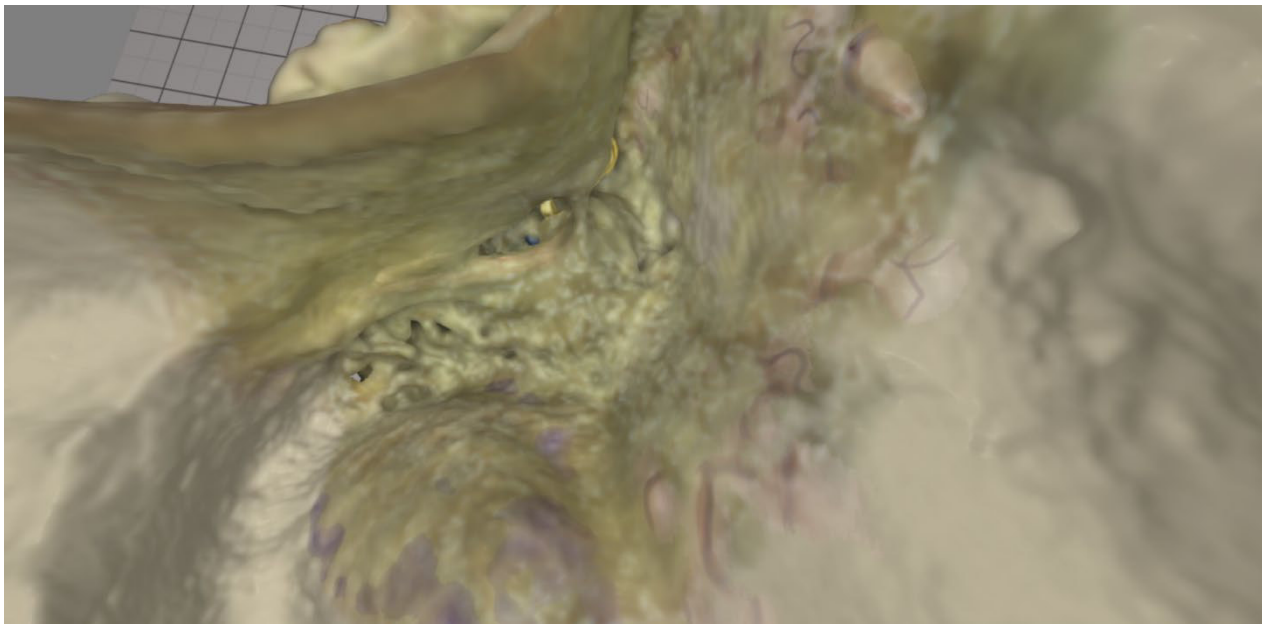

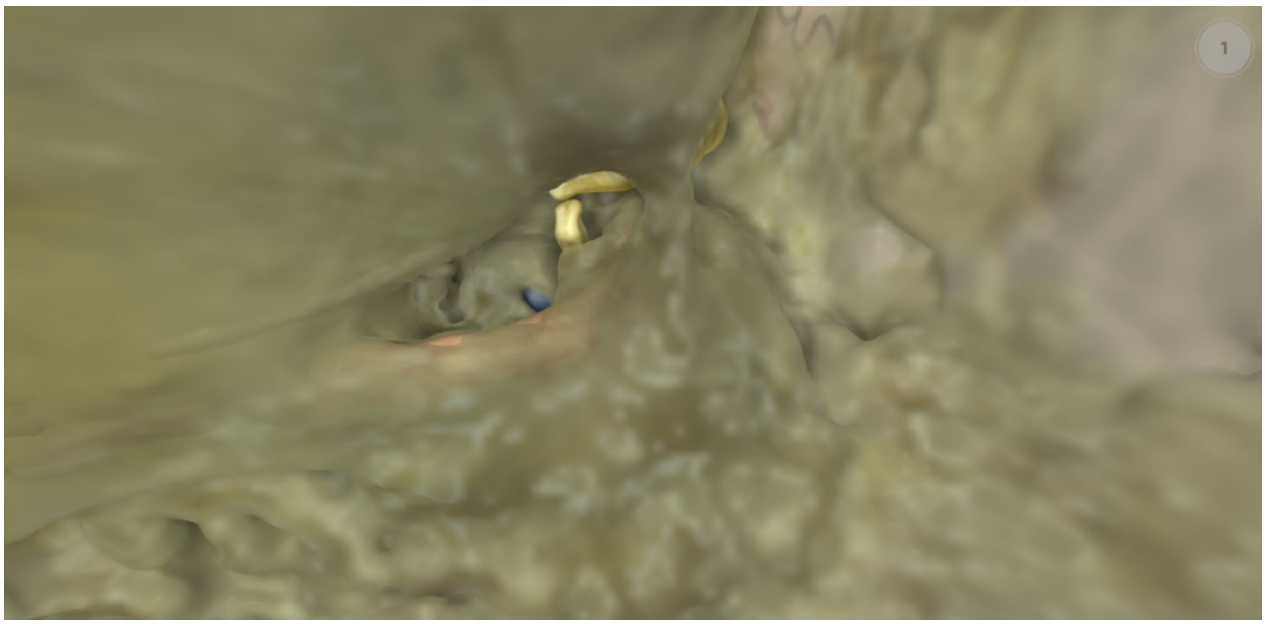

Evaluation of the VES3.5 OpenEar scenarios and controls.

Each page contains two images from a drilled mastoidectomy scenario in the Visible Ear Simulator.

Please consider if each structure listed is represented in a way that provides useful visual cues for surgical navigation.

Please rate the quality from 1 (poor-not useful) to 5 (good-sufficient for safe navigation) with X in the following table:

Gamma	Score				
Item	1	2	3	4	5
Dura					
Sigmoid sinus					
Lateral semicircular canal					
Incus					
Chorda tympani					
Facial nerve					
Stapes					
Round Window					

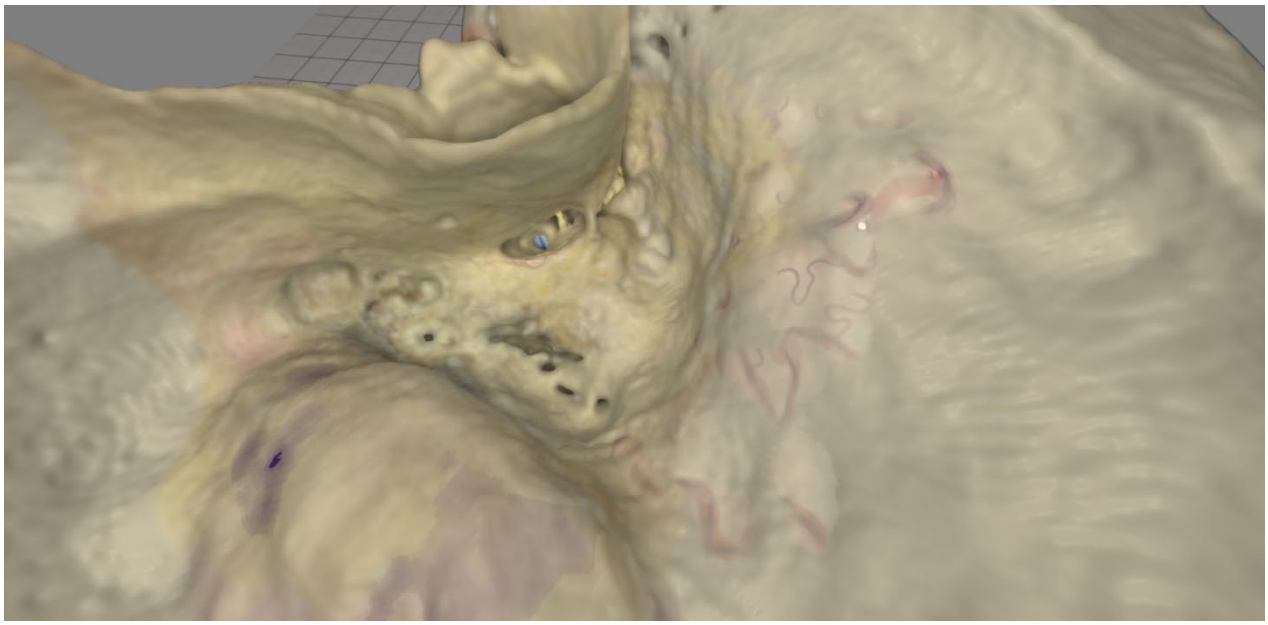

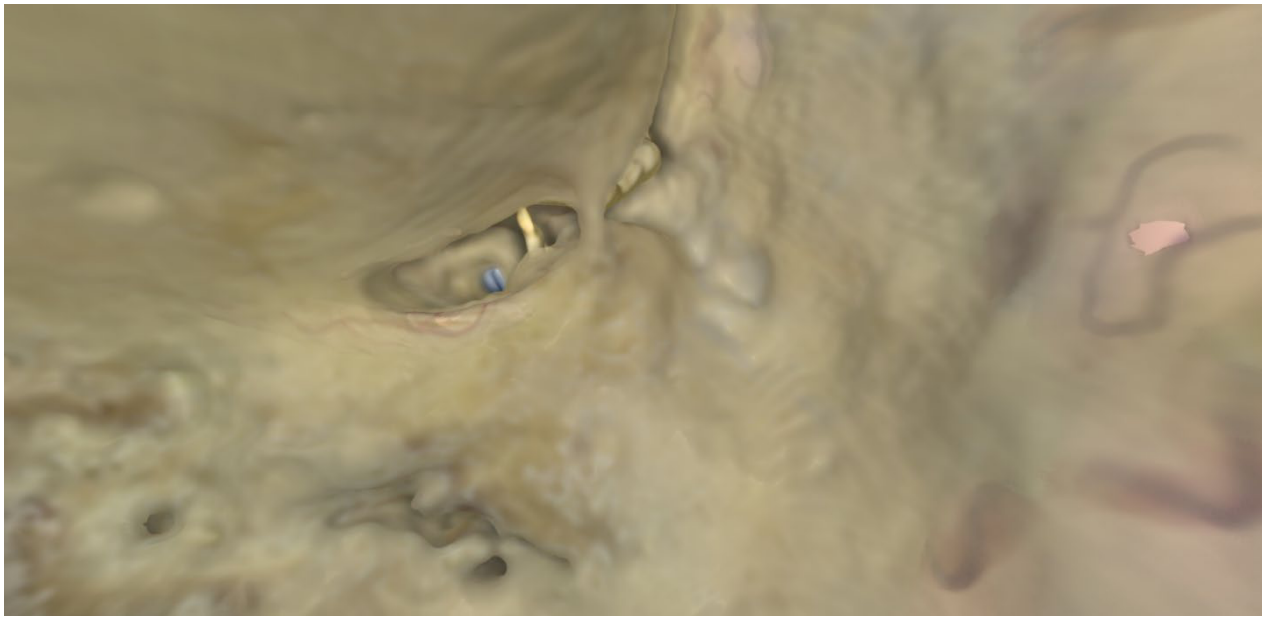

Evaluation of the VES3.5 OpenEar scenarios and controls.

Each page contains two images from a drilled mastoidectomy scenario in the Visible Ear Simulator.

Please consider if each structure listed is represented in a way that provides useful visual cues for surgical navigation.

Please rate the quality from 1 (poor-not useful) to 5 (good-sufficient for safe navigation) with X in the following table:

Theta	Score				
Item	1	2	3	4	5
Dura					
Sigmoid sinus					
Lateral semicircular canal					
Incus					
Chorda tympani					
Facial nerve					
Stapes					
Round Window					

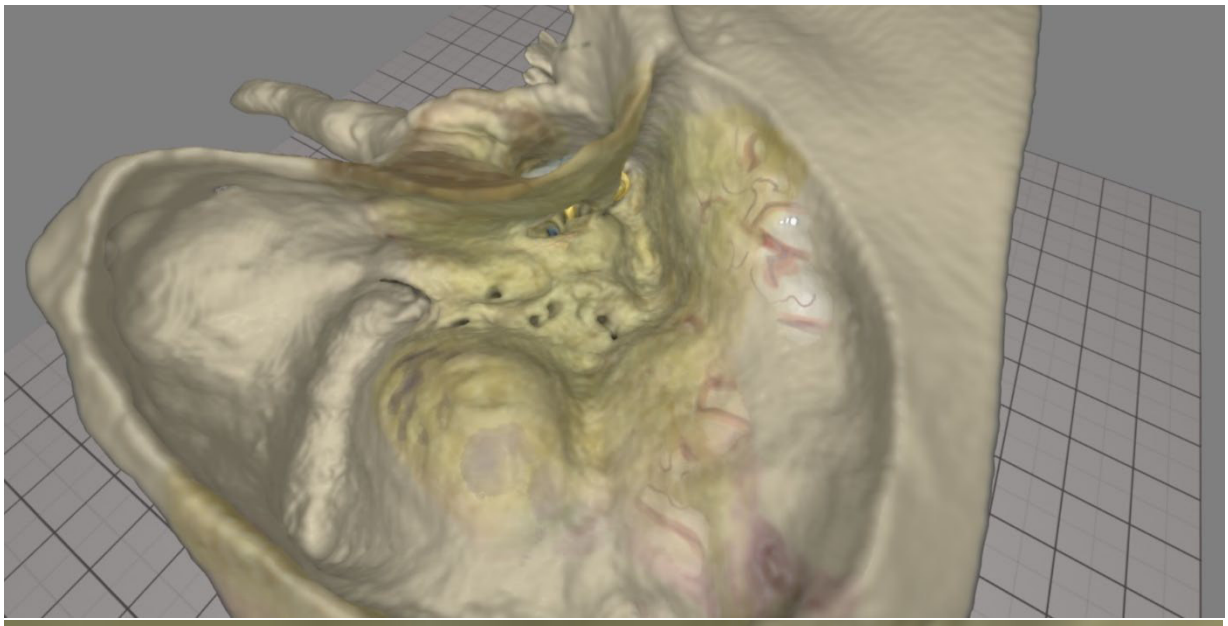

Evaluation of the VES3.5 OpenEar scenarios and controls.

Each page contains two images from a drilled mastoidectomy scenario in the Visible Ear Simulator.

Please consider if each structure listed is represented in a way that provides useful visual cues for surgical navigation.

Please rate the quality from 1 (poor-not useful) to 5 (good-sufficient for safe navigation) with X in the following table:

Zeta	Score				
Item	1	2	3	4	5
Dura					
Sigmoid sinus					
Lateral semicircular canal					
Incus					
Chorda tympani					
Facial nerve					
Stapes					
Round Window					

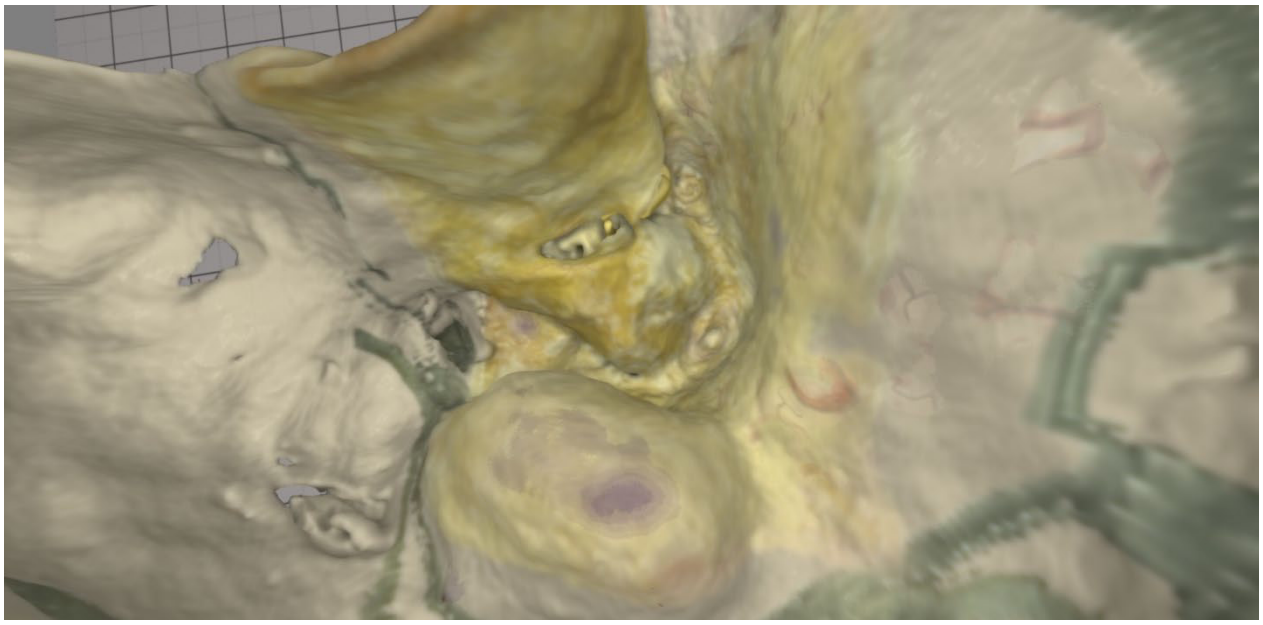

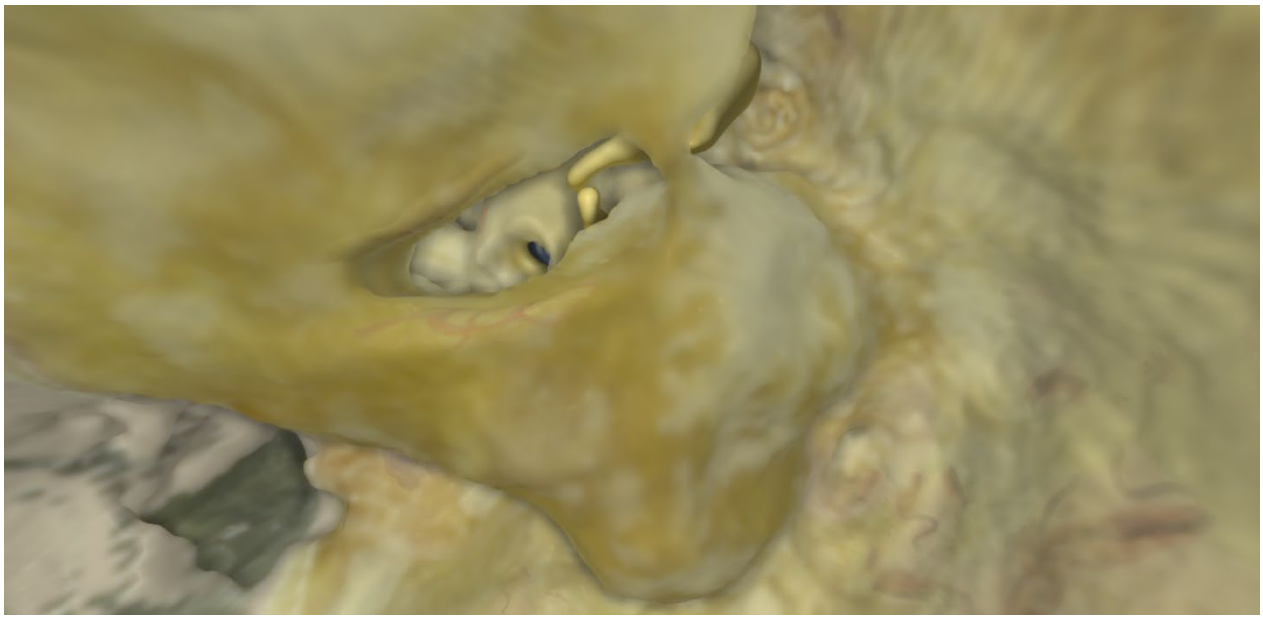

Supplemental table 1. Average rating of the nine rater for each structure.

Model	VES 3.5	VES 2.0	VES 1.3	Delta	Delta HR	Delta HRP	Epsilon	Eta	Gamma	Theta	Zeta
Average rating	4.2	3.8	3.7	3.4	3.6	4.1	3.9	3.7	3.9	4.0	3.8
Dura	3.8	3.3	2.8	3.2	3.8	4.6	4.4	3.6	4.0	4.6	4.1
Sigmoid sinus	3.9	3.3	2.8	3.9	4.1	4.4	4.0	3.6	4.2	3.8	3.8
Lateral semicircular canal	3.9	3.8	3.6	3.4	2.7	3.0	3.6	2.7	3.8	3.6	3.4
Incus	3.9	4.7	4.3	2.7	3.0	3.7	4.0	3.8	3.8	3.7	3.9
Chorda tympani	4.8	3.0	4.4	2.3	2.6	3.1	3.4	3.9	2.9	3.8	3.2
Facial nerve	4.7	4.0	4.1	3.8	4.6	4.7	4.3	4.3	4.0	4.2	3.9
Stapes	4.1	3.4	3.3	3.7	3.8	4.2	3.8	3.8	4.2	3.8	3.6
Round window	4.8	4.6	3.9	4.4	4.1	4.8	4.0	4.3	4.4	4.4	4.3

Supplementary Information:

Step-by-Step Protocols of OpenEar Creation Process

1. Protocol of micro slicing of epoxy embedded temporal bone specimen
2. Protocol of creation of target image from image stack
3. Protocol of alignment and interpolation of micro slicing data
4. Protocol of reconstruction / registration of micro slicing data
5. Protocol of segmentation and modelling of anatomy

Protocol of micro slicing of epoxy embedded temporal bone specimen

Aim

The aim of this process step is to acquire two dimensional images of an epoxy embedded temporal bone specimen at as many positions along the long axis of the specimen as possible. This is achieved by repeated grinding off a defined layer thickness from the specimen, and subsequent imaging by 2D optical microscopy. The layer thickness chosen is a compromise between the level of detail to be obtained and the time it takes to process specimen. Processing several specimens at the same time may improve the efficiency of the process but add risk of errors/mixup during the process.

Materials

- Buehler AutoMet250 with custom made specimen holder

- CarbiMet P1200 self-adhesive sand paper

- Keyence VHX-2000 with VH-Z20UR lens

- Micrometer DIN863 Set for 10-70mm

- Pressure air

Time planning

After a certain learning curve, about seven minutes per slice were needed

Protocol

<u>Setup Phase</u>

1. Setup Microscope
    - Initialize X/Y Stage and Autofocus “Automatically”
    - Adjust “Camera Settings”
        - Shutter: 1/60 sec
        - Gain: 0 dB
        - White Balance: Use the “Push Set” option placing and focusing a piece of white paper at approx. the same operating distance as the specimen
2. Setup Grinding Machine
    - Adjust Settings
        - Depth: 0.2 mm
        - Pressure: “ZAXIS”, 45N

    - Probe RPM: 40
    - Disc RPM: 500
    - Mode: “COMP”
    - Check in “WATER” Menu that “STAGE” is set to “ON”
    - Mount specimen in specimen holder with minimal hand torque
3. Setup Micrometer Screw
    - Use probes to ensure calibration is ok
    - Mount micrometer to allow for comfortable working

Slicing Phase

Before starting slicing, please make sure that everything that you need to perform the steps below is ready for many hours of work. Keep in mind that the following steps will be of destructive nature and cannot be reversed. A CBCT scan has to therefore be performed before starting the slicing process. To avoid deformations of the specimen mounting them in the specimen holder the epoxy embedding should have hardened at least 1-2 weeks.

1. Mount the specimen into the specimen holder and tighten screws carefully to avoid deformation of the specimen. In case of not using all slots in the specimen holder, use dummy epoxy overmolds to avoid any unbalanced mass.
2. Attach specimen holder to grinding machine
3. Start grinding machine
4. After completion of grinding dry the specimens
    - Dry specimen holder and specimens roughly using cotton blanket
    - Dry specimens surface and edges carefully using paper towel
    - Clean surface of specimens using pressure air
    - Visually check surfaces for remaining particles and remove if any are found
5. Make sure microscope’s X/Y table is centered
6. Position the specimen holder horizontally under microscope
7. Align specimen 1 to be roughly concentric with the light source of the microscope
8. Perform autofocus on specimen 1
9. Check result of autofocus procedure visually
10. Set borders of 2D image stitching functionality
11. Start 2D image stitching

12. Replace sandpaper on grinding machine while waiting for image stitching
13. Save image file for specimen 1 (Naming: 000.TIF, 001.TIF, 002.TIF and so on…)
14. Repeat steps 5-13 (not step 12) for specimen 2 and all further specimen accordingly
15. Measure remaining specimens height for all specimen and document in excel sheet
16. Check after every slice that enough specimen is sticking out of the specimen holder. Reposition the specimen when needed and carefully tighten screws at lowest possible torque to avoid deformation of specimen
17. Repeat steps 2-16 until the entire temporal bone is gone, or it becomes impossible to further advance and reposition the specimens in the specimen holder

Protocol of creation of target from image stack

Aim

The aim of this process step is to create a target image which can later be used to align all images from a micro slicing dataset. The alignment is performed by identifying and aligning the outline of the epoxy overmold in all images of the dataset. Therefore, a target image which is reduced to only contain the epoxy overmold outline information has to be created.

Materials

- WACOM Pen Digitizer Tablet Small (Model CTL-480 was used here)
- Gnu Image Manipulation Program (GIMP) version 2.8
- "Offset Path" script by user "RobA" available from http://www.silent9.com/incoming/scripts/ (version 2013-04-24)
- Micro slicing images, see "Protocol of micro slicing of epoxy embedded temporal bone specimen"

Installation

- Install GIMP
- Copy the offset_path.scm script into the GIMP scripts folder where all other '.scm' files are located

Protocol

1. Choose an image from the micro slicing
    - Preferably from a central position in the image stack
    - Try to choose a slice with minimal defects in the overmold outline
        - No air bubbles
        - No dust/grinding particles
        - No major deformations
2. Load the respective .tif file from the micro slicing to GIMP2
3. In the "Import from TIFF" dialog choose to import "Page 1"
4. Go to "Layer" -> "Transparency" -> "Add Alpha Channel" to add a transparency variable per pixel
5. Go to "Layer" -> "Duplicate Layer" to add a backup up of the original image
6. Go to "Tools" -> "Path" to activate the Paths module
7. Increase Zoom factor to 400%
8. Create a path along the outline of the overmold outline by left clicking on it using the Wacom digitizer; To correct mistaken points use "Strg+Shift" to delete them and draw a new point
9. To close the path after drawing the last point hold the "Strg" key and click on the first point again
10. Rename the path just created to "Outline"

11. Right click on the Outline path in the Paths Dialog and choose Offset Paths to run the script by RobA. Create and rename two new paths, one which is bigger and one which is smaller than the original outline. An offset of 20-50 pixels symmetric in both directions has proven to be good. For histologies with more deformation 50 is the better choice, for histologies with no visible outline deformation 20 seems the best choice. To get a “one fits all” process we ended up using a two-step process with a 50 target to search the rough outline, and a 20 target to find the precise outline.
12. Check the offset outline paths for points which were not correctly transformed. Such points can be moved by drag and drop or deleted using Strg+Shift.
13. Select the smaller outline and go to “Select” -> “From path”,
14. Go to “Select” -> “Feather” and choose a feathering of 5px
15. Go to “Edit” -> “Cut”. You should now see everything inside of the inner outline checkerboard style
16. Select the larger outline and go to “Select” -> “From path”
17. Go to “Select” -> “Invert”, feather as before, cut as before
18. Go to “Image” -> “Autocrop Image”
19. Now you may add rotation to the target. Rotating the target may help to overcome false minima in the search operation to find the outline in the image. These come from the fact that the original unrotated target is not interpolated, whereas all the other transformations of the target are interpolated pictures. So the unrotated image might be considered the best fit, just because it is not interpolated and results in a false low penalty function result. Rotating the target by 45° makes sure that all transformed picture undergo the same interpolation degradation eliminating the error source. In a two-step process the second step target must be vertical oriented again. To add rotation do the following:
    a. Go to “Tools” -> “Transform Tools” -> “Rotate” and rotate the image 45° (Make sure the Layer is selected in the Layers Dialog and in the “Tool Options” there is also “Layers” selected
    b. Right-click on the Outline path and select “Duplicate Path”
    c. Rename the new path to “Outline rotated”
    d. Switch “Tool Options” to “Path”, and use the rotate tool again to rotate the “Outline rotated” path by 45°
20. Go to “Image” -> “Canvas Size” and enter an odd number of pixels for both directions (e.g. 3701x3701px), click on “Center” in the “Offset” dialog
21. Export the target image by going to “File” -> “Export As”, set File Type to “PNG Image (*.png)”
22. In the Export dialog deactivate “Save background color” and “save color values from transparent pixels”
23. Export the path by right clicking on Outline rotated and selecting “Export Path”, use .SVG as filesuffix
24. Save your entire work by clicking “File” -> “Save as”

Protocol of alignment and interpolation of micro slicing data

Aim

The aim of this process step is to align all images of a micro slicing dataset by alignment along the epoxy overmold outline and subsequent interpolation of the images to allow 3D reconstruction of the dataset. Image alignment is performed by combination of a constrained brute search global optimization algorithm with a subsequent local optimization to find the transformation between target image and search image. Interpolation is performed using a virtual image stack which is filled with the acquired images from micro slicing and in which any slices which remain empty are then interpolated from the surrounding images.

Materials

- Micro slicing images, see “Protocol of micro slicing of epoxy embedded temporal bone specimen”
- Protocol of specimen height progression, see “Protocol of micro slicing of epoxy embedded temporal bone specimen”
- Target Image, see “Protocol of creation of target from image stack”
- Anaconda Python distribution plus several packages as listed below
- Python scripts and iPython Notebooks from Zenodo/Github

Installation

1. Make sure to install an up-to-date GPU driver and have an OpenCL compatible GPU
2. Install an up to date browser e.g. Firefox
3. Install Anaconda (Version used was Anaconda 3 2.5.0 64bit)
4. Install Anaconda packages (many downloadable from Christoph Gohlke’s web page) using the “pip install” function:
    - Appdirs (version used was 1.4.0)
    - Pytools (version used was 2016.1)
    - Pyopencl (version used was 2015.2.4)
    - Svg.path (version used was 2.1.1)
5. Download the versions of “pattern_finder_gpu” and “reconstruct_volume_from_RGB_slices” used to create the published dataset from Zenodo:
   https://doi.org/10.5281/zenodo.1344923
   https://doi.org/10.5281/zenodo.1400785
   Check the Github displayed on the respective Zenodo pages to check for potential updated versions on Github.

Protocol

Image alignment

1. Launch Anacondas “jupyter” GUI and open the “reconstruct_volume_from_RGB_slices.ipynb” notebook from the repository to perform image stack alignment
2. Scroll down to the “Start of main script” section and adjust the paths to the situation on your PC:
    - Set the path to the target image .PNG file
      (See “Protocol of creation of target from image stack”)
    - Set the path to the target outline .SVG file
      (See “Protocol of creation of target from image stack”)
    - Set the path to the folder containing all .TIF files from one micro slicing series
      (See “Protocol of micro slicing of epoxy embedded temporal bone specimen”)
3. In the “Definition of Search Strategy” adjust settings of the alignment
    - Rescale: Value for downsampling of the image (bigger than 0 and smaller or equal to 1= full res). To save computation time reduce this value, to increase accuracy increase this value.
    - Angle Range to search in during brute force optimization. Format: (Start_Angle, End_Angle, No of steps in between), Choose the search range large enough to be confident to be able to find the most rotated image of the stack. Subsequent steps will build on the best position found in previous steps, so search range is symmetrical to zero typically. Set number of steps sufficiently high to get a smooth curve plot for rotation vs. error value for plot = True or plot=’all’ as shown below

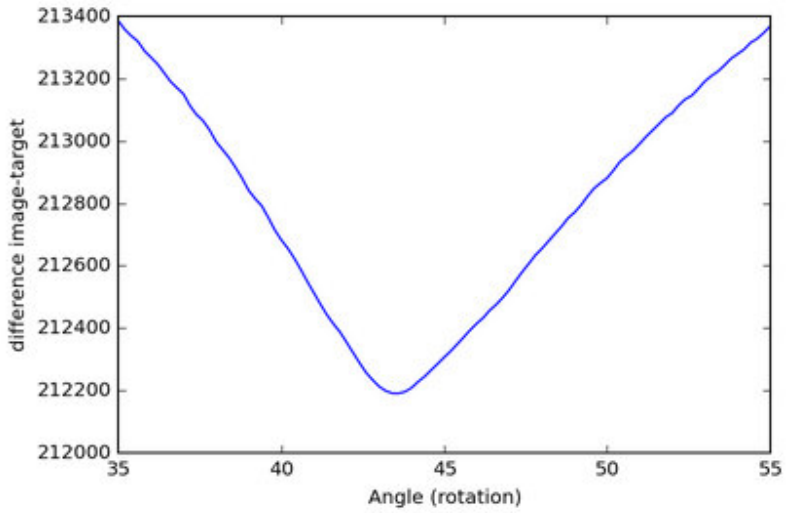

    - ROI Size for brute force optimization. Make sure the ROI is large enough, to allow for finding of the pattern in image. Check the heat plot in plot=’all’ to make sure it looks somewhat like below. Note that rescaling between steps can make a larger ROI

necessary even though the image is already aligned pretty well from previous steps.

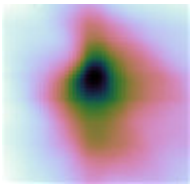

- Tolerance in local optimization: The higher the value, the faster the computation, the lower the value, the more accurate the result

4. In the "Execution of Image Alignment" section, adjust parameters to the situation on your PC:
   - Set the write_files variable to the path that aligned images shall be written to. Set it to 'False' if you do not want to write files to disc
   - Set the plot variable to "False", "True" or "all" to set the level of feedback you want to get from the optimization process
5. In jupyter choose "Cell"->"Run All" from the dropdown menu
6. The computation will now be performed for every image of the image stack. This can take several minutes to several days, depending on the settings chosen above. If errors occur, try to debug. If unsuccessful, contact the authors of the code (Daniel Sieber, Samuel John).

<u>Image Interpolation</u>

7. Next is the interpolation of the micro slicing images to create a homogeneously distanced image stack as required by most medical 3D viewers. As a prerequisite you need to export the positions of the layers from micro slicing as a comma separated value (CSV) list. If you used Excel to document slices, create a new tab and copy/recalculate your slice position data such, that every row represents one layer, with the first layer located at 0 representing the position of 000.TIF, and all further rows representing further layers and their distance to the first layer. Select all the rows in the column you created and use "Save as" to save as CSV and make sure that only the tab you just created is saved when asked.
8. Launch Anacondas "jupyter" GUI and open the "image_stack_interpolation.ipynb" notebook from the repository
9. Scroll down to "Definition of constants" and adjust the values/paths:
   - targetPixelNumXY: Sets the size to which every image is resampled to in X and Y direction, represented by two values separated by a comma; the higher the values chosen, the bigger the data volume created , the lower the values chosen the worse the image resolution
   - targetLayerSize: Sets the distance between slices in Z direction. Creates a homogenously spaced virtual image stack where the layers are spaced according to the value set.
   - csvfile: path to the .CSV file containing the positional data on the micro slicing slices as described in 7.)
   - images: path to the micro slicing images plus asterix based file name extension to create an image collection for interpolation of the images

- savedir: path which shall be used to store the images of the virtual image stack containing the micro slicing images amended by interpolated images in the empty positions in between

10. In jupyter choose “Cell”->”Run All” from the dropdown menu
11. The computation will now be performed and the original and interpolated images written to disc. This can take several minutes to hours, depending on the settings chosen above. If errors occur, try to debug. If unsuccessful, contact the author of the code (Daniel Sieber).

Protocol of reconstruction / registration of micro slicing data

Aim

The aim of this process step is to import the aligned and interpolated image stack from micro slicing into 3D Slicer and to reconstruct the dataset in three dimensions. In a second step the reconstructed dataset is registered to the corresponding CBCT datasets to allow seamless simultaneous use of the aligned datasets in further process steps.

Materials

- Aligned and interpolated micro slicing images, see “Protocol of alignment and interpolation of micro slicing data”
- CT scans of the unembedded and epoxy embedded specimen before micro slicing
- 3D Slicer multi-platform free medical imaging and computation software (version used was 4.8.0)
- Meshmixer software (version 11.0.544 was used here)
- Meshlab software (version 1.3.3 was used here)

Installation

- Install 3D Slicer software
- Install Meshmixer
- Install Meshlab

Protocol

<u>Alignment</u>

1. Use the “Load Data” Module, go to the folder where the interpolated micro slicing slices are located and select the first image of the image stack. Activate the “Show Options” checkbox and make sure that the “Single File” check box is deactivated
2. Use the “Volumes” Module, go to “Active Volume” and rename the volume to a meaningful name like “HISTO”, go to “Volume Information” and set the image spacing to the values which were used in interpolation, see “Protocol of alignment and interpolation of micro slicing data”
3. Check the “IJK to RAS Direction Matrix”. In case the first and second entry on the diagonal are negative, means that the X any Y coordinates are flipped. As this may result in issues later, it should be fixed now:
    1. Use the “Transforms” Module, go to “Active Transform” and create a new linear Transform
    2. Use “Rename current node” to name the transform “FlipXY”
    3. Under “Edit” invert the first and second diagonal entry of the “Transform Matrix”
    4. Under “Apply Transform”, apply the FlipXY transform to the HISTO dataset and push the “Harden Transform” button to make the change permanent.

4. In case you want to use the micro slicing in more than one resolution or an anisotropic/isotropic version, steps 1-3 have to be repeated for all datasets
5. Use the “DICOM” module to import and load the CBCT scan of the embedded specimen, and rename it to a useful name like CBCT
6. In the slice view visualization options set CBCT as foreground and HISTO as background dataset and adjust the visibility such that both datasets will be shown 50%/50% (although not yet aligned)
7. Use the “Transforms” module to create a new linear transform, give it a useful name e.g. CBCT_InitialGuess, apply the transformation to the CBCT dataset(s) using the “Apply Transformation” section, adjust the “translation” sliders in the “edit” section until the two datasets fit roughly onto each other. In case coordinates seem flipped, invert the signs of the main diagonal entries of the transform matrix. Harden the transformation in the “Apply Transformation” section when done.
8. Use the “Vector to Scalar Volume” module (under Converters) to create a scalar copy of the HISTO dataset, rename the new dataset to e.g. HISTO_Scalar
9. Use the “General Registration (BRAINS)” module (under Registration) and execute a new Registration with the following settings:
    - Fixed Volume: HISTO_Scalar
    - Moving Volume: CBCT
    - Percentage of Samples: 0.2 (run it at 0.002 first to see if it runs properly)
    - Slicer Linear Transform: Create a new one called CBCT_BrainsFit
    - Initialization Transform: None
    - Choose “Rigid 6DOF”
10. Use the “Transforms” module to harden the CBCT_Brainsfit transformation for the CBCT dataset
11. Use the “Volumes” module to rename the CBCT volume to CBCT_Registred
12. Use the “DICOM” module to import and load the CBCT scan of the unembedded specimen
13. Use the “Volumes” module to rename to a useful name like CBCTBig
14. Use the “Landmark Registration” module (under Registration) to roughly align the big and small CBCT scans with the following settings:
    1. Fixed Image: CBCT_Registred
    2. Moving Image: CBCTBig
    3. Use the “Add Landmark” feature to add three landmarks and identify them in both scans, for example:
        i. Apex
        ii. Center of RW
        iii. End of Malleus handle
    4. Registration Type: Affine Registration
    5. Registration Mode: Rigid (in some cases Rigid+Scale yields better results)
15. Use the “Transforms” module to rename the “Transform” transformation from the landmark registration to CBCTBig_InitialGuess, apply it to the CBCTBig volume and harden the transform

16. Use the “General Registration (BRAINS)” module and create a new Registration with the following settings:
    1. Fixed Volume: CBCT_Registred
    2. Moving Volume: CBCTBig
    3. Percentage of Samples: 0.2 (run it at 0.002 first to see if it runs properly)
    4. Output Slicer Linear Transform: Create a new one called CBCTBig_BrainsFit
    5. Initialization Transform: None
    6. Choose “Rigid 6DOF”
17. Use the “Transforms” module and harden the CBCTBig_Brainsfit transformation for the CBCTBig dataset(s)
18. Use the “Crop Volume” module (from Converters) to crop and resample the largest image of the scene:
    1. Input Volume: CBCTBig_Registred
    2. Input ROI: Create new Annotation Region of Interest (ROI)
    3. Change ROI size such that all relevant structures are included
    4. Use Interpolated cropping, interpolation option:
        i. Isotropic output voxel
        ii. Scaling factor: 0.5 (To upsample from 250µm to 125µm resolution)
        iii. Linear interpolation
19. Use the “Volumes” module to rename the CBCTBig-subvolume-scale0.5 volume to CBCTBig_Registred
20. Use the “Resample Image (BRAINS)” module (from Registration) to resample the CBCT_registred volume to have the exact same size and resolution as the CBCTBig_Registred volume for later segmentation:
    1. Image to Warp: CBCT_Registred
    2. Reference: CBCTBig_Registred
    3. Output Image: Create new image CBCT_Registred_FullKOS
    4. Pixel Type: Short
    5. Default value: Minimum Value of the CBCT_registred from Volumes module
21. Use the “Save File” widget to save your work

Accuracy Check

Two accuracy check measurements have been implemented for the datasets. The goal is to measure the geometric and volumetric errors in the micro slicing data in relation to the CBCT data.

Geometric error

The Hausdorff distances from one dataset to another is the distance between one voxel of the dataset and its closest voxel on the other dataset. In our case, the measured set is the outline of the epoxy mold of the micro-slicing data with the target being the same outline from the CBCT data.

1. Create a new Segmentation using the “Segment Editor” Module
2. First choose the CBCT_Registred_FullKOS dataset under “Master Volume”
3. Use the “Threshold” Effect and adjust the maximum value to the highest possible value, while setting the lower threshold to capture the entire epoxy overmold without getting too much noise like artifacts outside the epoxy mold
4. Now choose the HISTO_Scalar volume under “Master Volume” and use threshold effect as in 3.)
5. Use the “Export Models” function in the “Segmentations” module to export the segmentation, creating a new model hierarchy
6. Use the “Save File” widget to save the models over the overmold, select the .ply format
7. The models are then imported in *Meshmixer* to remove all the inner surfaces such as only the outer surface of the mold remains. The mesh operations used to do this in Meshmixer are Select (S), Replace (R), Remove (X), Invert Selection (I), and Fill (F).
8. Import the results from Meshmixer in Meshlab
9. The accuracy measurement is done by measuring the Hausdorff distance between the two models (under Filters/Sampling/Hausdorff distance).
10. The models are then colorized by Vertex Quality (Color Creation and processing/ Colorize by Vertex Quality) and a Quality Histogram is created (Render/Show Quality Histogram).

<u>Volumetric Error</u>

The Volumetric Error measurement is also based on the epoxy overmold segmentations from the micro-slicing and CBCT data. It gives the volume ratio between the subset of voxels contained in only one of the two sets and the CBCT set.

1. The 3DSlicer outline segments from the previous measurement are used again, the inner holes are filled using the *Scissors* tool. In the “Segment Editor” module a new segment named *Merged Error* is created. Using the *Logical operators* tool, the error between the two segments is computed using the following operations: (voxels of HISTO – voxels of CBXT) + (voxels of CBCT – voxels of HISTO). The newly created segment represents exclusive *or* between the CBCT and HISTO segments. This means it contains all the voxels that are only in one of the two sets.
2. The CBCT and Merged Error segments are now exported as ply models in analogy to steps 5./6. of the geometric error computation.
3. Import the two segments in *Meshlab*. For both model, the mesh volume is then calculated using *Filters/Quality Measure and Computations/ Compute Geometric Measures.* The volumetric error calculates as the volume of Merged Error divided by the volume of CBCT mesh.

Protocol of segmentation and modelling of anatomy

Aim

The aim of this process step is to delineate the different anatomical structures in the reconstructed and registered micro slicing and CBCT datasets, to allow subsequent creation of three-dimensional models of these anatomical structures. This is done by manual and in some cases, threshold supported segmentation techniques followed by an automatic triangulation of the segmented geometries.

Materials

- WACOM Pen Digitizer Tablet Small (Model CTL-480 was used here)
- 3D Slicer latest version (version 4.8.0 was used here)
- Reconstructed and Registered datasets, see “Protocol of reconstruction and registration of micro slicing data”
- Graphite software (version 3-1 Release 2015 was used here)
- Meshmixer software (version 11.0.544 was used here)
- Meshlab software (version 1.3.3 was used here)

Installation

- Install latest version of 3D Slicer
- Install the latest version of Graphite
- Install the latest version of Meshmixer
- Install the latest version of Mashlab

Protocol

Segmentation

Use the “Load Data” module in 3DSlicer to load the HISTO, CBCT_Registered_FullKOS and CBCTBig_Registred datasets, see “Protocol of reconstruction and registration of micro slicing data”. Segmentation is performed using the “Segment Editor” module. In the slice view visualization options set one of the CBCT datasets as foreground and HISTO as background dataset and adjust the visibility to show one of the datasets, or both datasets simultaneously. Which setting to use is dependent on the anatomical segment to be deliniated. Most of the segmentation can be done using the CBCT data. Micro-slicing data is mainly used to identify fine bony structures (e.g. stapes) and soft tissue structures (e.g. tympanic membrane, basilar membrane) and to help finding landmarks (e.g. junction between Facial Nerve and Chorda Tympani).

As an initial step the bone threshold value (BTV) is determined, all voxels with an intensity higher than BTV will be considered as bone. The BTV is chosen such that most of the air cells partition are kept while

no artifact due to soft tissue is added on the surface of the bone. The value must be manually adjusted while segmenting, until the resulting segmentations have an adequate size.

The segments were created in the following order, using the “Add new empty segment” function:

1) Scala Tympani, Scala Vestibuli, Ossicles, Facial Nerve, Chorda and Carotis

The “Paint” tool is the main tool used to do the segmentation in these segments and the Digitizer Pen is used to control the brush. It is important to always check that two segments are not overlapping by setting the editable area to “Outside all segments”. Activating the “Editable Intensity Range” allows the user to set a range of voxel values outside of which the tool does not work. For the bony structures, this range is from the BTV to the max value. For cavities and other structures, the range is from the min value to the BTV. The “Scissors” tool is used to create clean cuts on the outer ends of ducts of nerve structures and the Carotid artery. To check the results of segmentation and optimize them, the “Show 3D” function can be used, this is particularly helpful for surface optimization and small structures like the Stapes.

2) Tympanic Membrane

The membrane segment is created using the micro-slicing data. First, the segment is painted on the slices where the image is not interpolated (so it’s an original picture of the sample). The gaps between each painted slice are then filled using the “Fill between Slices” tool. The remaining holes are then filled directly on the 3D window using the “Paint” effect with the “Sphere brush” function activated.

3) Bone

The bone segment is obtained using the “Threshold” effect (From the BTV to the max value). The “Keep largest island” function from the “Islands” effect is used to discard undesired and unconnected regions of the segmentation. The “Scissors” effect is used to remove any possible artifact. The integrity of the bone surfaces is checked and holes on surfaces which should be closed are manually closed using a sphere brush eventually combined with the “Editable Intensity Range” function and gradually reducing the lower value below the BTV value until a smooth surface is achieved.

In normal temporal bone specimen, the ossicles are not be embedded in bone and the Facial Nerve should be surrounded by a bony canal. This can be checked using the “Show 3D” function and if necessary the bone segment must be modified using “Paint” and “Erase”.

4) External Auditory Canal

Before segmenting the EAC, the holes between the Tympanic membrane and the Bone must be filled so that the junction is completely seamless. The EAC segment is then created using the Paint tool. The Scissors effect is used to obtain a clean cut at the outer end of the EAC.

5) Sinus-Dura

A large sphere brush (e.g. Size 20) is used to roughly obtain a first version of the segment representing Sinus and Dura. The “Keep the Largest Island” operation is used to remove unconnected islands. At this point, a lot of the air cells are still filled with Dura. The goal of the next steps is to remove it. The “Margin/Shrink” operation is applied with a 3mm margin for example. This operation can take several minutes and aims to separate the parts of the segment that are in the air cells from the main island. “Keep the Largest island” is then used again. Most of the air cells if not all are empty at this point. For the main island to fit the bone again, it is necessary to use the Margin/Grow operation with the same margin value as for the Shrink operation. It lasts also several minutes. The outer border of this segment must be cleaned using Scissors such as clean cuts are obtained and that the Sinus and Dura are hidden behind the bone from the surgeons pre-operative viewpoint.

Modelling

Once it has made been sure that all segments are acceptable in the 3D view and not overlapping, the models are exported using the “Segmentations” module (Operation : Export, Output type : Models) and subsequently saved as .ply files using the “Save Data” Widget. The Bone segment is exported as a Labelmap (Operation : Export, Output Type : Labelmap) and subsequently saved as .nrrd file using the “Save Data” Widget.

1) Repairing and Remeshing the models

The steps described in this paragraph are applied for all exported models except for the bone. Performing these steps will greatly improve the mesh quality and reduce complexity of the models.

1) Start the Graphite software
2) Use File->Load to load the ply file from Slicer
3) Use the Surface->Repair->repair surface operation with the following parameters
    a. Epsilon: 0,1
    b. Min comp area: 0,03
    c. Max hole area: 1e-3
    d. Max hole edges: 2000
    e. Max degree3
    f. dist: 0,0
4) Use the the Surface->Repair->merge vertices operation with the following parameter
    a. Epsilon: 0,01
5) Remesh the model, this means creating a new mesh based on the former one with a new amount of points and improved mesh quality. The operation is Surface->Remesh->remesh smooth with the following parameters:

a. Nb points : See table below
b. Tri shape adapt : 1.0
c. Tri size adapt : 0.0)

Segment	Stapes	Incus, Malleus	Chorda Tympani	Tympanic Membrane	Scala Tympani, CochleoVestibular Nerve	Carotis, Facial Nerve, Scala vestibuli, External Auditory Canal	Sinus-Dura
Nb points	1000	2000	3000	4000	8000	10000	50000

This should result in a relatively homogenous mesh element size. If this is not the case, the number of points may have to be adjusted.

Once the operation is complete, the newly created remeshed model is exported using the File->save current function.

If needed, open the remeshed model in Meshmixer to fix remaining defects of the surface by replacing them using a smoothed surface.

In the MeshLab software, import the remeshed models. Sometimes the imported models appear with a completely dark surface. In this case the surface normal are falsely inverted, this can be corrected by applying the Filters->Normals, Curvatures and Orientation-> invert face orientation. The model is then saved again.